STUDY S-382

STUDY OF DoD AUTOMATED ENVIRONMENTAL SERVICES SUPPORT SYSTEMS

Appendix E: Numerical Simulation of Global Circulation of the Atmosphere up to an Altitude of 300 Km

Alan J. Grobecker

June 1971

INSTITUTE FOR DEFENSE ANALYSES
SCIENCE AND TECHNOLOGY DIVISION

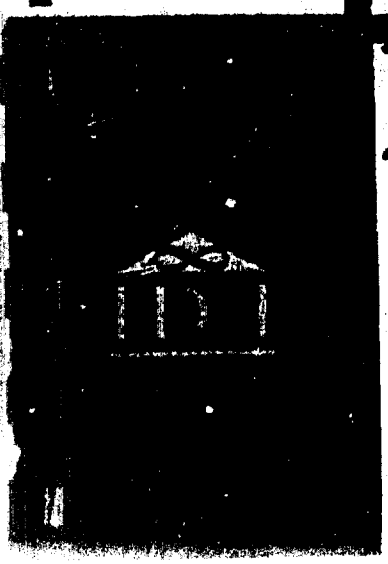

IDA Log No. HQ 71-12457
Copy 139 of 200 copies

127
R

The work reported in this document was conducted under contract DAHC15 67 C 0011 for the Department of Defense. The publication of this IDA Study does not indicate endorsement by the Department of Defense, nor should the contents be construed as reflecting the official position of that agency.

Approved for public release; distribution unlimited.

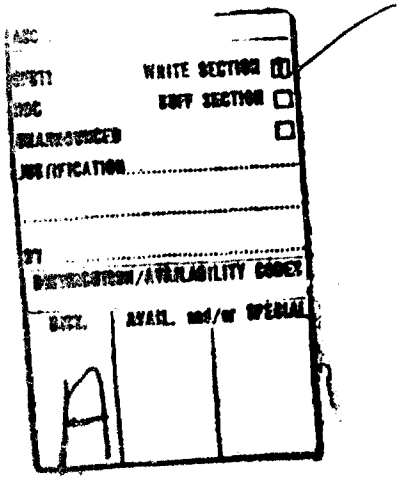

UNCLASSIFIED
Security Classification

DOCUMENT CONTROL DATA - R & D
(Security classification of title, body of abstract and indexing annotation must be entered when the overall report is classified)

1 ORIGINATING ACTIVITY (Corporate author) INSTITUTE FOR DEFENSE ANALYSES 400 Army-Navy Drive Arlington, Virginia 22202	2a. REPORT SECURITY CLASSIFICATION UNCLASSIFIED 2b. GROUP --

3 REPORT TITLE
Study of DoD Automated Environmental Services Support Systems
Appendix E: Numerical Simulation of the Global Circulation of the Atmosphere up to an Altitude of 300 Kilometers

4 DESCRIPTIVE NOTES (Type of report and inclusive dates)
Study S-382 - June 1971

5 AUTHOR(S) (First name, middle initial, last name)
Alan J. Grobecker

6 REPORT DATE June 1971	7a. TOTAL NO OF PAGES 128	7b. NO OF REFS 47
8a CONTRACT OR GRANT NO DAHC15 67 C 0011 b PROJECT NO Task T-80 c d	9a. ORIGINATOR'S REPORT NUMBER(S) S-382 9b. OTHER REPORT NO(S) (Any other numbers that may be assigned this report) None	

10 DISTRIBUTION STATEMENT
Approved for public release; distribution unlimited.

11 SUPPLEMENTARY NOTES NA	12 SPONSORING MILITARY ACTIVITY Advanced Research Projects Agency Arlington, Virginia 22209

13 ABSTRACT

This Appendix to IDA Study S-382 describes a numerical model for the global stratosphere, mesosphere, and thermosphere. The model is intended to be used solely as a basis for estimating the size of the computational problem. The model attempts to define the motions of the atmosphere, including the troposphere, up to altitudes of 300 kilometers. Only those atmospheric motions which are of horizontal scale lengths greater than 1000 km and of vertical scale lengths greater than 10 km are considered.

Annexes to this document detail various factors to be considered in specifying a model of the upper atmosphere.

DD FORM 1 NOV 68 1473

UNCLASSIFIED
Security Classification

14 KEY WORDS	LINK A		LINK B		LINK C	
	ROLE	WT	ROLE	WT	ROLE	WT
stratosphere, mesosphere and thermosphere						
global circulation						
computational model						

STUDY S-382

STUDY OF DoD AUTOMATED ENVIRONMENTAL SERVICES SUPPORT SYSTEMS

Appendix E:
Numerical Simulation of Global Circulation of the Atmosphere up to an Altitude of 300 Km

Alan J. Grobecker

June 1971

INSTITUTE FOR DEFENSE ANALYSES
SCIENCE AND TECHNOLOGY DIVISION
400 Army-Navy Drive, Arlington, Virginia 22202
Contract DAHC15 67 C 0011
Task T-80

READER'S REFERENCE

This Study of DoD Automated Environmental Services Support Systems consists of the following documents:

Report of Findings

Appendix A. DoD Needs for Environmental Support Services

Appendix B. Navy Environmental Support Services in 1970

Appendix C. Air Force/Army Environmental Support Services in 1970

Appendix D. Sources of Data for DoD Environmental Services Support Systems of 1975-80

Appendix E. Numerical Simulation of Global Circulation of the Atmosphere up to an Altitude of 300 km

Appendix F. Data Processing for DoD Environmental Services Support Systems of 1975-80

Appendix G. Costs of a Spectrum of Options for Data Processing of DoD Environmental Services Support Systems of 1975-80

ABSTRACT

This Appendix to IDA Study S-382 describes a numerical model for the global stratosphere, mesosphere, and thermosphere. The model is intended to be used solely as a basis for estimating the size of the computational problem. The model attempts to define the motions of the atmosphere, including the troposphere, up to altitudes of 300 kilometers. Only those atmospheric motions which are of horizontal scale lengths greater than 1000 km and of vertical scale lengths greater than 10 km are considered.

Annexes to this document detail various factors to be considered in specifying a model of the upper atmosphere.

ABSTRACT

This Appendix to IDA Study S-382 describes a numerical model for the global stratosphere, mesosphere, and thermosphere. The model is intended to be used solely as a basis for estimating the size of the computational problem. The model attempts to define the motions of the atmosphere, including the troposphere, up to altitudes of 300 kilometers. Only those atmospheric motions which are of horizontal scale lengths greater than 1000 km and of vertical scale lengths greater than 10 km are considered.

Annexes to this document detail various factors to be considered in specifying a model of the upper atmosphere.

CONTENTS

TABLES

FIGURES

I. INTRODUCTION

OBJECTIVE

The objective of IDA Study S-382 is to examine the feasibility of a collocation and/or consolidation of the Navy and Air Force current and programmed (five years) operational environmental services computer centers.

As part of this task, we present here a numerical model for the global circulation in the strato-, meso-, and thermosphere (S-M-T), showing features of horizontal scale larger than 1000 km. Since the troposphere represents a lower boundary to the upper atmosphere described, the model describes the troposphere also in mesh coarser than that commonly used for weather prediction.

The present model is set up solely to provide a basis for estimating the scale of the computational problem and should not be used in any other way. Since the described model, or any other model of comparable complexity, has never been proven in practice, the details may certainly be considered controversial, but such controversy need not affect the utility of the model for the intended purpose of computer estimation.

ORGANIZATION OF THIS DOCUMENT

The S-M-T Model described in the main body of this text includes some but not all of the various considerations leading to a specification of a model for purposes of its numerical computation. In Annex A, the basic conservation equations are given in as complete a form as may be necessary to describe all effects, large and small, that may obtain in the altitude range from sea level to 300 km. In Annex B the region up to the 300-km altitude is subdivided into several domains. The terms described in Annex A that are applicable to each of these

domains, and the boundaries that limit each domain, are also given. In Annex C the conservation equations, described in vector notation in Annex A, are described in spherical coordinates (r, θ, λ, t). In Annex D the parameters described in Annex C are given in terms of the mean quantity and a small perturbation. These relations may be used to treat the nonlinear terms descriptive of the advection. In Annex E schemes of difference equations are described. Leith's (1965) method of treating advection is described, as is the 4-point explicit scheme, with forward time difference, reviewed by Richtmyer (1967), which is computationally stable if grid spacing and time steps are suitably chosen. With computational stability and Nyquist sampling considerations as given in Annex F, the time and space steps are defined to be 500 km horizontally, 5 to 20 km vertically and 10 min in time. A summary listing by name of heat sources that are to be considered in each domain is given in Annex G. In Annex H are listed photo processes and chemical reactions described by Bortner and Kummler (1968), as significant in the tropo-, strato-, meso-, and thermosphere. These reactions lead to definition of the production and loss terms of the number continuity equations and of important heat contributions in the atmosphere. Annex I presents a timing analysis of radiation energy and heat equations.

OVERVIEW

Beginning with the effort of L.F. Richardson (1922), a number of attempts to compute the global circulation of the atmosphere have been undertaken. The recent efforts of Leith (1965), Mintz and Arakawa (1965), Smagorinsky and co-workers (1963), and Kasahara and Washington (1967) have been confined largely to simulations of the troposphere, problems of such magnitude as to exceed the capacity for the fastest computers of the day. The 1971 advent of "fourth-" and "fifth-generation" computers, with capacity approaching a thousand times that of computers used for tropospheric simulation, promises that we will have the capacity to simulate the atmosphere up to and including the thermosphere, to meet needs for data suggested by application of

radio propagation for purposes of communication and radar, and of orbit prediction of low-altitude earth satellites.

The S-M-T Model is one intended to define the motions of the atmosphere, including also the troposphere up to altitudes of about 300 km, which are of horizontal scale lengths greater than 1000 km and of vertical scale lengths greater than 10 km.

In Fig. 1, horizontal scale lengths characteristic of various modes of atmospheric motion are described. The S-M-T Model described herein will not resolve most motions of turbulence the size of hurricanes or smaller.

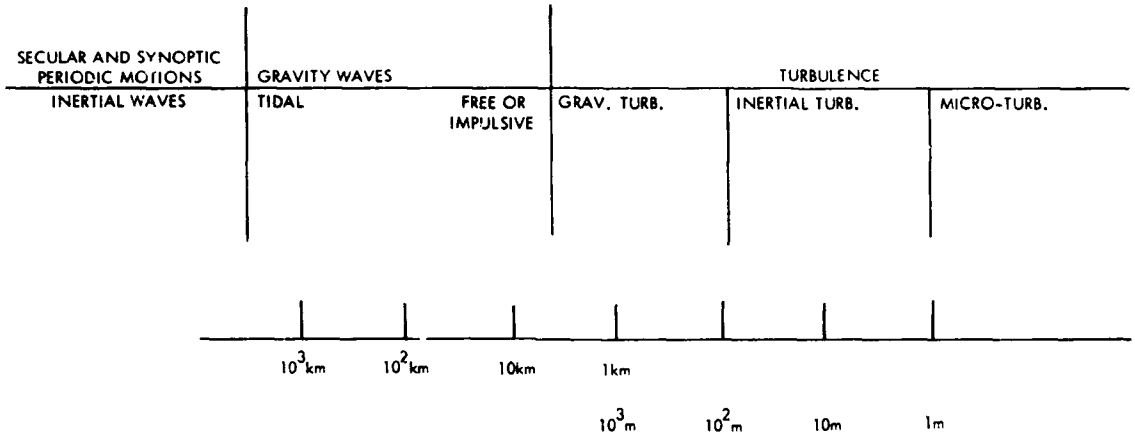

55-12-71-6

FIGURE 1. Horizontal Scale Lengths

The method of computation suggested herein for the S-M-T Model follows the pattern and has many of the conventions described by Leith (1965). The Annexes detail various considerations leading to a specification of a model for purposes of its numerical computation: The S-M-T Model described in the main body of this text includes some but not all of these considerations, neglecting others as elements of negligible importance.

In Annex A, the basic conservation equations are given in as complete a form as may be necessary to describe all effects, large and small, that may obtain in the altitude range from sea level to 300 km. In Annex B the region up to the 300-km altitude is subdivided into several domains. The terms described in Annex A that are applicable

to each of these domains, and the boundaries that limit each domain, are also given. In Annex C the conservation equations, described in vector notation in Annex A, are described in spherical coordinates (r, θ, λ, t). In Annex D the parameters described in Annex C are given in terms of the mean quantity and a small perturbation. These relations may be used to treat the nonlinear terms descriptive of the advection. In Annex E schemes of difference equations are described. Leith's (1965) method of treating advection is described, as is the 4-point explicit scheme, with forward time difference, reviewed by Richtmyer (1967), which is computationally stable if grid spacing and time steps are suitably chosen. With computational stability and Nyquist sampling considerations as given in Annex F, the time and space steps are defined to be 500 km horizontally, 5 to 20 km vertically and 10 min in time. A summary listing by name of heat sources that are to be considered in each domain is given in Annex G. In Annex H are listed photo processes and chemical reactions described by Bortner and Kummler (1968), as significant in the *tropo-*, *strato-*, *meso-*, and thermosphere. These reactions lead to definition of the production and loss terms of the number continuity equations and of important heat contributions in the atmosphere. Annex I presents a timing analysis of radiation energy and heat equations.

I. COORDINATES

It is assumed in the model that the atmosphere is always in hydrostatic equilibrium. This means that the pressure at a given point is determined by the weight per unit area of the air above that point. A differential expression of this assumption is the hydrostatic relation.

$$dp = -g\rho\, dz = -g \sum_a m_a n_a\, dz \qquad (1)$$

giving the increment in pressure dp in terms of an increment in height dz for given density ρ. Here g is the (assumed constant) acceleration of gravity that transforms the mass element $\rho\, dz$ into a weight element $g\rho\, dz$, where $\rho = \sum_a m_a n_a$, the sum of the mass densities of all atmospheric constituents.

The hydrostatic assumption rules out in particular the possibility of dynamic pressure differences leading to vertical accelerations. For horizontal scales of motion large compared to the thickness of the atmosphere, this assumption is thought to be quite valid.

Another dependent variable that is used is the geopotential $\phi = gz$, giving the potential energy per unit mass and serving as a measure of the height of a given pressure surface. In the topography of pressure surfaces a region of lower pressure corresponds to a higher altitude in the z coordinate.

The coordinate system by which the atmosphere is described in this report is given in Fig. 2. The earth is considered to be a sphere of radius $a = 6366$ km. Horizontal position coordinates are latitude θ and east longitude λ. The vertical position coordinate is $r = a + z$.

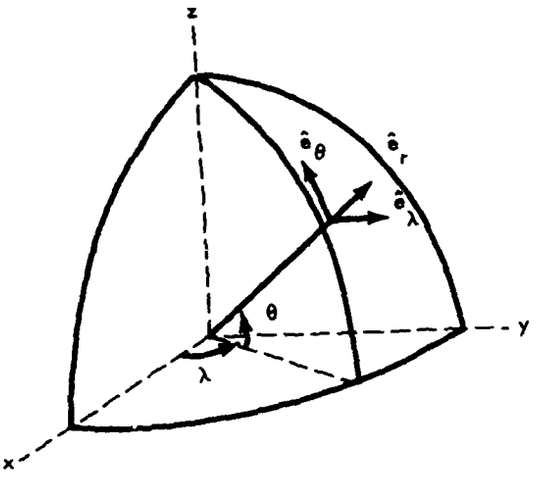

S 5-12-71-S

FIGURE 2. Spherical Coordinate System

II. KINEMATIC RELATIONS

It is important to distinguish 2 kinds of time derivative. The Eulerian time derivative $\partial/\partial t$ is based on the time rate of change at a fixed point in the space coordinates (θ, λ, r), and thus corresponds to the usual notion of partial derivative. The Lagrangian or substantive time derivation D/Dt on the other hand is based on the time rate of change at a point imbedded in and moving with the fluid. It is this Lagrangian time derivative that enters quite naturally in the expression of many of the physical laws governing the hydrodynamics of the atmosphere.

The horizontal velocity components are

$$u = a \cos \theta \frac{D\lambda}{Dt} \tag{2}$$

$$v = a \frac{D\theta}{Dt} \tag{3}$$

positive toward the east and pole, respectively.

In the altitude coordinate system the vertical "velocity" component is

$$w = \frac{Dr}{Dt} \tag{4}$$

positive upward. In terms of these velocity components the relation between the two kinds of time derivative is

$$\frac{D}{Dt} = \frac{\partial}{\partial t} + u \frac{1}{a \cos \theta} \frac{\partial}{\partial \lambda} + v \frac{1}{a} \frac{\partial}{\partial \theta} + w \frac{\partial}{\partial r} \quad . \tag{5}$$

The terms involving space derivatives and velocity components are referred to as the advection terms.

The equation of <u>continuity</u> is, for each of the atmospheric constituents (denoted by subscript a), as follows:

$$\frac{\partial n_a}{\partial t} + \frac{1}{r^2}\frac{\partial}{\partial r}(n_a r^2 w_a) + \frac{1}{r\cos\theta}\frac{\partial}{\partial \lambda}(n_a v_a) + \frac{1}{r\cos\theta}\frac{\partial}{\partial \theta}(n_a \cos\theta\, u_a)$$

$$= P_a - L_a \qquad (6)$$

wherein

P_a = production of number density of constituent ($_a$), i.e., by dissociation.

L_a = loss of number density of constituent ($_a$), i.e., by reconstruction.

The conservation of mass requires the continuity relation of the nondivergent flow of mixture of constituents:

$$\mathcal{D} + \frac{\partial w}{\partial z} = 0 \qquad (7)$$

where $\mathcal{D}$ is the horizontal divergence of the two-dimensional wind field calculated in an altitude surface from horizontal components u, v, i.e.,

$$\mathcal{D} = \frac{1}{a\cos\theta}\left[\frac{\partial u}{\partial \lambda} + \frac{\partial v\cos\theta}{\partial \theta}\right] . \qquad (8)$$

Using the boundary conditions $w = 0$ at $z = 300$ km, Eq. 7 can be integrated downward to give

$$w(z) = \int_z^{300\ \mathrm{km}} \mathcal{D}(z)\, dz \ . \qquad (9)$$

The acceleration equations in the altitude coordinate system are the following, after Godske et al. (1957):

$$m_a n_a \Bigg\{ \hat{e}_r \left[\frac{dw}{dt} - \frac{u^2}{r} - \frac{v^2}{r} + \frac{\partial \phi}{\partial r} + s \frac{\partial p}{\partial r} 2\,\Omega \left[(\sin \lambda)\, u - (\sin \theta \cos \lambda) v \right] - S_r \right]$$

$$+ \hat{e}_\lambda \left[\frac{dv}{dt} - \frac{uv}{r} \tan \theta + \frac{wv}{r} + \frac{1}{r \cos \theta} \frac{\partial \phi}{\partial \lambda} + \frac{s}{r \cos \theta} \frac{\partial p}{\partial \lambda} \right.$$

$$\left. - 2\,\Omega \left[(\sin \theta \cos \lambda)\, w + (\cos \theta \cos \lambda) u \right] - S_\lambda \right]$$

$$+ \hat{e}_\theta \left[\frac{du}{dt} + \frac{uw}{r} + \frac{v^2}{r} \tan \theta + \frac{1}{r} \frac{\partial \phi}{\partial \theta} + 2\,\Omega \left[(\sin \lambda)\, w + (\cos \theta \cos \lambda) v \right] - S_\theta \right] \Bigg\}_a$$

$$= \underline{F}_a + \underline{F}_{em} + \underline{F}_{coll} \qquad (10)$$

wherein Ω = vector of rotation

ϕ = geotential (gz)

s = specific volume $= \frac{1}{\rho} = \frac{1}{\sum m_a n_a}$

p = pressure

S = force of friction $= \mu \left[\nabla^2 \underline{V} + \frac{1}{3} \nabla (\nabla \cdot \underline{V}) \right]$ (11)

$$= \hat{e}_r \left[\mu \left(\frac{1}{r} \frac{\partial^2 (rw)}{\partial r^2} + \frac{1}{r^2} \frac{\partial^2 w}{\partial \theta^2} - \frac{1}{r^2 \cos^2 \theta} \frac{\partial^2 w}{\partial \theta^2} \right.\right.$$

$$+ \frac{\tan \theta}{r^2} \frac{\partial w}{\partial \theta}$$

$$- \frac{2}{r^2} \frac{\partial v}{\partial \theta} + \frac{2}{r^2 \cos \theta} \frac{\partial u}{\partial \lambda} - \frac{2w}{r^2} - \frac{2 \tan \theta}{r^2} v$$

$$\left.\left. + \frac{1}{3} \nabla (\nabla \cdot \underline{V}) \right) \right]$$

$+ \hat{e}_\lambda [\quad] + \hat{e}_\theta [\quad]$. (Landau & Lefshitz (1959) 15.08, p. 52)

The equation of state of the atmospheric constituents may be represented by the following:

$$P_a = n_a' k T_a \quad . \tag{12}$$

k = Boltzmann's constant

The thermodynamical equation of energy conservation is written as follows:

$$\dot{w} + s\delta = \dot{e} + p\dot{s} \tag{13}$$

wherein $\dot{w}$ = rate of heat input from sources radiative + conductive

$$= \sum_a \frac{dQ_a}{dt} + \nabla(\lambda_a \nabla T_a)$$

$s\delta$ = rate of heat increase by Rayleigh dissipation (friction)

s = unit volume

$$s\delta = \left[\frac{1}{2}\eta\left(\frac{\partial u_i}{\partial x_k} + \frac{\partial u_k}{\partial x_i} - \frac{2}{3}\delta_{ik}\frac{\partial u_\ell}{\partial x_\ell}\right)^2 + \zeta(\nabla \cdot \underline{u})^2\right] \tag{14}$$

$\dot{e}$ = rate of heat increase (increase of internal energy

$= c_p \theta$

$p\dot{s}$ = compression energy

and symbol ($\dot{}$) denotes $\frac{d(\ )}{dt} = \frac{\partial(\ )}{\partial t} + \underline{u}\nabla \cdot (\ )$. (15)

In the altitude coordinate system the thermodynamical equation of energy becomes:

$$m_a n_a c_v \left(\frac{\partial T_a}{\partial t} + w \frac{\partial T_a}{\partial r} + \frac{u}{r \cos\theta} \frac{\partial T_a}{\partial \lambda} + \frac{v}{r} \frac{\partial T_a}{\partial \theta} \right)_a$$

$$- kT_a \left(\frac{\partial n_a}{\partial t} + w \frac{\partial n_a}{\partial r} + \frac{u}{r \cos\theta} \frac{n_a}{\partial \lambda} + \frac{v}{r} \frac{\partial n_a}{\partial \theta} \right)_a$$

$$= \frac{\lambda_a}{r^2 \cos\theta} \left\{ \frac{\partial}{\partial r} \left(r^2 \cos\theta \frac{\partial T_a}{\partial r} \right) + \frac{\partial}{\partial \lambda} \left(\frac{1}{\cos\theta} \frac{\partial T_a}{\partial \lambda} \right) + \frac{\partial}{\partial \theta} \left(\cos\theta \frac{\partial T_a}{\partial \theta} \right) \right\}$$

$$+ \frac{1}{2} \eta \left\{ \left[\frac{\partial w}{r \partial \theta} + \frac{\partial u}{\partial r} - \frac{2}{3} \left(\frac{\partial w}{\partial r} \right) - \frac{2}{3} \left(\frac{\partial u}{r \cos\theta \, \partial \lambda} \right) \right]^2 + \left[\frac{\partial v}{\partial r} + \frac{\partial w}{r \partial \theta} - \frac{2}{3} \frac{\partial v}{r \partial \theta} - \frac{2}{3} \frac{\partial w}{\partial r} \right]^2 \right.$$

$$\left. + \left[\frac{\partial u}{r \partial \theta} + \frac{\partial v}{r \cos\theta \, \partial \lambda} - \frac{2}{3} \frac{\partial u}{r \cos\theta \, \partial \lambda} - \frac{2}{3} \frac{\partial v}{r \partial \theta} \right]^2 \right\}$$

$$+ \zeta \left[\frac{1}{r^2} \frac{\partial}{\partial r} (r^2 w) + \frac{1}{r \cos\theta} \frac{\partial u}{\partial \lambda} + \frac{1}{r \cos\theta} \frac{\partial}{\partial \theta} (\cos\theta \, v) \right]^2 \qquad (16)$$

wherein η, ζ are the coefficients of viscosity.

The force on a unit volume of atmosphere due to the moon's gravity is given in Jeffreys (1960), pp. 231-233.

$$\underline{F}_a = m_a r_a \left(\frac{K_g M_n}{D_m^3} \right) \left\{ \left[r \left\{ \left(\frac{1}{2} - \frac{3}{2} \cos^2 \Delta\lambda_n \right) + \frac{3}{2} \sin^2 \Delta\lambda_n \cos\theta \right\} \right] \hat{e}_\Omega \right.$$

$$+ \left[\frac{r}{\cos\theta} \left\{ \frac{3}{2} \cos \Delta\lambda_m \sin \Delta\lambda_m (1 + \cos 2\theta) \right\} \right] \hat{e}_\lambda$$

$$\left. + \left[\frac{3}{2} r \sin^2 \Delta\lambda_m \sin 2\theta \right] \hat{e}_\theta \right. \qquad (17)$$

wherein $\Delta\lambda_m = \lambda - \lambda_m$; λ_m = longitude of moon. The electromagnetic force on a unit volume of atmosphere is

$$\underline{F}_{em} = e_a n_a \left(E_{o_r} + E_{s_r} + u_\lambda \frac{B_\theta}{c} - u_\theta \frac{B_\lambda}{c} \right) \hat{e}_r +$$

$$+ \left(E_{o_\lambda} + E_{s_\lambda} + u_\theta \frac{B_r}{c} - u_r \frac{B_\theta}{c} \right) \hat{e}_\lambda$$

$$+ \left(E_{o_\theta} + E_{s_\theta} + u_r \frac{B_\lambda}{c} - u_\lambda \frac{B_r}{c} \right) \hat{e}_\theta \quad . \tag{18}$$

The collisional force is

$$\underline{F}_{coll} = m_a n_a \nu_{an} \left\{ (w_a - w_n) \hat{e}_r + (u_a - u_n) \hat{e}_\lambda + (v_a - v_n) \hat{e}_\theta \right\} \tag{19}$$

where n denotes a neutral particle, e.g. nitrogen,

e_a is the electric charge of species $(_a)$

$\underline{E}_o$ is the external electric field

$\underline{E}_s$ is the self-consistent or induced electric field

$\underline{B}$ is the magnetic field.

III. FINITE DIFFERENCE MESH

The finite difference equations are based on 2 separate fixed, Eulerian space-time meshes that are conveniently distinguished as even and odd. Some dependent variables such as temperature and water vapor concentration are defined on the even mesh; others such as horizontal velocity components are defined on the odd mesh.

Altitude z is used as a vertical coordinate; even mesh points are at 41 pressure levels (0, 5, 10, 15, ..., 115, 120 km in 5-km steps; 130, 140, ..., 180, 200 km in 10-km steps; and 220, 240, 260, 280, and 300 km in 20-km steps).

Latitude θ and longitude λ are used as horizontal coordinates. Even mesh points are at even multiples of 5° in latitude and in longitude between the equator and 60° latitude. Poleward of 60° a coarsening of the mesh in the longitudinal direction is introduced. For 65°, 70°, and 75° latitude the even mesh points are at even multiples of 10° in longitude; for 80° at even multiples of 20°, and for 85° at even multiples of 40°. The pole finally is an even mesh point. There are 2072 grid points in the horizontal mesh of a single altitude level.

The time variable t is Greenwich time. The even mesh times are even multiples of 10 min starting from midnight.

The odd mesh points are at the centers of the boxes defined by the even mesh points. They are thus at altitude levels of 2.5, 7.5, 12.5, etc., and at times 5 min later (or earlier) than an even mesh time.

Indexing of the even mesh is by the letters k, l, m, n. The index k increases with E longitude being 0 at Greenwich meridian. For latitudes up to 60° the Greenwich meridian is reached again for $k = 72$, but for example at latitude 80°, it is reached again for $k = 18$.

The index l increases with latitude from 0 at the equator to 18 at the pole. Note that no distinction has been made between N latitude and S latitude; the two hemispheres are treated in the same way, but this implies that the coordinate system in the southern hemisphere is the (left-handed) reflection of that in the northern hemisphere.

The index m increases (upward) with altitude from 1 for 5 km to 40 for 300 km.

The index n increases with time.

The odd mesh is then most naturally indexed with the appropriate half-integer indices. For purposes of problem organization and memory storage assignment, a link has been established between the odd indices $k = \frac{1}{2}$, $l - \frac{1}{2}$, $m - \frac{1}{2}$, $n + \frac{1}{2}$ and the even indices k, l, m, n.

The global indexing system described is supplemented by a local indexing system, shown in Fig. 3. In this system, attention is fixed on a particular even mesh point, which is given the single letter index V corresponding, say, to the global index (k, l, m, n). The even mesh point neighboring toward the pole (k, l + 1, m, n) is designated by P. The one toward the equator (k, l - 1, m, n) is designated by Q. The lower neighbor corresponding to higher pressure (k, l, m - 1, n) is designated by U. The neighbor above corresponding to lower pressure (k, l, m + 1, n) is designated by T. The new value at the same mesh point (k, l, m, n + 1) is designated by W. This leaves variation in the longitudinal direction, which is indicated by addition and subtraction; thus, the east neighbor (k + 1, l, m, n) is designated by V + 1, the west neighbor (k - 1, l, m, n) by V - 1.

The odd mesh also uses this local indexing system with the same letter designations through the link described earlier between the 2 meshes. Thus a westerly wind component u indexed by P and written as u_P is defined at the odd mesh point $(k - \frac{1}{2}, l + \frac{1}{2}, m - \frac{1}{4}, n + \frac{1}{2})$. The conceptual complication here is the price paid for a shortening of the notation.

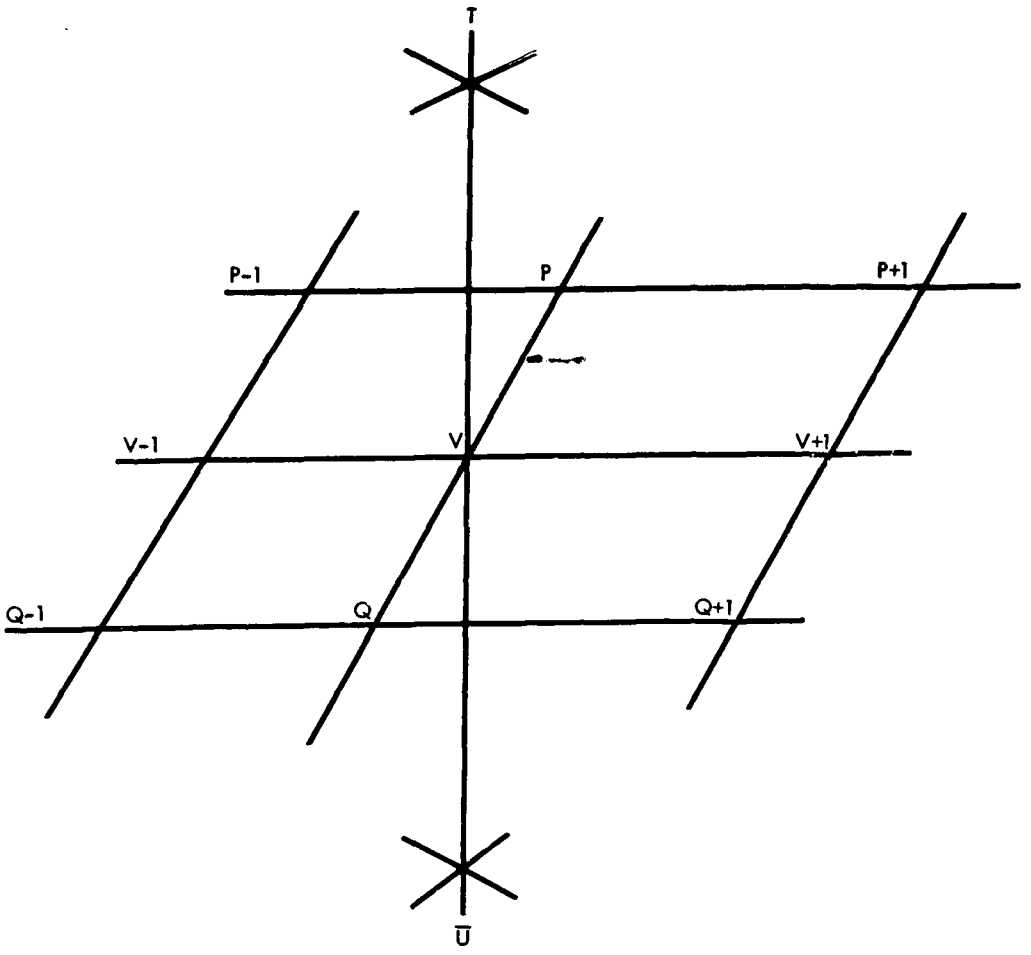

S 5-12-71-4

FIGURE 3. Local Indexing System

IV. VARIABLES

The independent variables whose subdivision into a discrete grid has been described are latitude, θ, longitude, λ, altitude, z, and time, t.

The dependent variables are of 2 sorts, prognostic and diagnostic. Of these the prognostic variables are the more fundamental in that they define at any given time the state of the atmosphere and its change. For each of 33 constituents, there are 4 variables: temperature T, number density n_a, and horizontal wind velocity components a toward the east and v toward the pole, all 4 being defined as functions of latitude, longitude, altitude, and time. Of these 4 variables, 2, namely T and n, are defined at even grid points and at even times; whereas the other 2, namely, the wind velocity components u and v, are defined at odd grid points and at odd times. There is 1 final prognostic variable, the surface pressure, $dp_s = \Sigma m_a n_a g\, dz$, which is a function of latitude, longitude, time, and altitude. The surface pressure p_s is defined at even latitude and longitude grid points and at even times. The prognostic variables are characterized by being advanced in time through integration of a first-order time differential equation approximated numerically by summation of a first-order time difference equation. This numerical process is of the marching type, explicit, and involving only single time differences.

Any other dependent variables are of the diagnostic sort. They are completely determined at any given time by the fields of prognostic variables at the same time. The most important of these are the horizontal wind divergence δ defined at odd pressure levels, even latitude and longitude grid points, and odd times; the vertical "velocity" component w defined at even spatial grid points but odd times;

and the geopotential $\phi = gz$ defined at odd pressure levels, even latitude and longitude grid points, and even times. These assignments of variables to even or odd grid points are summarized in Table 1.

TABLE 1. EVEN-ODD GRID ASSIGNMENTS

	Independent Variable Grid			
Dependent Variables	Altitude	Latitude	Longitude	Time
Prognostic:				
T	even	even	even	even
n	even	even	even	even
u	odd	odd	odd	odd
v	odd	odd	odd	odd
p_s	even	even	even	even
Diagnostic:				
Ω	odd	even	even	odd
w	even	even	even	odd
ϕ	odd	even	even	even

V. ADVECTION

One of the crucial aspects of numerical models of Eulerian flow is the approximation of advection terms in a stable and accurate way. The approach used in this model is that of Leith (1965), which follows the method of fractional time steps used by Marchuk (1964) and others (Bagrinovsky and Godunov (1957), D'yakonov (1962)).

In applying this scheme the difference equation can be written as a sequence of two equations, determining $\frac{\partial \psi}{\partial t}(y,t)$ and $\frac{\partial \psi}{\partial t}(y,t+\frac{1}{2})$:

$$\psi_{j,k}^{n+\frac{1}{2}} = \psi_{j,k}^{n} - \frac{\beta}{2}\left(\psi_{j,k+1}^{n} - \psi_{j,k-1}^{n}\right) + \frac{\beta^2}{2}\left(\psi_{j,k+1}^{n} - 2\psi_{j,k}^{n} + \psi_{j,k-1}^{n}\right)$$

$$\psi_{j,k}^{n+1} = \psi_{j,k}^{n+\frac{1}{2}} - \frac{\alpha}{2}\left(\psi_{j+1,k}^{n+\frac{1}{2}} - \psi_{j-1,k}^{n+\frac{1}{2}}\right) + \frac{\alpha^2}{2}\left(\psi_{j+1,k}^{n+\frac{1}{2}} - 2\psi_{j,k}^{n+\frac{1}{2}} + \psi_{j-1,k}^{n+\frac{1}{2}}\right) \quad (20)$$

where $\alpha = \frac{u\Delta t}{\Delta x}$ and $\beta = \frac{v\Delta t}{\Delta y}$.

The computational process involved in a single time step is divided into 2 cycles. In the first of these, advection in the y-direction only is evaluated whereas in the second advection in the x-direction only is evaluated starting, of course, with the results of the first cycle. The fractional time step notation is a convenience, but the results of the first cycle have no particular physical significance.

VI. HORIZONTAL DIVERGENCE

The differential expression equation (8) for the horizontal divergence is

$$\mathcal{D} = \frac{1}{a \cos \theta} \left[\frac{\partial u}{\partial \lambda} + \frac{\partial v \cos \theta}{\partial \theta} \right] \tag{8}$$

where a is the (assumed constant) radius of the earth.

In choosing an appropriate finite difference estimate of the divergence, it is convenient to return to the fundamental definition of divergence as net outflow per unit area. Figure 4 shows a piece of the grid in an odd pressure level showing variables and indices appropriate to a single divergence calculation. The divergence $\mathcal{D}_v$ is that calculated for the element of area enclosed by dotted lines whose vertices are odd horizontal grid points. Assuming a linear dependence of u, v on position, the net outflow from this element of area is

$$\frac{u_{p+1} + u_{v+1}}{2}(a\Delta\theta) - \frac{u_p + u_v}{2}(a\Delta\theta) + \frac{v_p + v_{p+1}}{2}\left(a \cos \theta_{l+\frac{1}{2}}\Delta\lambda\right)$$

$$- \frac{v_v + v_{v+1}}{2}\left(a \cos \theta_{l-\frac{1}{2}}\Delta\lambda\right)$$

and the area of the element is

$$a^2\left(\sin \theta_{l+\frac{1}{2}} - \sin \theta_{l-\frac{1}{2}}\right)\Delta\lambda \quad .$$

Thus the average outflow per unit area is

$$D_v = \frac{\Delta\theta}{\Delta \sin\theta}\left[\frac{u_{p+1} + u_{v+1} - u_p - u_v}{2a\,\Delta\lambda} + \frac{(u_p + u_{p+1})\cos\theta_{l+\frac{1}{2}} - (u_v + u_{v+1})\cos\theta_{l-\frac{1}{2}}}{2a\Delta\theta}\right] \qquad (21)$$

This difference form is conservative of mass since the flow from one grid element across a boundary is numerically identical to the flow across the boundary to the adjacent grid element.

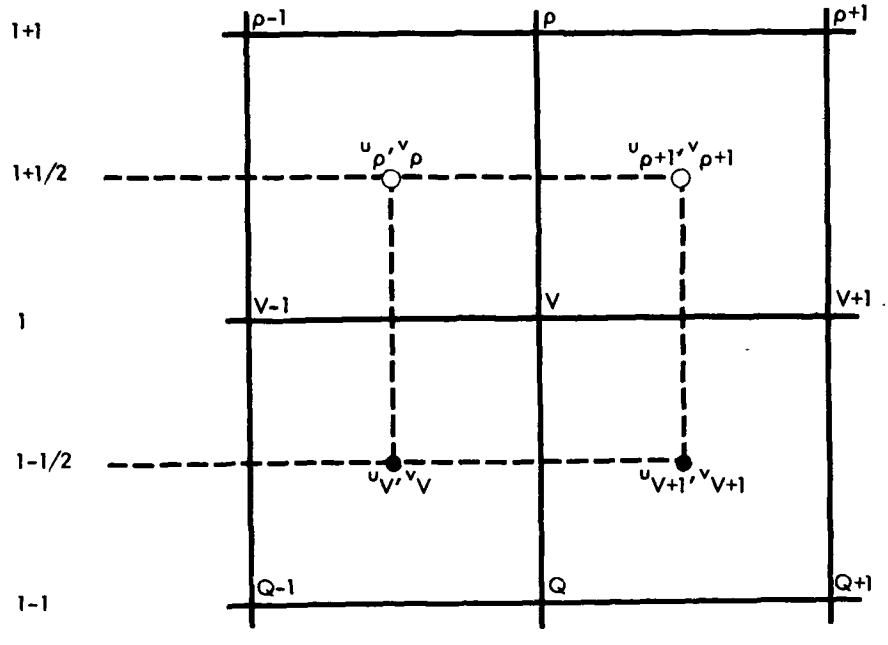

55-12-71-3

FIGURE 4. Divergence Calculation

Horizontal divergence $\mathcal{D}$ determines the vertical motion field w by Eq. 9 repeated here

$$w(p) = -\int_{300}^{z} \mathcal{D}(z')dz' . \qquad (9)$$

Between 2 even altitude levels, winds and therefore also divergence are assumed to be independent of pressure, thus

$$w_m = w_{m-1} + \delta_{m-\frac{1}{2}}(z_m - z_{m-1}) \qquad (22)$$

with $w_{300} = 0$ in accordance with the kinematic boundary condition at $z = 300$.

VII. EDDY TRANSPORT

The atmosphere is in fact in turbulent motion. Any finite difference description of its state of motion cannot describe accurately those scales of motion that are small compared to the grid size. These scales are not capable of explicit description and thus must somehow be described implicitly or statistically. Since they are not, then error can result from the natural transfer of energy from the large scales of motion to the small scales of motion, which comes about through nonlinear interactions. As was pointed out by Phillips (1959), there can be aliasing error that in fact leads to assignment of energy increments to waves that have a large rather than a small scale and thus falsify the long waves for which the calculation pretends to be valid. One thing to be done about these small-scale eddies is to put in some sort of eddy diffusion terms that would diffuse away singularities by damping short-wave-length components, and serve then as smoothing terms. This method of Leith's (1965) has been used in design of this model. Leith found that a value for the horizontal eddy diffusion term coefficient of 10^{10} cm^2/sec leads to a stable calculation. This value is about 1/4 of the gross Austausch coefficient of Defant; i.e., should this value have been in the calculation 4 times greater than it was, presumably no interesting explicit eddies would have developed. The same horizontal eddy diffusion coefficient has been used to diffuse water vapor, temperature, and u and v components of the velocity.

Although the value of 10^{10} cm^2/sec for the horizontal eddy diffusion coefficient was found by experimentation with the Leith (1965) model itself, there is observational evidence that indicates that a value of about this magnitude is to be expected.

L. F. Richardson observed that the eddy diffusion coefficient appropriate for estimating dispersion of clusters in the atmosphere was a function of the size of the cluster. Thus, he formulated the empirical law

$$D = 0.2L^{4/3} \quad cm^2/sec \tag{23}$$

where L is in cm that hold over a range of L from 10^2 cm to 10^7 cm. For $L = 2 \times 10^8$ cm, we would accordingly have $D = 10^{10}$ cm^2/sec.

According to this empirical law, the largest scale disturbances in the atmosphere with wavelengths of the order of 500 km would have $D = 8 \times 10^{10}$ cm^2/sec, not much different than Defant's gross Austausch coefficient.

This 4/3 power law of Richardson (1926) has received some theoretical justification (Batchelor, 1950) from the Kolmogoroff similarity hypothesis for equilibrium turbulent motions.

The introduction of a horizontal eddy diffusion term in the finite difference equations is particularly simple. The quadratic advection scheme (Eq. 20) used has already introduced a second difference term with a dimensionless coefficient depending on the advection velocity. To this coefficient, one need add only another dimensionless term of the form

$$r = \frac{D\Delta t}{(\Delta x)^2} \tag{24}$$

to include the eddy diffusion with the quadratic advection calculation. Since D is constant, r is a precalculated field of values of the order of 0.002, depending only on latitude.

Also included are vertical eddy diffusion terms for most of these quantities. The vertical eddy diffusion coefficient has been chosen as 2.4×10^5 cm^2/sec at the surface of the earth, decreasing as one goes to higher levels. This value, determined more or less empirically by Leith, produced an upward transport of water vapor that

in turn produced proper rainfall and release of latent heat in the general circulation calculation made with his model. The u and v components of the wind are diffused vertically using the same eddy diffusion coefficient as for water vapor. However, entropy is not diffused according to the eddy diffusion coefficient prescription, for, if it were, the heat flow would be downward, whereas it is observed generally to be upward. This counter radiant flow of entropy is of course due to the correlation that exists between the vertical motion and excess temperature. To take this effect into account at least qualitatively, a convection prescription has been introduced, according to which the vertical flux of heat, always upward, is made a function of the stability of the atmosphere. This convection function decreases with increased stability for a stable layer, but is constant and equal to 340 cal/cm^2 day for an unstable layer. This prescription permits a return to stability in the model atmosphere without the necessity of the overturning of masses of air on a scale comparable to the mesh size.

Neither the vertical eddy diffusion nor the convection prescription permits eddy transport across the boundary defined by ($p = 0$, $Z = 300$ km), which is effectively insulating and frictionless. There are, however, fluxes of momentum, energy, and water vapor across the $p = p_s$ boundary. This boundary is at present taken as a sea level in the model, with surface temperature T_s and the associated saturation water vapor mixing ratio μ_s specified as a function of latitude and longitude. Certain arid land areas are specified by setting $\mu_s = 0$, but no mountains should be included.

Similar flux formulas are used at the surface. If we let

$$V_s = (u_s^2 + v_s^2)^{\frac{1}{2}} \tag{25}$$

be the magnitude of the surface wind, and let u_s and v_s be the components of diffusion velocity from the surface, we can write the flux as follows:

$$F_{xs} = -C_v V_s u_s$$
$$F_{ys} = -C_v V_s v_s \qquad (26)$$

where C_v is a constant drag coefficient. On the other hand, the vertical eddy diffusion of velocity gives fluxes between the surface and level 1/2 in the amount

$$F_x = k_v \frac{u_s - u_{1/2}}{p_s - p_{1/2}}$$
$$F_y = k_v \frac{v_s - v_{1/2}}{p_s - p_{1/2}} \quad . \qquad (27)$$

The surface velocity components u_s, v_s are determined to maintain a balance between the stresses in Eqs. 26 and 27. Thus, we find

$$u_s = Au_{1/2}$$
$$v_s = Av_{1/2} \qquad (28)$$

with

$$A = \frac{k_v}{k_v + c_v V_s (p_s - p_{1/2})}$$

Similarly, sensible heat flux from the surface is calculated according to a conduction formula

$$F_T = C_T V_s (T_s - T) \qquad (29)$$

where C_T is a conduction coefficient. Water vapor flux from the surface is calculated according to an evaporation formula

$$E = c_\mu V_s (\mu_s - \mu) \qquad (30)$$

where C_μ is an evaporation coefficient. These fluxes enter into the calculation of the changes in T and μ, respectively. The coefficients C_v, C_T, C_μ are determined somewhat empirically and are about 10^{-5} gm/cm^3.

VIII. RADIATION ENERGY BALANCE

The heating of each layer by incoming solar radiation depends on the zenith angle of the sun, the energy absorption along the slant path by atmospheric constituents in the layer, and the heat capacity of the layer.

The very important absorption, scattering, and reradiations of solar energy by clouds and dust is herein taken into account only parametrically, in terms of an effective and time-variable opacity, rather than explicitly. This parametrization is particularly sensitive to the effect of clouds in the troposphere and may be estimated on the basis of cloud pictures from geosynchronous satellites. Such an estimation method is not developed in the present section, in which the older method of Leith (which does not incorporate explicit cloud data) is described.

The solar declination δ is the latitude of the sun, a function of the day of the year. The hour angle λ_s is the longitude of the sun, a measure of the hour of the day. At a given latitude θ and longitude λ, the zenith angle ϕ is given by

$$\cos \phi = \cos \delta \cos \theta \cos(\lambda_s - \lambda) + \sin \delta \sin \theta \ . \qquad (31)$$

The sun is above the horizon if $\cos \phi > 0$, on the horizon if $\cos \phi = 0$, and below the horizon if $\cos \phi < 0$. The absorption of electromagnetic radiation energy in the band λ_1 to λ_2 along a slant path of zenith angle χ is

$$\left(\frac{dQ}{dt}\right)_{EM} = \sum_i J_i(z)\, n_i(z) \qquad (\text{ergs cm}^{-3}\ \text{sec}^{-1}) \qquad (32)$$

$$J_i(z) = \int_{\lambda_1}^{\lambda_2} \sigma_i(\lambda)\, I_o(\lambda)\, \exp\left[-F(X) \sum_j \sigma_j(\lambda)\, N_j(z)\right] d\lambda \qquad (33)$$

$$(\text{erg sec}^{-1}\ (\text{particle}))^{-1}$$

I_o = Solar electromagnetic flux outside the absorbing atmosphere at wave length λ.

$F(X)$ = Chapman function denoting the effective thickness factor of spherical shell atmosphere $\simeq \sec X$.

$\sigma_j(\lambda)$ = Chapman cross section, a function of wavelength, of the j^{th} atmospheric constituent.

$N_j(z) = \int_{300\ km}^{z} n_j(z)\, dz$ = integral number in column along vertical path of atmospheric constituent j.

The flux $\int_{\lambda}^{\lambda_2} I_o(\lambda)\, d\lambda$ is determined by SOLRAD HI Satellite (to be launched in 1973) for the bands listed in Table 2.

The deposition of the particulate energy of solar origin, as measured outside the magnetosphere from about 20 kev to 100 Mev is more difficult to determine as a function of latitude, longitude, altitude, and time than is that of the solar electromagnetic radiation.

The solar wind energy after the SOLRAD HI determination passes through the magnetosheath where it is thermalized by turbulence and is rendered isotropic (Gosling et al., JGR 72, 101-112, 1967). Within the magnetopause, the solar wind fills first the outer zone, with a spectral distribution $N(E) = k \exp(-E/E_o)$. The outer zone, in turn, empties into the inner zone, at about 10 R_E, presumably with further thermalizing and isotropizing due to collisions, and hardening due to magnetic pinch. The latter increases the population of outer zone $E > 40$ kev protons by a factor of about 10^5 (Anderson et al., JRG 70, 1039, 1965).

TABLE 2. PLANNED SOLAR ENERGY MEASUREMENTS BY SOLRAD XI SATELLITE, 1973

Electromagnetic Radiation	Particles	Band Coverage
0.5 - 3A	> 0.5 Mev	1350 - 1550A
1 - 5A	> 1.0 Mev	1225 - 1350
1 - 8A	> 2.0 Mev	1216
8 - 16A	> 5.0 Mev	1080 - 1225
1 - 20A	> 10.0 Mev	170 - 600
44 - 60A	> 20.0 Mev	44 - 60
170 - 600A	> 50.0 Mev	16 - 20
1080 - 1350A	> 100.0 Mev	8 - 16
1225 - 1350A	0.1 - 0.5A (20-150kev)	5 - 8
1350 - 1550A	0.1 - 1.5A (7-150kev)	1 - 5
		0.5 - 1
		0.1 - 0.5A

Electromagnetic ↓

Particles ↑
20 - 150 Kev
500 - 1 Mev
1 - 2 Mev
2 - 5 Mev
5 - 10 Mev
10 - 20 Mev
20 - 50 Mev
50 - 100 Mev

The consequent spectrum is then assumed to propagate along the lines of magnetic flux (along path s), to be absorbed according to the law of energy loss in an electronic plasma (Jackson, [13.88], p. 451, 1962), which may be rewritten as:

$$\frac{dE}{dj} \cong (4\pi NZe^2/m)\ \frac{(ze)^2}{v^2}\ \ell n\left(\frac{1.123v}{(kT/m)^{\frac{1}{2}}}\right) \qquad (34)$$

where the particles have a charge number z, a mass m, and a velocity v; while the plasma has a density N, a charge number Z, and a temperature T.

Cooling by radiative loss of heat, by emission from atomic oxygen, molecular oxygen, ozone, carbon dioxide, and water vapor, also affects the heat content of the atmosphere. A. C. Aiken and S. J. Bauer (1968) have found the auroral precipitation in geomagnetic latitudes 60-70° to be shown in Fig. 5.

Bates (1956) has described the radiative heat loss from atomic oxygen, by the reaction

$$O\left(^3P_1\right) \rightarrow O\left(^3P_2\right) + h\nu(\lambda = 63\mu) \tag{35}$$

to be

$$\rho q_{0\lambda} = n_o A_{12} E_1 \left[\frac{\bar{W}_1 \, e^{-E_1/kT}}{\bar{W}_2 + \bar{W}_1 \, e^{-E_1/kT} + \bar{W}_o \, e^{-E_o/kT}} \right] \tag{36}$$

$$= n_o \left[\frac{-1.68(10)^{-18} \, e^{-228/T}}{1 + 0.6 \, e^{-228/T} + 0.2 \, e^{-325.3/T}} \right]$$

$$\sim 6(10)^{-7} n_o \text{ for } 120 \text{ km} < z < 160 \text{ km}$$

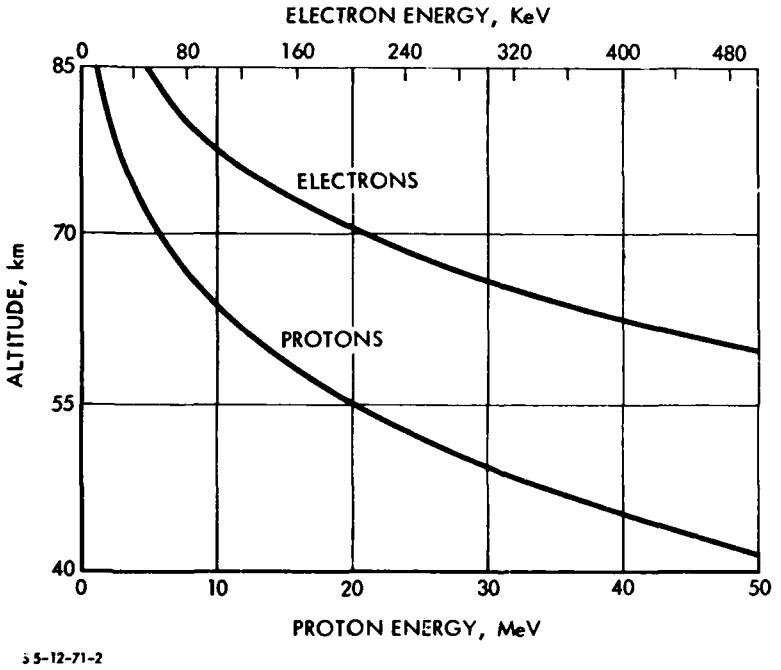

FIGURE 5. Atmospheric Penetration Depth of Energetic Particles (After A.C. Aikan and S.J. Bauer 1968)

wherein

n_o = number density of atomic oxygen

$$E_1 = h\left(\nu_{3_{P_2}} - \nu_{3_{P_1}}\right)$$

$$E_o = h\left(\nu_{3_{P_2}} - \nu_{3_{P_o}}\right)$$

$$\left.\begin{aligned} \bar{W}_o &= 1 \\ \bar{W}_1 &= 3 \\ \bar{W}_2 &= 5 \end{aligned}\right\} \quad \text{statistical weight}$$

A_{12} = Einstein coefficient for $O\left({}^3P_1\right) \rightarrow O\left({}^3P_2\right) = 8.9(10)^{-5}$.

Leith (1965) describes cooling by outgoing terrestrial radiation by specifying a cooling rate as a function of pressure alone, independent of latitude or atmospheric conditions, as shown in Table 3. He hopes eventually to replace the table by a calculation of terrestrial radiation balance. Meanwhile, the prescribed cooling rate interferes with a possible feedback control mechanism in the model.

TABLE 3. TERRESTRIAL RADIATION COOLING RATE

m	P_m	Cooling rate (deg/day)
1	100	0.21
2	200	1.31
3	400	2.49
4	600	1.74
5	850	0.65
6	1000	0.37

The treatment of the radiation and heat source problem, from the standpoint of the computer programming, is elaborated in Annex I, which also gives estimates of central processor times required for execution of the computation.

IX. CONTINUITY EQUATION

The consideration of the equation continuity for each of the important constituents of the atmosphere requires taking into account the mechanisms for production and loss.

$$\frac{dn_a}{dt} = \frac{\partial n_a}{\partial t} + \nabla \cdot (n_a \underline{u}_a) = P - L \quad . \tag{37}$$

The principal production and loss mechanism, with greatest time and space variability, is that due to ionization and dissociation resulting from the solar electromagnetic radiation, which depends on length and flux.

The dissociation energies and ionization potentials of atmospheric species of interest, as listed by Bortner and Kummler (1968), are given in Annex H. The method for estimating the effect of dissociation is illustrated for the production of atomic oxygen by radiation of the Schumann-Runge continuum

$$1300 < \lambda < 1750 \text{ A} \tag{38}$$

for example, is given as follows:

$$O_2 + h\nu \rightarrow O + O \; ; \; \lambda_D = 1751 \text{ A} \tag{39}$$

$$\left(\frac{dn(O)}{dt}\right)_{SR} = P(O) = 2J(O_2)\, n(O_2) \; .$$

The i^{th} constituent is dissociated according to

$$J_i(\lambda_i,\lambda_2) = \int_{\lambda 1}^{\lambda 2} \sigma_i(\lambda)\ I_o(\lambda)\ \exp\left[-F(X) \sum_j \sigma_{j_{d\lambda}}(\lambda)\ N(z)\right] \quad (40)$$

wherein

$$N_i(z) = \int_z^{\infty} n_i(z)\ dz \text{ for } i^{th} \text{ constituent}$$

$I_o(\lambda)$ = solar flux outside the atmosphere

$F(X)$ = Chapman function of solar zenith angle X

$\cos X = \cos \delta \cos \theta \cos \Delta\lambda + \sin \delta \sin \theta$

δ = solar

θ = latitude angle

$\Delta\lambda$ = hour angle of radiation vector with respect to longitude (GHA + λ).

Since the radiation which is more energetic than the Schumann-Runge continuum may also cause ionization, it will produce ion pairs at a rate proportional to the next-smaller-integer value of (J/IP).

Another important source of production and loss of chemical constituents is the chemical processes, defined by Bortner and Kummler (1968) in their Figs. 5-1 to 5-31, inclusive, which are also described in Annex H. Only the most important reactions and their effects are shown. The species are arranged in the following order:

a. Major neutral species: H_2O, CO_2, O_2

b. Minor neutral species: O, $O(^1D)$, $O_2(^1\Delta)$, $O_2(^1\Sigma)$, O_3, N, NO, NO_2, N_2O, H, H_2, OH, HO_2, H_2O_2

c. Positive ions: N_2^+, N^+, O^+, O_2^+, NO^+

d. Negatively charged species: e, O_2^-, O^-, O_3^-, CO_3^-, NO_2^-, NO_3^-

e. Metallic species: of form M, MO, MO_2, M^+ of metals, Na, Mg, and Cu.

For each of the reactions shown in Appendix H, a rate coefficient is given in centimeter-gram-sec (cgs) units, that is, in $cm^3\ sec^{-1}$ per particle for two body and in $cm^6\ sec^{-1}$ per $(particle)^2$ for three body reactions. Particle densities are in cm^{-3} and temperature in ^oK. M is used to represent a collision partner. All values for rate constants are given by the constants a, b, and c for a rate constant of the form $R = a\left(\frac{T}{300}\right)^b \exp(-c/T)$. The rate coefficients of Appendix H may have error factors of 2 to 10.

Bortner and Kummler (1968) list 33 atmospheric species, with approximately 8 reactions each, or 244 reactions. The reactions are to be accounted in each of 33 equations of the form of Eq. 6, in general, or, for example, following Fig. H-4, of that for n(O):

$$\frac{dn(o)}{dt} = 2\left(\frac{J(O_2)}{IP(O_2)}(\lambda<1750A)\right) n(O_2) + \left(\frac{J(O_3)}{IP(O_3)}(\lambda<3105A)\right) n(O_3)$$

$$+\left(\frac{J(NO_2)}{IP(NO_2)}(\lambda<3981A)\right) + 2R_i\, n(O_2^+)\, n(e) - R_j N(O) n(O_2) n(M) - R_k n(O^2) n(M) \tag{41}$$

$$- R_1 n(O) n(OH) - R_M n(O) n(HO_2) - R_n n(O) n(O_3)$$

where the J/IP expressions take the value of the next smaller integer. The 33 continuity equations are solved simultaneously at each grid location.

X. PRECIPITATION

Tentative new values of temperature, $\tilde{T}$, and water vapor mixing ratio, $\mu = n_w/\sum_i n_i$ are calculated by Leith (1965) ignoring the possibility of condensation and associated release of latent heat, but taking into account all other sources and sinks. This tentative thermodynamic state is then examined to see if it corresponds to a state of supersaturation. If not, these tentative values of T and μ are taken as the final values. Otherwise, condensation occurs leading to a decrease in μ and an increase in T to establish saturation.

Let $S(T) - p\mu_s(T)$ be the tabulated function proportional to vapor pressure defining saturation values μ_s of μ; then the adjustment calculation is based on the following two equations

$$S'(\tilde{T}) = \frac{S(T^{n+1}) - S(\tilde{T})}{T^{n+1} - \tilde{T}} \tag{42}$$

and

$$C_p(T^{n+1} - \tilde{T}) = L(\mu^{n+1} - \tilde{\mu}) \tag{43}$$

where

$$S(T^{n+1}) = p\mu_s(T^{n+1}) = p\mu^{n+1}$$

and L is the latent heat of vaporization.

We solve this pair of equations in the 2 unknown quantities T^{n+1}, μ^{n+1} by eliminating $T^{n+1} - \tilde{T}$; we have

$$-S'(\tilde{T})\frac{L}{C_p}(\mu^{n+1} - \tilde{\mu}) = p\mu^{n+1} - S(\tilde{T}) \tag{44}$$

giving

$$\mu^{n+1} \leq \frac{S(\tilde{T}) + (L/C_p)S'(\tilde{T})\tilde{\mu}}{p + (L/C_p)S'(\tilde{T})} \tag{45}$$

$$T^{n+1} = \tilde{T} + \frac{L}{C_p}(\tilde{\mu} - \mu^{n+1}) \quad . \tag{46}$$

Here $L/C_p = 2483$ deg.

XI. HYDROSTATIC PRESSURE

The hydrostatic integration can be carried out after a new value of surface pressure is obtained.

The downward integration of the horizontal divergence to determine ω terminates at the surface pressure p_s with a surface value ω_s.

From the kinematic surface boundary condition as given by Eq. 9, we have the surface pressure evolution equation

$$\frac{\partial p_s}{\partial t} = \omega_s - u_s \frac{1}{a \cos\theta}\left(\frac{\partial p_s}{\partial \lambda}\right)_s - v_s \frac{1}{a}\left(\frac{\partial p_s}{\partial \theta}\right)_s \quad . \tag{47}$$

The advection involves surface wind components. It is evaluated as all other terms by quadratic interpolation in separate sweeps for north-south and east-west contribution. The pressure at altitude Z may now be determined by integrating

$$p(Z) = p_s - g \int_{Z_s}^{Z} \left(\sum_a m_a n_a\right) dZ \quad . \tag{48}$$

XII. CALCULATION OF ACCELERATION

The acceleration term coming from the gradient of pressure is approximated as follows:

$$\left(\frac{\partial p}{\partial x}\right) v = \frac{P_v + P_Q - P_{v-1} - P_{Q-1}}{2\Delta x}$$

$$\left(\frac{\partial p}{\partial y}\right) v = \frac{P_v - P_{v-1} + P_Q - P_{Q-1}}{2\Delta y} \quad . \tag{49}$$

The centering of these estimates can be seen in Fig. 6.

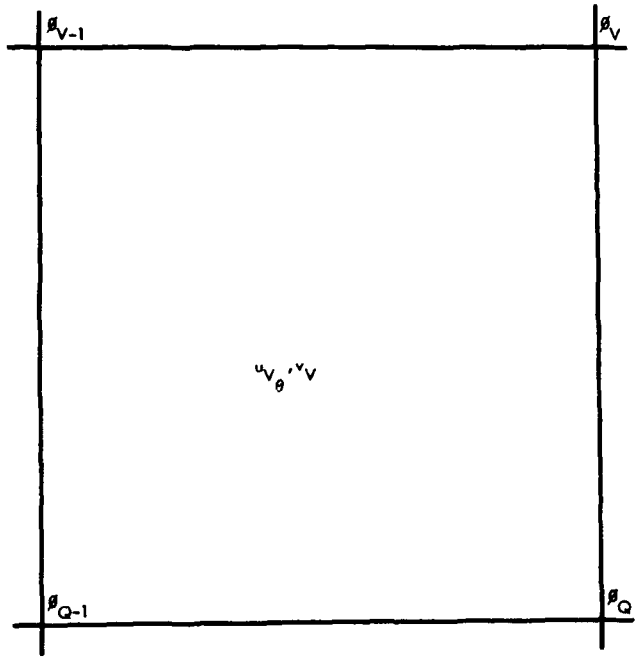

FIGURE 6 Calculation of Acceleration

The Coriolis terms are evaluated at the new time; thus, if

$$F = \left[2\Omega \sin \theta + \frac{u^{n+1/2} \tan \theta}{a}\right] \Delta t \tag{50}$$

the acceleration equations become

$$\begin{aligned} u_v^{n+3/2} - u_v^{n+1/2} &= \Delta_a u_v^{n+1/2} + F u_v^{n+3/2} - \left(\frac{\partial p}{\partial x}\right)_v \Delta t \\ u_v^{n+3/2} - u_v^{n+1/2} &= \Delta_a u_v^{n+1/2} - F u_v^{n+3/2} - \left(\frac{\partial p}{\partial y}\right)_v \Delta t \end{aligned} \tag{51}$$

where Δ_a indicates the change due to advection and diffusion. If now

$$\begin{aligned} G &= u_v^{n+3/2} + \Delta_a u_v^{n+1/2} - \left(\frac{\partial p}{\partial x}\right)_v \Delta t \\ H &= u_v^{n+3/2} + \Delta_a u_v^{n+1/2} - \left(\frac{\partial p}{\partial y}\right)_v \Delta t \end{aligned} \tag{52}$$

we have finally

$$\begin{aligned} u_v^{n+3/2} &= \frac{G + FH}{1 + F^2} \\ u_v^{n+3/2} &= \frac{H - FG}{1 + F^2} \end{aligned} \tag{53}$$

XIII. GENERAL PLAN OF CALCULATION

The way in which the various influences described are assembled into a single complex model, follows the method of fractional time steps used by Marchuk (1964) and described in the discussion of advection.

The prognostic variables are assumed to be known at a given time; the calculational cycle for 1 time step advances these variables to new values for a time 10 min later. It is assumed at the beginning of the calculational time step that the u, v, components are known at the odd time 1/2 time interval or 5 min later than the time at which the variables n_a, T, p_s are known.

The calculation for a complete time step is broken down into separate cycles. The first of these computes by Eq. 20a new values of all dependent variables based solely on advection in the north-south direction. Using these results, the next cycle computes by Eq. 20b new values based solely on advection in the east-west direction. The coefficients for the advection calculations for the even mesh variables n_a and T are obtained by averaging the 8 surrounding values of velocities defined on the odd mesh. All the rest of the contributions to change in the values of the dependent variables are computed in a final cycle.

In this final cycle, one starts at the top of the atmosphere and evaluates by Eq. 21 successively working downward the horizontal divergence δ of the wind at odd altitude levels but at even horizontal mesh points. The negative of this divergence, $-\delta$, is integrated downward from the top to give by Eq. 22 the vertical "velocity" w on the basis of the continuity equation describing conservation of mass. In this way the diagnostic variable w is defined at even mesh points.

A tentative new value of T is obtained by satisfying the finite difference approximation to the law of conservation of energy Eq. 16 taking into account the vertical advection terms as well as any possible energy sources or sinks but excluding temporarily the source coming from the release of latent heat associated with possible condensation. Similarily a tentative new value of μ is obtained by taking into account vertical advection of constituents in satisfying the finite difference approximation to the law of conservation of numbers (Eqs. 6, 37) taking into account any sources and sinks but ignoring for the moment the possible loss of water vapor by condensation and precipitation. Should the resulting tentative new values of $\mu = {}^{n}(H_2O)/\sum_{a} n_a$ and T represent an atmospheric state in a condition of supersaturation, then using Eqs. 45 and 46 the appropriate amount of water vapor is removed and the corresponding amount of energy is introduced to return the atmosphere to exact saturation. The resulting values of μ and T are taken as final for that time step. In the other case, that is of subsaturation conditions after the tentative μ, T, calculation, then the tentative results are taken as final. This calculatical process, which results in the new values of μ and T proceeds from layer to layer down through the atmosphere to the bottom.

At the bottom by carrying the integration of $-\mathfrak{D}$ to the limit p_s the value of w_s appropriate to the surface is obtained. This together with an extrapolated value of the wind fields to give an estimate of the surface wind components u_s, v_s permits an evaluation of the new surface pressure through the pressure tendency Eq. 47.

Knowing the new value of surface pressure and knowing from surface topography the geopotential ϕ_s to which it relates, it is possible to integrate the hydrostatic Eq. 47 upward now making use of the newly acquired values of water vapor and temperature to find new values of the pressure at the odd altitude levels. These new values of pressure are known 1/2-time step later than the u,v, components on the same altitude levels but at the surrounding even horizontal mesh points. This permits their gradients to be appropriately

centered for purposes of evaluating the acceleration term in the momentum Eq. 51. For evaluating the vertical advection terms in the momentum equation, it is necessary to average surrounding values to find a w appropriate to the odd mesh point at which u, v, components are defined. In the u momentum equation, the v entering into the Coriolis term is taken at the new time; and for the v equation the Coriolis term value of u is taken at the new time. This represents an evaluation of the Coriolis terms 1/2-time step too late and is done as a practical matter to provide a small amount of damping of inertial oscillations in the model. This calculational process of evaluating new values of p by integration of the hydrostatic Eq. 48 and evaluation of new values u and v by time integration of the momentum Eq. 51 proceeds upward through the atmosphere. Finally, when the top of the atmosphere is reached, again 1 time step has been completed in the calculation; and new u, v, Na, T, and p_s values have been determined.

ANNEX A

BASIC CONSERVATION EQUATIONS

MOMENTUM (I, II, III)

$$m_a n_a\left(\frac{\partial \underline{u}_a}{\partial t} + \underline{u}_a \cdot \nabla \underline{u}_a\right) = \underline{F}_a - k(T_a \nabla n_a + n_o \nabla T_a) + n_a e_a(\underline{E}_o + \underline{E}_s + \underline{u}_a \times \frac{\underline{B}}{C}) -$$

$$- m_a n_a \sum_b \nu_{a_b}(\underline{u}_a - \underline{u}_b) + \nu_a(\nabla^2 \underline{u}_a + \frac{1}{3}\nabla \cdot \underline{u}_a) + m_a n_a \underline{g} + m_a n_a \underline{u}_a \times \underline{\Omega}$$

(1) (2) (3) (4) (5) (6) (7) (8) (9)

(1)	(2)	(3)+(4)	(5)	(6)	(7)	(8)	(9)
Inertia	Ext. Forces	Pressure Gradient	E M Force	Collision Force	Viscous Damping	Gravity	Coriolis Force

NUMBER DENSITY (IV)

$$\frac{\partial n_a}{\partial t} + \nabla \cdot (n_a \underline{u}_a) = [P - L]$$

(1) (2) (3) (4)

(1)	(2)	(3)	(4)
Time Evaluation	Advection by Flux	Production (i.e., Dissociation)	Loss (i.e., Recombination)

ENERGY (V)

$$\dot{e} + p\dot{s} = S\delta + \dot{\omega}$$

rate of increase of internal energy; rate of increase of compression energy; rate of increase by Rayleigh dissipation; rate of increase from radiative and conductive heat sources

$$m_a n_a C_v\left(\frac{\partial T_a}{\partial t} + \underline{u}_a \cdot \nabla T_a\right) = \nabla \cdot (\lambda_a \nabla T_a) + \frac{1}{2}\sigma_{ik}\left(\frac{\partial u_i}{\partial x_k} + \frac{\partial u_k}{\partial x_i}\right) + \sum\left(\frac{dQ_a}{dt}\right)$$

(1) (2) (3) (4) (5) (6)

(1)	(2)	(3)	(4)	(5)	(6)
Temporal Change	Advection	Compression	Rate of heat increase by conductivity	Rate of heat increase by Raleigh dissipation	Rate of heat input from heat sources and radiation

EQUATION OF STATE (VI)

$$p = nkT$$

ANNEX B

DOMAINS & APPLICABILITY OF TERMS OF CONSERVATION EQUATIONS

Domain	Approx. Altitude (km)	Boundary Condition	Term Applicability		
Troposphere	0-20	Surface Temp. Minimum	I-1 2 3 4 \ \ 7 8 9	IV-1 2 \ \	V-1 2 3 4 \ 6
Stratosphere	20-50	Temp. Maximum	I-1 2 3 4 \ 6 7 8 9	IV-1 2 3 4	V-1 2 3 4 5 6
Mesosphere	50-90	Temp. Minimum	I-1 2 3 4 \ 6 7 8 9	IV-1 2 3 4	V-1 2 3 4 5 6
Lower Thermosphere	90-150	Collision Freq = Gyro Freq	I-1 2 3 4 5 6 7 8 9	IV-1 2 3 4	V-1 2 3 4 5 6
Upper Thermosphere	150-300	F_2 Ionization Max	I-1 2 3 4 5 6 7 8 9	IV-1 2 3 4	V-1 2 3 4 5 6

I-1 Inertia
2 External Force
3 Forces (times) (∇m_a)
4 Pressure Gradient (∇T_a)
5 E M force
6 Collision force
7 Viscous Damping
8 Gravity
9 Coriolis Force

IV-1 Time Deriv. in Density
2 Advection in Density
3 Production
4 Loss

V-1 Time Deriv. in Int. En.
2 Advection in Int. En.
3 Compression
4 En. by conductivity
5 En. by Raleigh dissipation
6 Heat imput by radiation

ANNEX C
CONSERVATION EQUATIONS IN SPHERICAL COORDINATES

The following description of the conservation equations, in the form of the spherical coordinate system employed for the S-M-T Model, is adapted from that of Godske et al. (1957), for the mixture of all constituents as one fluid.

THE EULERIAN EQUATIONS OF MOTION AND CONTINUITY

In spherical coordinates (r, λ, φ) as given in Fig. C-1, suppose the vector of rotation Ω to be situated in the meridian plane $\lambda = 0$, and to form an angle φ_o with the equatorial plane $\varphi = 0$. Then, the components of Ω are,

$$\begin{aligned} \Omega_r &= \Omega \cdot i_r = \Omega_x \cos\varphi \cos\lambda + \Omega_y \cos\varphi \sin\lambda + \Omega_s \sin\varphi \\ &= \Omega(\sin\varphi_o \sin\varphi + \cos\varphi_o \cos\varphi \cos\lambda) \ , \\ \Omega_\lambda &= \Omega \cdot i_\lambda = -\Omega \cos\varphi \sin\lambda \ , \\ \Omega_\varphi &= \Omega \cdot i_\varphi = \Omega(\sin\varphi_o \cos\varphi - \cos\varphi_o \sin\varphi \cos\lambda) \ . \end{aligned} \tag{C-1}$$

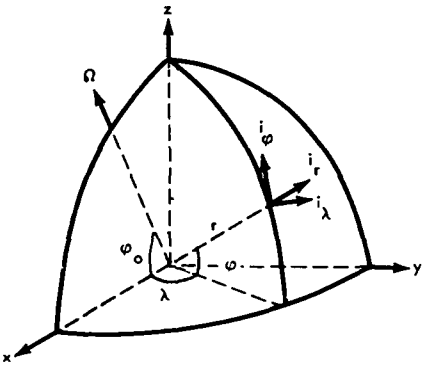

55-12-71-7

FIGURE C-1. The Position of the Rotation Vector Ω in the System Spherical Coordinates

We introduce the abbreviations

$$\left(\frac{d}{dt}\right)_s = \frac{\partial}{\partial t} + v_r \frac{\partial}{\partial r} + \frac{v_\lambda}{r \cos \varphi} \frac{\partial}{\partial \lambda} + \frac{v_\varphi}{r} \frac{\partial}{\partial \varphi} \tag{C-2}$$

$$\nabla \phi \equiv \frac{\partial}{\partial r} \phi i_r + \frac{1}{r \cos \varphi} \frac{\partial}{\partial \lambda} \phi i_\lambda + \frac{1}{r} \frac{\partial}{\partial \varphi} \phi i_\varphi \tag{C-3}$$

$$\nabla . \underline{v} = \frac{1}{r^2} \frac{\partial}{\partial r} (r^2 v_r) + \frac{1}{r \cos \varphi} \frac{\partial v_\lambda}{\partial \lambda} + \frac{1}{r \cos \varphi} \frac{\partial (v_\lambda \cos \varphi)}{\partial \varphi} \tag{C-4}$$

$$\nabla x \underline{v} = \frac{i_r}{r \cos \varphi} \left[\frac{\partial v_\varphi}{\partial \lambda} - \frac{\partial}{\partial \lambda} (\cos \varphi \, v_\lambda) \right] + \frac{i_r}{r} \left[\frac{\partial v_r}{\partial \varphi} - \frac{\partial}{\partial r} (r v_\varphi) \right]$$

$$+ \frac{i_\varphi}{r \cos \varphi} \left[\frac{\partial}{\partial r} (r \cos \varphi \, v_\lambda) - \frac{\partial v_r}{\partial \lambda} \right] \tag{C-5}$$

$$\nabla^2 \phi = \nabla . \nabla \phi = \frac{1}{r^2 \cos \varphi} \left[\frac{\partial}{\partial r} \left(r \cos \varphi \frac{\partial \phi}{\partial r} \right) + \frac{\partial}{\partial \lambda} \left(\frac{1}{\cos \varphi} \frac{\partial \phi}{\partial \lambda} \right) \right.$$

$$\left. + \frac{\partial}{\partial \phi} \left(\cos \varphi \frac{\partial \phi}{\partial r} \right) \right] \tag{C-6}$$

and the nomenclature

Ω = vector of earth's rotation
$\underline{v}$ = velocity
ϕ = geopotential (gz)
s = specific volume
S = force of friction
p = pressure
ρ = density
θ = temperature
δ = dissipation
e = internal energy per unit mass
w = heat per unit mass from sources
$\underline{F}$ = lunar tide force

$$= \rho\nabla\cdot\left[\frac{3}{4}\frac{K_g M_m}{D_m^3} r^2\left\{3 - \cos^2\lambda_m + \sin^2\lambda_n \cos^2\varphi\right\}\right]$$

$\underline{F}_{em}$ = electromagnetic force (C-8)

$\underline{F}_{coll}$ = collision force = $\sum_b \nu_{ab}(\underline{v}_a - \underline{v}_b)$ (C-9)

P-L = rates of production minus loss of number density

we find for the equation of motion

$$\left.\begin{aligned}
&i_r\left[\left(\frac{dv_r}{dt}\right)_s - \frac{v_\varphi^2}{r} - \frac{v_\lambda^2}{r} + \frac{\partial\phi}{\partial r} + s\frac{\partial p}{\partial r} - 2\Omega\cos\varphi_o\sin\lambda\, v_\varphi\right.\\
&\qquad\left. - 2\Omega(\cos\varphi\sin\lambda - \sin\varphi\cos\varphi_o\cos\lambda)v_\lambda - S_r\right]\\
&+ i_\lambda\left[\left(\frac{dv_\lambda}{dt}\right)_s - \frac{v_\lambda v_\varphi}{r}\tan\varphi + \frac{v_r v_\lambda}{r} + \frac{1}{r\cos\varphi}\frac{\partial\phi}{\partial\lambda} + \frac{s}{r\cos\varphi}\frac{\partial p}{\partial\lambda}\right.\\
&\qquad + 2\Omega(\sin\varphi_o\cos\varphi - \cos\varphi_o\sin\varphi\cos\lambda)r_v\\
&\qquad\left. - 2\Omega(\sin\varphi_o\sin\varphi + \cos\varphi_o\cos\varphi\cos\lambda)v_\varphi - S_\lambda\right]\\
&+ i_\varphi\left[\left(\frac{dv_\varphi}{dt}\right)_s + \frac{v_\varphi v_r}{r} + \frac{v_\lambda^2}{r}\tan\varphi + \frac{1}{r}\frac{\partial\phi}{\partial\varphi} + 2\Omega\cos\varphi_o\sin\lambda\, v_r\right.\\
&\qquad\left. + 2\Omega(\sin\varphi_o\sin\varphi + \cos\varphi_o\cos\varphi\cos\lambda)v_\lambda - S_\varphi\right]\\
&= \underline{F} + \underline{F}_{em} + \underline{F}_{coll}
\end{aligned}\right\} \text{C-10)}$$

Similarly, the equation of continuity can be written in the form

$$s^{-2}\frac{\partial s}{\partial t} - \frac{1}{r^2}\frac{\partial}{\partial r}(s^{-1}r^2 v_r) - \frac{1}{r\cos\varphi}\frac{\partial s^{-1}v_\lambda}{\partial \lambda} - \frac{1}{r\cos\varphi}\frac{\partial}{\partial \varphi}(\cos\varphi s^{-1}v_\varphi) = P - L \qquad \text{(C-11)}$$

or

$$\frac{\partial \rho}{\partial t} + \frac{1}{r^2}\frac{\partial}{\partial r}(\rho r^2 v_r) + \frac{1}{r\cos\varphi}\frac{\partial}{\partial \lambda}(\rho v_\lambda) + \frac{1}{r\cos\varphi}\frac{\partial}{\partial \varphi}(\rho\cos\varphi\, v_\varphi) = P-L \qquad \text{(C-12)}$$

The equation of motion is essentially simplified if Ω vanishes, or is directed along the axis of the system of coordinates, so that $\varphi_o = \pi/2$.

THE BOUNDARY CONDITIONS

The equations of motion and continuity apply directly only to the interior of a fluid. At external boundaries, or at internal surfaces of discontinuity, the solutions of those equations have to satisfy certain boundary conditions. We shall here consider only the frictionless case.

Let

$$f(x, y, z, t) = 0 \qquad \text{(C-13)}$$

denote the equation of a surface of discontinuity, generally moving in space, but at rest if t does not appear.

The kinematic boundary conditions,

$$\frac{\partial f}{\partial t} + \underline{v}\cdot\nabla f = 0\,, \qquad \frac{\partial f}{\partial t} + \underline{v}'\cdot\nabla f = 0\,, \qquad \text{(C-14)}$$

express the fact that the particles of velocities $\underline{v}$ and $\underline{v}'$ on both sides near the surface of discontinuity will follow this surface during its motion.

Formula C-14 can also be written

$$v \cdot \nabla f = v' \cdot \nabla f = - \frac{\partial f}{\partial t} \quad , \qquad \text{(C-15)}$$

an equation that states that the velocity satisfies the solenoidal boundary condition expressing the continuity of the normal velocity; in a sense it is the form taken by the equation of continuity near a surface of discontinuity.

The dynamic boundary condition,

$$p(x, y, z, t) = p'(x, y, z, t) \quad , \qquad \text{(C-16)}$$

expresses the continuity of the pressure at the surface of discontinuity, and may thus be said to represent the equation of motion at such a surface.

In many applications the mixed boundary conditions

$$\frac{\partial(p - p')}{\partial t} + v \cdot \nabla(p - p') = 0, \qquad \frac{\partial(p - p')}{\partial t} + v' \cdot \nabla(p - p') = 0 \qquad \text{(C-17)}$$

found by combining the kinematic and dynamic conditions are especially useful.

The conditions at a free surface where the pressure vanishes are obtained by simply annulling all primed letters in the above expressions. The condition at a rigid surface is represented by the first of equations C-14 stating that the normal velocity of the fluid is equal to the known normal velocity of the boundary.

The above boundary conditions can easily be written explicitly in a component form in any system of orthogonal coordinates.

THE EQUATIONS OF STATE AND ENERGY

It can be shown by physical experiments that the variables of state--pressure, temperature, and density--are mutually related by the so-called equation of state. This equation can be shown to be independent of the motion (see, for instance, O. Björgum, 1944, pp. 26-27). The equation of state may be fairly easily expressed

in Langrangian coordinates that refer directly to the moving particles. If, however, the Eulerian coordinates (x, y, z) are used, the problem of expressing the equation of state by means of these coordinates arises. The solution of this problem is generally very difficult, but becomes simple for an atmosphere whose particles do not change their composition.

Combining the equation of state with the equations of motion and continuity, we arrive at a system of 5 scalar equations. In general this system is incomplete, for there are 6 dependent variables. It is therefore necessary in the general case to introduce the energy equation as a sixth relation.

EULERIAN FORM OF THE SIMPLIFIED EQUATION OF STATE

In the Eulerian system of coordinates, the values A, B, ... of the coordinates of numeration are unknown until all integrations have been carried through. The Lagrangian form $\chi P - \rho R\theta = 0$ of the equation of state is therefore impractical. An equation of state adapted to the Eulerian method is found through elimination of the quantities A, B, ... This elimination is effected by means of the Lagrangian equation and those obtained from it by individual differentiations, namely,

$$\dot{\chi} = \frac{\partial \chi}{\partial t} + \underline{v} \cdot \nabla \chi, \quad \ddot{\chi} = \left(\frac{\partial}{\partial t} + \underline{v} \cdot \nabla \right)^2 \chi \ , \ldots \qquad \text{(C-18)}$$

In the general case where the parameters A, B, ... are variable with time, new unknown variables $\dot{A}$, $\dot{B}$, ..., $\ddot{A}$, $\ddot{B}$, ... are thereby introduced, and it is necessary to add more equations, namely those which characterize the individual variation of A, B, ..., e.g., the variation of water vapor. When, however, A, B, ... are assumed to be individually constant, $\dot{A}$, $\dot{B}$, ..., $\ddot{A}$, $\ddot{B}$, ... all vanish. Then A, B, ... can be directly eliminated and a Eulerian equation of state can be obtained having the following form:

$$\chi(p, s, \theta, \dot{p}, \dot{s}, \dot{\theta}, \ddot{p}, \ldots) = 0 \qquad \text{(C-19)}$$

The equation of state is thus much more complicated in Eulerian than in Lagrangian coordinates. Although the Eulerian system is preferable to the Lagrangian from purely dynamical and kinematical points of view, the Lagrangian method must be considered the simpler from a thermodynamical viewpoint; the Eulerian is the more practical method for discussion of problems which are mainly dynamic, e.g., complicated motions of simple fluids, the Lagrangian for the study of problems which are mainly thermodynamic, e.g., simple motions of media having complex thermodynamic properties. If the amount of water vapor is assumed to be constant in time, and no fluid or solid water is supposed to be present, the equation of state for the air can be written

$$ps = R\theta \quad . \tag{C-20}$$

When the air is dry, or of constant composition, the individually constant R is the same for all particles, i.e., constant in time and space. In this case C-20 can be used directly in the Eulerian system. When the parameter R varies from one particle (a, b, c) to another, or from one geometric point (x, y, z) to another, R is easily eliminated by an individual logarithmic differentiation of Equation C-20. Hence,

$$\frac{\dot{p}}{p} + \frac{\dot{s}}{s} = \frac{\dot{\theta}}{\theta} \tag{C-21}$$

represents a more general form of the atmospheric equation of state.

THE ENERGY EQUATIONS

According to the first principle of thermodynamics, the change in the total energy of any fluid particle is equal to the work done upon it by all forces, external as well as internal, plus the energy added to it in the form of heat. In meteorology we neglect for the most part the forms of energy due to electric and magnetic forces, and consider only the two dynamically and thermodynamically most important types, namely the kinetic and the internal energies. The

kinetic energy, equal to $1/2v^2$ per unit mass, is a measure of the intensity of the macroscopic motions of the air particles. The internal energy, denoted by e, is an expression of the intensity of the molecular motions; in an ideal gas, this energy is simply proportional to the temperature. The heat added to the mass unit, by processes of radiation, condensation, etc., is denoted by δw; it will be considered a well-defined function of time and space, and its value per unit time will be denoted by $\dot{w} = Dw/Dt$. The principle of energy can thus be written:

$$\frac{D}{Dt}\left(e + \frac{1}{2}\underline{v}^2\right) = -\underline{v}\cdot\nabla\phi - s\underline{v}\cdot\nabla p - p\dot{s} + s\underline{v}\cdot\underline{S} + s\delta + \dot{w} \quad . \qquad (C\text{-}22)$$

This equation will be called the complete energy equation or the dynamical-thermodynamical energy equation, since it contains quantities of dynamical as well as thermodynamical nature.

A special dynamical equation of energy, independent of all transformations of heat into energy, can be derived from the equation of motion through a scalar multiplication by $\underline{v}$,

$$\frac{D}{Dt}\left(\frac{1}{2}\underline{v}^2\right) = -\underline{v}\cdot\nabla\phi - s\underline{v}\cdot\nabla p + s\underline{v}\cdot\underline{S} \quad . \qquad (C\text{-}23)$$

This equation simply establishes an equality between changes in kinetic energy and the external work done by gravity, pressure, and friction, and contains neither the internal work of pressure and friction, nor the internal energy, nor the added heat. If, in particular, the geopotential ϕ at a fixed geometric point is independent of time, we find

$$\frac{D}{Dt}\left(\frac{1}{2}\underline{v}^2 + \varphi\right) = s\underline{v}\cdot(-\nabla p + S) \quad . \qquad (C\text{-}24)$$

In this form the dynamical energy equation states that the sum of kinetic and potential energies is changed only by the external work done by the forces of pressure and friction.

Subtracting Equation C-23 from C-22 now gives the thermodynamical equation of energy,

$$\dot{w} + s\delta = \dot{e} + p\dot{s} \qquad \text{(C-25)}$$

or if $e = c_v\theta$ and the potential temperature $\vartheta = \left(\frac{p_o}{p}\right)^k \theta$ are introduced

$$\dot{w} + s\delta = c_p \frac{\theta}{\vartheta} \dot{\vartheta} \quad . \qquad \text{(C-26)}$$

This equation connects the heat supply with the internal work of pressure and friction and with changes in the internal energy, but contains neither the kinetic energy nor the external work.

Equations C-22, C-23, and C-24 which establish relations between different forms of energy, do not say that one definite form of energy is transformed into another definite form. The relations in no way enable us to follow the transformation of some well-defined "amount" of energy. Such transformations are different in different motions, and a complete determination for a given motion can be carried through only by a complete knowledge of the dynamics of the motion.

If the energy of the suspended water and ice is negelected, the internal energy of moist air is equal to $c_v\theta$. Since the quantity c_v varies only slightly from one particle to another, we can in practice consider it constant and equal to the specific heat c_{vd} at constant volume of dry air.

The heat $\dot{w}$ given to or taken from the air particles is due to process of evaporation, condensation, and radiation, and also to eddy conductivity if we consider smoothed motions. If we assume the composition of a particle to remain constant, there will be no heat exchange associated with evaporation and condensation. There still remains, however, the radiative heat which is always a rather complex quantity, depending, among other things, on the absorptive power of the air, i.e., on the amounts of atmospheric water in different phases. It seems possible to discuss the large-scale atmospheric motions by means of the several equations governing this type of motion. These equations form a complete system for the variables, including the three velocity components v_x, v_y, v_z, the pressure p,

the density ρ (or the specific volume s), and the temperature θ. solution of this system will contain a certain number of arbitrary functions and constants. Some of them can be determined by the boundary conditions, whereas others are given by the initial conditions,

$$\left.\begin{aligned} v(x, y, z, t_o) &= v_o(x, y, z) , \\ p(x, y, z, t_o) &= p_o(x, y, z) , \\ s(x, y, z, t_o) &= s_o(x, y, z) , \\ \theta(x, y, z, t_o) &= \theta_o(x, y, z) . \end{aligned}\right\} \qquad \text{(C-2}$$

Here t_o is a certain initial time, and v_o, p_o, s_o, and θ_o are given functions, to be determined empirically by observations.

ANNEX D

CONSERVATION EQUATIONS IN PERTURBATION FORM

The solution of the nonlinear hydrodynamical equations is extremely difficult. In most cases it is therefore necessary to substitute for the exact system of equations other approximate systems. The method of perturbation, introduced systematically in hydrodynamics by V. Bjerknes (1927), enables us to discuss, by means of linear differential equations, all motions that lie in the vicinity of any known so-called fundamental motion. The difference between the fundamental motion and the motion differing only slightly from the fundamental motion is termed the motion of perturbation. The latter motion, if sufficiently small, satisfies a particularly simple system of equations. It may be that treatment by the method of perturbation is the best way as a starting point of dealing with the nonlinearity of advection in the Eulerian system. The following treatment of the method of perturbation as applied to advection of meteorologic phenomena is that given by Godske et al. (1957), who omitted description of external forces ($\underline{F}_a$, $\underline{F}_{em}$, $\underline{F}_{coll}$), production and loss mechanisms, and heating terms. Inclusion of those may, however, be treated.

FUNDAMENTAL MOTION AND PERTURBATION

Let the velocity, specific volume, pressure, and temperature characterizing such a fundamental motion be represented, in the Eulerian system of coordinates, by the quantities

$$\underline{V} = iV_x + jV_y + kV_z, S, P, \theta \qquad \text{(D-1)}$$

supposed to be known functions of the independent variables. The velocity, specific volume, pressure, and temperature characterizing a motion that differs only slightly from the fundamental one can be represented by the quantities

$$\underline{V} + \underline{v} = i(V_x + v_x) + \underline{j}(V_y + v_y) + \underline{k}(V_z + v_z) ,$$

$$S + s, P + p, \Theta + \theta . \qquad \text{(D-2)}$$

Here the small letters

$$\underline{v} = \underline{i}v_x + \underline{j}v_y + \underline{k}v_z, s, p, \theta \qquad \text{(D-3)}$$

characterize the small, unknown "motion of perturbation"; when added to the fundamental motion (Eq. D-1), they are determined by the above-discussed hydrodynamical equations. If the perturbation is small, squares and products of the quantities D-3 are supposed to be negligible, so that a "linear system of equations of perturbation" can be derived. If the quantities D-3 represent a solution of this system approximate solutions of the hydrodynamical equations are thus obtained by adding D-1 and D-3. The accuracy of the approximation improves as the intensity of the motion of perturbation decreases.

THE GENERAL EQUATIONS OF PERTURBATION

Let us now consider the equations of perturbation for a frictionless fluid. The resultant motion must satisfy the Eulerian equations of motion, continuity, state and thermodynamical energy. So that

$$\frac{\partial(\underline{V} + \underline{v})}{\partial t} + (\underline{V} + \underline{v})\cdot\nabla(\underline{V} + \underline{v}) + 2\underline{\Omega} \times (\underline{V} + \underline{v}) + (S + s)\nabla(P + p)$$

$$+ \nabla(\Phi + \phi_t) = 0 \qquad \text{(D-4)}$$

$$\frac{1}{S + s}\left[\frac{\partial}{\partial t}(S + s) + (\underline{V} + \underline{v})\cdot\nabla(S + s)\right] - \nabla\cdot(\underline{V} + \underline{v}) = 0 \qquad \text{(D-5)}$$

$$\chi(S + s,\ P + p,\ \Theta + \theta,\ \hat{S} + \hat{s},\ \ldots) = 0 \qquad \text{(D-6)}$$

$$\dot{W} + \dot{w} = \hat{E} + \hat{e} + (P + p)(\hat{S} + \hat{s}) \qquad \text{(D-7)}$$

where the perturbation in Φ (produced, for instance, by tidal forces) is denoted by ϕ_t so as to avoid confusion with the latitude.

When the perturbation is produced by some impulse changing neither the external forces nor the heat supply to a physical particle, the quantities $\nabla\phi_t$ and $\dot{w}$ vanish; such a perturbation will be called "free." If the perturbation is caused by a small additional force whereas the heat supply to the particles remains unchanged, we have $\nabla\phi_t \neq 0$, $\dot{w} = 0$. Finally, if the perturbation is produced by a small additional heat supply (e.g., a daily variation of insolation), we have $\dot{w} \neq 0$, $\nabla\phi_t = 0$.

Equations D-4 to D-7 inclusive must be supplemented by boundary conditions. Since the surface of discontinuity, assumed to consist always of the same particles, is generally also disturbed, its equation in the motion D-2 can be written

$$F(x, y, z, t) + f(x, y, z, t) = 0 \qquad \text{(D-8)}$$

where f characterizes the perturbation in the position of the surface. At this surface the kinematic boundary conditions

$$\frac{\partial(F + f)}{\partial t} + (\underline{V} + \underline{v})\cdot\nabla(F + f) = 0,$$

$$\frac{\partial(F + f)}{\partial t} + (\underline{V}' + \underline{v}')\cdot\nabla(F + f) = 0 \qquad \text{(D-9)}$$

must be satisfied, as well as the dynamic boundary condition

$$P + p - P' - p' = 0 \qquad \text{(D-10)}$$

and the mixed boundary conditions

$$\frac{\partial(P + p - P' - p')}{\partial t} + (\underline{V} + \underline{v})\cdot\nabla(P + p - P' - p') = 0$$

$$\frac{\partial(P + p - P' - p')}{\partial t} + (\underline{V}' + \underline{v}')\cdot\nabla(P + p - P' - p') = 0 \quad . \quad \text{(D-11)}$$

The known fundamental motion D-1 satisfies a corresponding system of equations, obtained simply by neglecting all small letters in equations D-4 to D-11. Thus the differential equations of motion, continuity, state, and energy characterizing the fundamental state become

$$\frac{\partial \underline{V}}{\partial t} + \underline{V}\cdot\nabla\underline{V} + 2\underline{\Omega}\times\underline{V} + S\ \nabla P + \nabla\Phi = 0 \qquad \text{(D-12)}$$

$$\frac{\partial S}{\partial t} + \underline{V}\cdot\nabla S - S\ \nabla\cdot\underline{V} = 0 \qquad \text{(D-13)}$$

$$\chi(S,\ P,\ \Theta,\ \dot{S},\ \ldots) = 0 \qquad \text{(D-14)}$$

$$\dot{W} - \dot{E} - P\dot{S} = 0 \quad . \qquad \text{(D-15)}$$

The undisturbed surface of discontinuity has the form

$$F(x,\ y,\ z,\ t) = 0 \qquad \text{(D-16)}$$

and the corresponding kinematic, dynamic, and mixed boundary conditions can be written

$$\frac{\partial F}{\partial t} + V\cdot\nabla F = 0, \qquad \frac{\partial F}{\partial t} + \underline{V}'\cdot\nabla F = 0 \qquad \text{(D-17)}$$

$$P - P' = 0 \qquad \text{(D-18)}$$

$$\frac{\partial(P - P')}{\partial t} + \underline{V}\cdot\nabla(P - P') = 0$$

$$\frac{\partial(P - P')}{\partial t} + \underline{V}'\cdot\nabla(P - P') = 0 \quad . \qquad \text{(D-19)}$$

The system of Equations D-12 to D-15 can now be subtracted from the system D-4 to D-7 valid for the overall resultant motion. If after subtraction squares and products of the small quantities characterizing the perturbation are neglected (or if a variation is performed on the equations of the fundamental motion), the following linear equations of perturbation (linear and homogeneous in v, s, p, ...) are obtained:

$$\frac{\partial \underline{v}}{\partial t} + \underline{V}\cdot\nabla\underline{v} + \underline{v}\cdot\nabla\underline{V} + 2\underline{\Omega}\times\underline{v} + S\ \nabla p + s\ \nabla P + \nabla\phi_t = 0 \qquad \text{(D-20)}$$

$$\frac{\partial s}{\partial t} + \underline{V}\cdot\nabla s + \underline{v}\cdot\nabla S - S\ \nabla\cdot\underline{v} - s\ \nabla\cdot\underline{V} = 0 \qquad \text{(D-21)}$$

$$\frac{\partial \chi}{\partial \rho} s + \frac{\partial \chi}{\partial P} p + \frac{\partial \chi}{\partial \theta} + \frac{\partial \chi}{\partial S}\left(\frac{\partial s}{\partial t} + \underline{V}\cdot\nabla s + \underline{v}\cdot\nabla S\right) + \ldots = 0 \qquad \text{(D-22)}$$

$$\frac{\partial w}{\partial t} - \frac{\partial e}{\partial t} - P\frac{\partial s}{\partial t} - p\frac{\partial S}{\partial t} + \underline{V}\cdot(\nabla w - \nabla e - P\nabla s - p\nabla S)$$

$$+ \underline{v}\cdot(\nabla W - \nabla E - P\nabla S) = 0\ . \qquad \text{(D-23)}$$

In Equation D-23 we have expanded $\dot{W}$ and $\dot{w}$, although they are not functions of state, in a local and a convective part.

The equation of the surface of discontinuity is of the form D-8

$$F(x, y, z, t) + f(x, y, z, t) = 0 \qquad \text{(D-24)}$$

thus linear in f, but inhomogeneous. The formulas representing the kinematic and mixed boundary conditions, however, are of the homogeneous type, since by means of D-17 to D-19 Equations D-9 to D-11 can be reduced to

$$\frac{\partial f}{\partial t} + \underline{V}\cdot\nabla f + \underline{v}\cdot\nabla F = 0, \qquad \frac{\partial f}{\partial t} + \underline{V}'\cdot\nabla f + \underline{v}'\cdot\nabla F = 0 \qquad \text{(D-25)}$$

$$P + p - P' - p' = 0 \tag{D-26}$$

$$\frac{\partial(p - p')}{\partial t} + \underline{V}\cdot\nabla(p - p') + \underline{v}\cdot\nabla(P - P') = 0$$

$$\frac{\partial(p - p')}{\partial t} + \underline{V}'\cdot\nabla(p - p') + \underline{v}'\cdot\nabla(P - P') = 0 \ . \tag{D-27}$$

The system of differential Equations D-20 to D-23 contains the potentials Φ and ϕ_t, assumed to be known field functions, constant in time or variable, and the internal energies E and e, dependent on the temperature Θ and its perturbation θ. Finally, the equations contain the amount of heat $\dot{W}$ given to the particle, as well as its variation $\dot{w}$. These quantities generally depend on external agencies; only when they are assumed to be known beforehand will the system of Equations D-20 to D-23 be complete, containing just as many variables as equations.

PERTURBATION EQUATIONS IN SPHERICAL COORDINATES

Introducing

$$\left(\frac{D}{Dt}\right)_s = \frac{\partial}{\partial t} + V_r \frac{\partial}{\partial r} + \frac{V_\lambda}{r \cos \varphi} \frac{\partial}{\partial \lambda} + \frac{V_\varphi}{r} \frac{\partial}{\partial \varphi} \ ,$$

$$\left(\frac{d}{dt}\right)_s = v_r \frac{\partial}{\partial r} + \frac{v_\lambda}{r \cos \varphi} \frac{\partial}{\partial \lambda} + \frac{v_\varphi}{r} \frac{\partial}{\partial \varphi} \tag{D-28}$$

we find for the fundamental state, D-12 and D-13, the following equations of motion and of continuity in spherical coordinates in the case of absolute motion:

$$\left.\begin{aligned}
&\left(\frac{DV_r}{Dt}\right)_s - \frac{V_\varphi^2}{r} - \frac{V_\lambda^2}{r} + S\,\frac{\partial P}{\partial r} + \frac{\partial \Phi}{\partial r} = 0 \\
&\left(\frac{DV_\lambda}{Dt}\right)_s - \frac{V_\lambda V_\varphi}{r}\tan\varphi + \frac{V_\lambda V_r}{r} + \frac{S}{r\cos\varphi}\,\frac{\partial P}{\partial \lambda} + \frac{1}{r\cos\varphi}\,\frac{\partial \Phi}{\partial \lambda} = 0 \\
&\left(\frac{DV_\varphi}{Dt}\right)_s + \frac{V_\varphi V_r}{r} + \frac{V_\lambda^2}{r}\tan\varphi + \frac{S}{r}\,\frac{\partial P}{\partial \varphi} + \frac{1}{r}\,\frac{\partial \Phi}{\partial \varphi} = 0
\end{aligned}\right\} \quad \text{(D-29)}$$

$$\left(\frac{DS}{Dt}\right)_s - \frac{S}{r^2}\frac{+\partial}{\partial r}\left(r^2 V_r\right) - \frac{S}{r\cos\varphi}\,\frac{\partial V_\lambda}{\partial \lambda} - \frac{S}{r\cos\varphi}\,\frac{\partial}{\partial \varphi}\left(\cos\varphi\, V_\varphi\right) = 0 \quad \text{(D-30)}$$

and the corresponding equations of perturbation D-20 and D-21:

$$\left.\begin{aligned}
&\left(\frac{Dv_r}{Dt}\right)_s + \left(\frac{dV_r}{dt}\right)_s - \frac{2V_\varphi v_\varphi}{r} - \frac{2V_\lambda v_\lambda}{r} + S\frac{\partial p}{\partial r} + s\frac{\partial P}{\partial r} + \frac{\partial \phi_t}{\partial r} = 0 \\
&\left(\frac{Dv_\lambda}{Dt}\right)_s + \left(\frac{dV_\lambda}{dt}\right)_s - \frac{V_\lambda v_\varphi + v_\lambda V_\varphi}{r}\tan\varphi + \frac{V_\lambda v_r + v_\lambda V_r}{r} \\
&\qquad + \frac{S}{r\cos\varphi}\,\frac{\partial p}{\partial \lambda} + \frac{s}{r\cos\varphi}\,\frac{\partial P}{\partial \lambda} + \frac{1}{r\cos\varphi}\,\frac{\partial \phi_t}{\partial \lambda} = 0 \\
&\left(\frac{Dv_\varphi}{Dt}\right)_s + \left(\frac{dV_\varphi}{dt}\right)_s + \frac{V_\varphi v_r + v_\varphi V_r}{r} + \frac{2V_\lambda v_\lambda}{r}\tan\varphi \\
&\qquad + \frac{S}{r}\,\frac{\partial p}{\partial \varphi} + \frac{s}{r}\,\frac{\partial P}{\partial \varphi} + \frac{1}{r}\,\frac{\partial \phi_t}{\partial \varphi} = 0
\end{aligned}\right\} \quad \text{(D-31)}$$

$$\left(\frac{Ds}{Dt}\right)_s + \left(\frac{dS}{dt}\right)_s - \frac{S}{r^2}\frac{\partial}{\partial r}\left(r^2 v_r\right) - \frac{S}{r\cos\varphi}\frac{\partial v_\lambda}{\partial\lambda} - \frac{S}{r\cos\varphi}\frac{\partial}{\partial\varphi}\left(\cos\varphi\, v_\varphi\right)$$

$$- \frac{s}{r^2}\frac{\partial}{\partial r}\left(r^2 V_r\right) - \frac{s}{r\cos\varphi}\frac{\partial V_\lambda}{\partial\lambda} - \frac{s}{r\cos\varphi}\frac{\partial}{\partial\varphi}\left(\cos\varphi\, V_\varphi\right) = 0 \,. \qquad \text{(D-32)}$$

The equations of state, energy, and so forth are easily written down by means of the general expressions for the fundamental state D-14 to D-19 and for the perturbation D-22 to D-27.

ANNEX E

DIFFERENCE EQUATIONS

As a means of expressing in terms of discrete steps the continuous functions of differential equations, we resort to the analogous difference equations. The difference equation analogs of differential equations may take a variety of forms, each having different ease of computation, truncation error, and stability of solution when the time and space steps are made to be small.

If the discrete space positions taken by the space steps are denoted by subscripts (i, j, k) in the (x, y, z) directions and the time position taken by the time step is denoted by the superscript (n) in the time dimension, then we may write the difference equation analog of a differential by reference to the position or time for which the evaluation is made. Thus, a space differential may be expressed as "forward," "centered," or "backward," as follows:

$$\left(\frac{\partial \phi}{\partial x}\right)_i = \frac{\phi^n_{i+1} - \phi^n_i}{\Delta x} \qquad \text{Forward space difference (in x-dimension)} \tag{E-1}$$

$$= \frac{\phi^n_{i+1/2} - \phi^n_{i-1/2}}{\Delta x} = (\delta\phi)^n_i \qquad \text{Centered space difference (in x-dimension)} \tag{E-2}$$

$$= \frac{\phi^n_i - \phi^n_{i-1}}{\Delta x} \qquad \text{Backward space difference (in x-dimension)} . \tag{E-3}$$

Similar analogs may be written for the 2 other space dimensions and the time dimension.

We may write difference equation analogs for the simple diffusion equation

$$\frac{\partial u}{\partial t} = \sigma \frac{\partial^2 u}{\partial x^2}, \qquad \sigma = \text{constant} > 0 \tag{E-4}$$

as an explicit difference equation

(a) in terms of a "forward time difference, centered space difference" form:

$$\frac{u_j^{n+1} - u^n{}_j}{\Delta t} = \sigma \, (\delta^2 u)^n{}_j = \sigma \left(\frac{u^n_{j+1} - 2u^n{}_j + u^n_{j-1}}{(\Delta x)^2} \right) \tag{E-5}$$

(b) or a "backward time difference, centered space difference" form:

$$\frac{u_j^{n+1} - u^n{}_j}{\Delta t} = \sigma \, (\delta^2 u)^{n+1}_j = \sigma \, \frac{u^{n+1}_{j+1} - 2u^{n+1}_j - u^{n+1}_{j-1}}{(\Delta x)^2} \tag{E-6}$$

or as a combination of the "backward" and "forward" forms, which is an implicit scheme for evaluating Eq. E-4, is given by

$$\frac{u_j^{n+1} - u^n{}_j}{\Delta t} = \sigma \left[\frac{\theta \, (\delta^2 u)^{n+1}_j + (1 - \theta)(\delta^2 u)^n_j}{(\Delta x)^2} \right]_i \qquad 0 \le \theta \le 1 . \tag{E-7}$$

Richtmyer and Morton (1967) have described a review of the several approximations, as given in Table E-1. In this summary of various difference systems for the simple diffusion equation, the diagram at the left indicates the type of differencing. The points shown are those points of the net in the x, t plane used in one application of the formula; the t-axis points to the top of the page and x-axis horizontally to the right. Where three points are connected by a horizontal line, they are used in forming the second space difference ($\delta^2 u$), and where two points are connected by a

TABLE E-1. FINITE DIFFERENCE APPROXIMATIONS TO

$$\frac{\partial u}{\partial t} = \sigma \frac{\partial^2 u}{\partial x^2}\ , \quad \sigma = \text{constant} > 0$$

(after Richtmyer & Morton 1967)

1.

1. $$\frac{u_j^{n+1} - u_j^n}{\Delta t} = \sigma \frac{(\delta^2 u)_j^n}{(\Delta x)^2}$$

$e = O(\Delta t) + O[(\Delta x)^2]$

explicit, stable if $\sigma \Delta t/(\Delta x)^2 = \text{constant} \leq 1/2$

2.

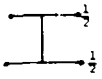

2. $$\frac{u_j^{n+1} - u_j^n}{\Delta t} = \sigma \frac{(\delta^2 u)_j^n + (\delta^2 u)_j^{n+1}}{2(\Delta x)^2}$$

Crank and Nicholson (1947)

$e = O[(\Delta t)^2] + O[(\Delta x)^2]$

implicit, always stable.

3.

3. $$\frac{u_j^{n+1} - u_j^n}{\Delta t} = \sigma \frac{(\delta^2 u)_j^{n+1}}{(\Delta x)^2}$$

Laasonen (1949)

$e = O(\Delta t) + O[(\Delta x)^2]$

implicit, always stable.

4.

4. Same as 1, but with $\sigma \Delta t/(\Delta x)^2 = 1/6$

$e = O[(\Delta t)^2] = O[(\Delta x)^4]$

special case of 1, stable.

5.

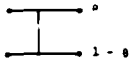

5. $$\frac{u_j^{n+1} - u_j^n}{\Delta t} = \sigma \frac{\theta(\delta^2 u)_j^{n+1} + (1-\theta)(\delta^2 u)_j^n}{(\Delta x)^2}$$

where θ = constant, $0 \leq \theta \leq 1$

$e = O(\Delta t) + O[(\Delta x)^2]$

for $0 \leq \theta < 1/2$, stable if $\sigma \Delta t/(\Delta x)^2 =$ constant $\leq 1/(2 - 4\theta)$; for $1/2 \leq \theta \leq 1$ always stable

includes 1, ..., 4 as special cases.

6.

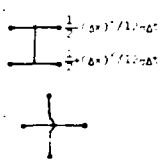

6. Same as 5, but with $\theta = 1/2 + (\Delta x)^2/12\sigma\Delta t$

$e = O[(\Delta t)^2] + O[(\Delta x)^4]$

stable.

7.

7. $$\frac{u_j^{n+1} - u_j^{n-1}}{2\Delta t} = \sigma \frac{(\delta^2 u)_j^n}{(\Delta x)^2}$$

always unstable.

8.

8. $$\frac{u_j^{n+1} - u_j^{n-1}}{2\Delta t} = \sigma \frac{u_{j+1}^n - u_j^{n+1} - u_j^{n-1} + u_{j-1}^n}{(\Delta x)^2}$$

where $\sigma^*/\Delta x = 0$ as $\Delta t, \Delta x \to 0$

$e = O[(\Delta t)^2] + O[(\Delta x)^2] + O\left[\left(\frac{\Delta t}{\Delta x}\right)^2\right]$

Du Fort and Frankel (1953)

Explicit, always stable.

9.

9. $$\frac{3}{2}\frac{u_j^{n+1} - u_j^n}{\Delta t} - \frac{1}{2}\frac{u_j^n - u_j^{n-1}}{\Delta t} = \sigma \frac{(\delta^2 u)_j^{n+1}}{(\Delta x)^2}$$

$e = O[(\Delta t)^2] + O[(\Delta x)^2]$

always stable.

10.

10. $$(1+\theta)\frac{u_j^{n+1} - u_j^n}{\Delta t} - \sigma\frac{u_j^n - u_j^{n-1}}{\Delta t} = \sigma \frac{(\delta^2 u)_j^{n+1}}{(\Delta x)^2}$$

where θ = constant ≥ 0, $\sigma \Delta t/(\Delta x)^2 =$ constant

$e = O(\Delta t) + O[(\Delta x)^2]$

always stable

contains 3, 9 as special cases.

11.

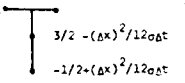

11. Same as 10 but with

$$\theta = \frac{1}{2} + \frac{(\Delta x)^2}{12\sigma\Delta t}$$

$e = O[(\Delta t)^2] = O[(\Delta x)^4]$

always stable.

12.

12. $$\frac{1}{12}\frac{u_{j+1}^{n+1} - u_{j+1}^n}{\Delta t} + \frac{5}{6}\frac{u_j^{n+1} - u_j^n}{\Delta t} + \frac{1}{12}\frac{u_{j-1}^{n+1} - u_{j-1}^n}{\Delta t} = \sigma \frac{(\delta^2 u)_j^{n+1} + (\delta^2 u)_j^n}{2(\Delta x)^2}$$

$e = O[(\Delta t)^2] + O[(\Delta x)^4]$

always stable

identical with 6.

13.

13. $$\frac{1}{12}\frac{3/2\, u_{j+1}^{n+1} - 2u_{j+1}^n + 1/2\, u_{j+1}^{n-1}}{\Delta t} + \frac{5}{6}\frac{3/2 u_j^{n+1} - 2u_j^n + 1/2\, u_j^{n-1}}{\Delta t} + \frac{1}{12}\frac{3/2 u_{j-1}^{n+1} - 2u_{j-1}^n + 1/2\, u_{j-1}^{n-1}}{\Delta t} = \sigma \frac{(\delta^2 u)_j^{n+1}}{(\Delta x)^2}$$

$e = O[(\Delta t)^2] + O[(\Delta x)^4]$

always stable.

14.

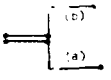

14a. $$u_j^{n+1} - u_j^n = \sigma\left(u_{j+1}^n - u_j^n - u_j^{n+1} + u_{j-1}^{n+1}\right)$$

14b. $$u_j^{n+2} - u_j^{n+1} = \sigma\left(u_{j+1}^{n+2} - u_j^{n+2} - u_j^{n+1} + u_{j-1}^{n+1}\right)$$

where $\sigma = \sigma \Delta t/(\Delta x)^2$

Saul'ev (1957)--see text.

vertical line they are used in forming the time difference. When there are two or more sets of points of either kind, the weights used are indicated at the side or underneath. The table also shows the order of the truncation error (e) and the conditions for stability of solution.

The 5-point explicit scheme (#1 of Table E-1) with forward time difference is that employed by Leith (1965) and to be used for the S-M-T Model.

Richtmyer and Morton (1967) point out that in general the stability of an approximation's solution is determined by the stability of the solution of the highest order derivative.

As a means of replacing a complicated (say multidimensional) problem by a succession of simpler (say 1-dimensional) ones, the methods of splitting, or methods of fractional steps, were devised by Soviet mathematicians (Bagrinovski and Godunov 1957, D'yakonov, 1962, Marchuk 1964). These have been applied by Leith (1965) and are proposed for the S-M-T Model in the following form:

$$\psi_{j_i k}^{n+1/2} = \psi_{j_i k}^{n} - \frac{1}{2}\left(\frac{v\Delta t}{\Delta x}\right)\left(\psi_{j_i k+1}^{n} - \psi_{j_i k+1}^{n}\right) + \frac{1}{2}\left(\frac{v\Delta t}{\Delta x}\right)^2\left(\psi_{j_i k+1}^{n} - 2\psi_{j_i k}^{n} + \psi_{j_i k-1}^{n}\right) \tag{E-8}$$

$$\psi_{j_i k}^{n+1} = \psi_{j_i k}^{n+1/2} - \frac{1}{2}\left(\frac{u\Delta t}{\Delta x}\right)\left(\psi_{j+1_i k}^{n+1} - \psi_{j-1_i k}^{n+1/2}\right) + \frac{1}{2}\left(\frac{u\Delta t}{\Delta x}\right)^2\left(\psi_{j+1_i k}^{n+1/2} - 2\psi_{j_i k}^{n+1/2} + \psi_{j-1_i k}^{n+1/2}\right) \tag{E-9}$$

The computational process involved in a single time step is divided into two cycles. In the first of these, advection in the y-direction only is evaluated; whereas in the second, advection in the x-direction only is evaluated starting of course with the results of the first cycle. The fractional time step notation is a convenience, but the results of the first cycle have no particular physical significance.

ANNEX F

CONSIDERATIONS FOR CHOICE OF SPACE AND TIME STEPS

Criteria	Δx(m)	Δz(m)	Δt(sec)
TEMPERATURE STRATIFICATION Nyquist Criteria on T(z)		Take $\Delta z = \begin{cases} 5(10)^3 & z < 120 \text{ km} \\ (10)^4 & 120 \leq z \leq 200 \text{ km} \\ 2(10)^4 & 200 \leq z \leq 300 \text{ km} \end{cases}$	
WIND SPECTRA Surface Wind Period > 3 hr Advect at 10 m sec^{-1} $\lambda > 108$ km Advect at 50 m sec^{-1} $\lambda > 540$ km	> 108 km > 540 km		
	Take $\Delta x = 500 \text{ km} = 5(10)^5 \text{m}$		
HORIZONTAL GRAVITY WAVE $\Delta t < \frac{\Delta x}{2V_H}$; $V_H < 200$ m sec			$< \left[\frac{5(10)^5}{4(10)^2} = 1.25(10)^3 \text{ sec} = 20.8 \text{ min}\right]$
VERTICAL GRAVITY WAVE $V_z \sim 0.01 V_H$ $\Delta t < \frac{\Delta z}{2V_z}$			$< \left[\frac{5(10)^3}{2} = 2.5(10)^3 \text{ sec} = 41.6 \text{ min}\right]$ $z < 120$ km) $< [83.2 \text{ min}]$; $(120 \leq z < 200$ km) $< [166.4 \text{ min}]$; $(200 < z \leq 300$ km)
COMPUTATION STABILITY for $\left(\frac{\partial \phi}{\partial t}\right) = \sigma \frac{\partial^2 \phi}{\partial x^2}$ if $\phi = u$, $\sigma = \nu = 1.3(10)^{-4}$ g cm^{-1} sec^{-1} if $\phi = T$, $\sigma = \frac{\lambda}{c_p \rho} = \frac{0.15}{\rho}$ $\Delta t < \frac{1}{2\sigma} (\Delta x)^2$			< large number ($> 10^{14}$) < large number $[1.3(10)^6$ @ 300 km Take $\Delta t = 10$ km

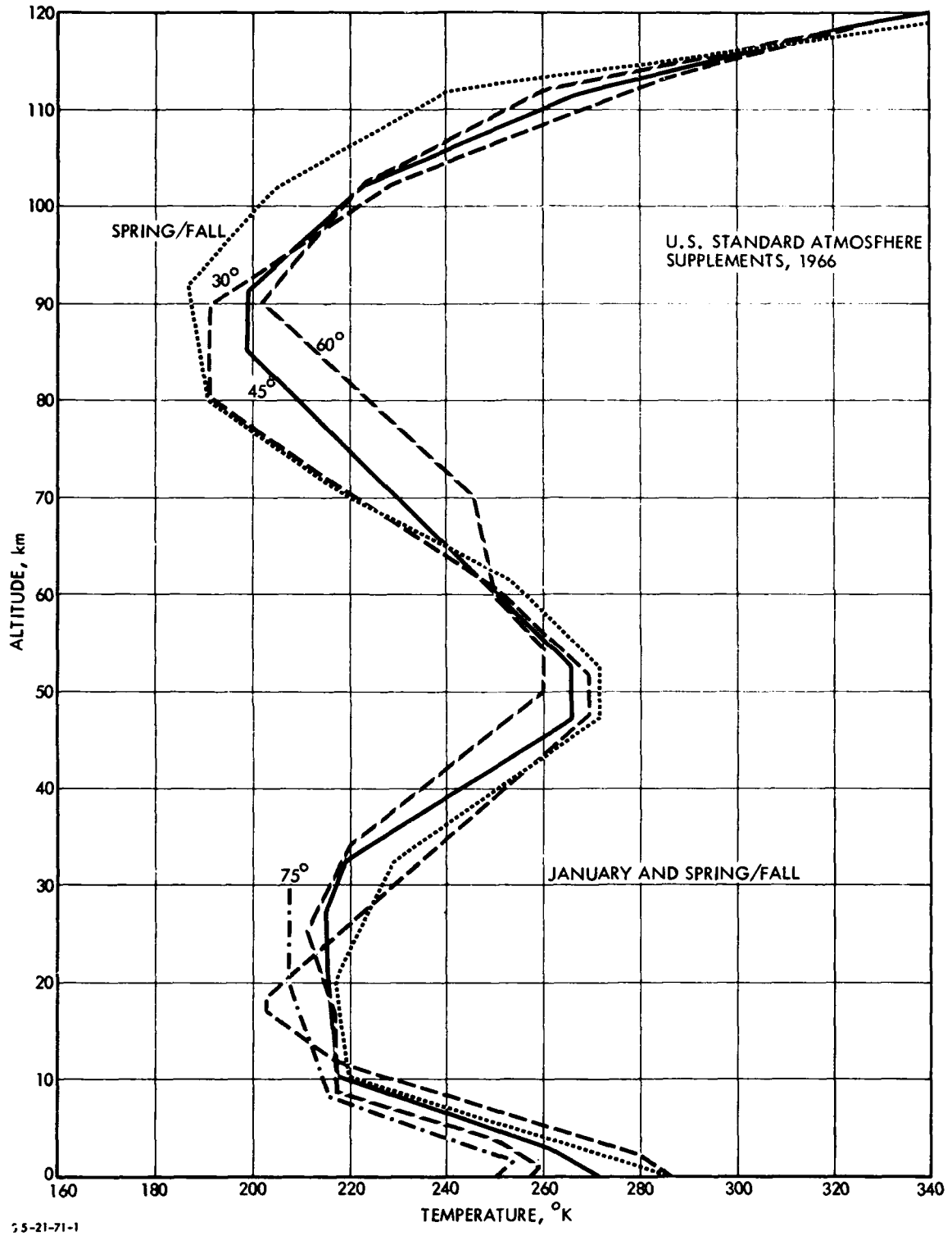

FIGURE F-1. Temperature-Altitude Profiles of the 30°, 45°, 60°, and 75° N. January and Mid-Latitude Spring/Fall Supplement

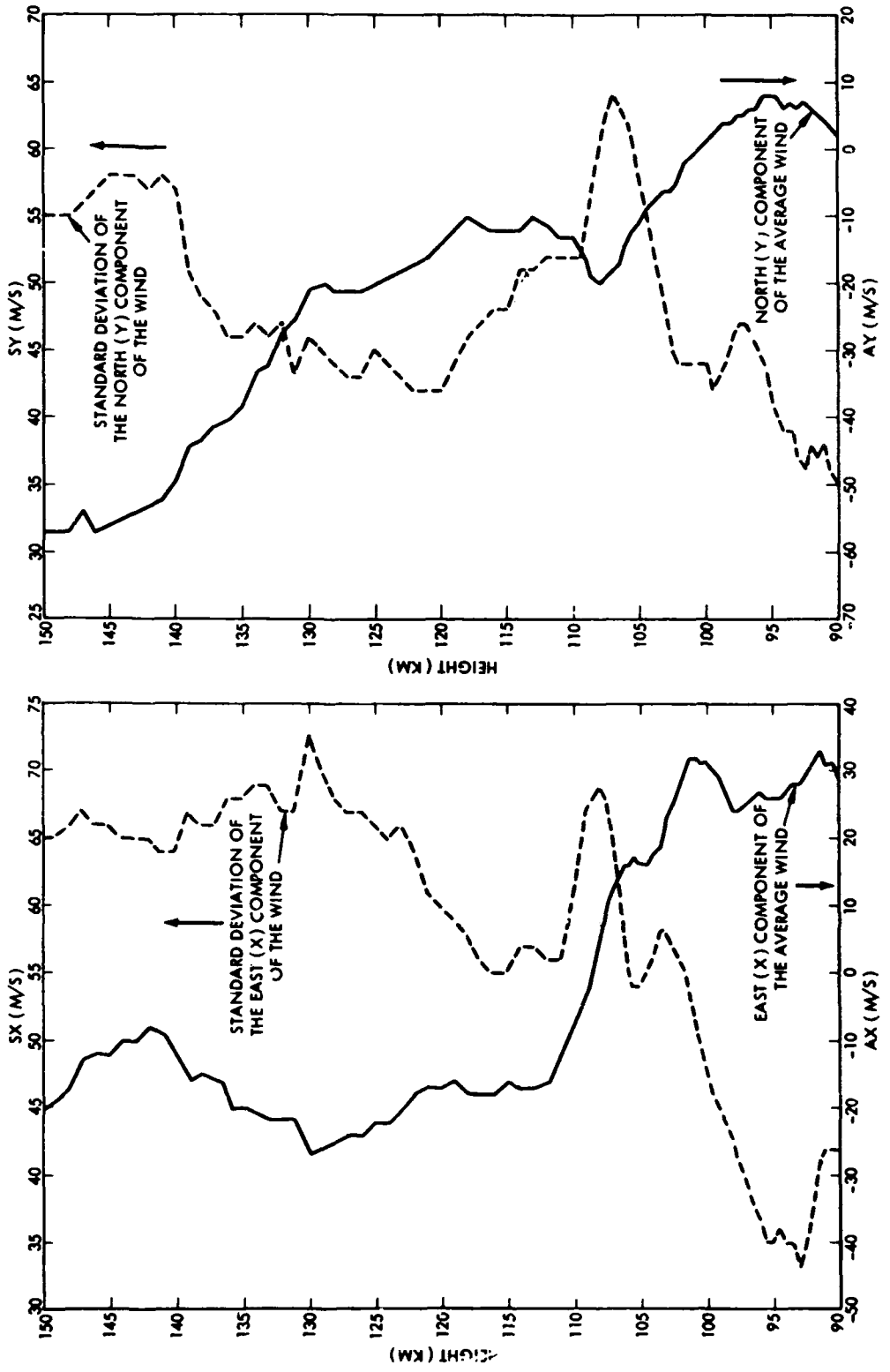

FIGURE F-2. Components of Wind Velocity (After Bedinger and Constantinides, 1969)

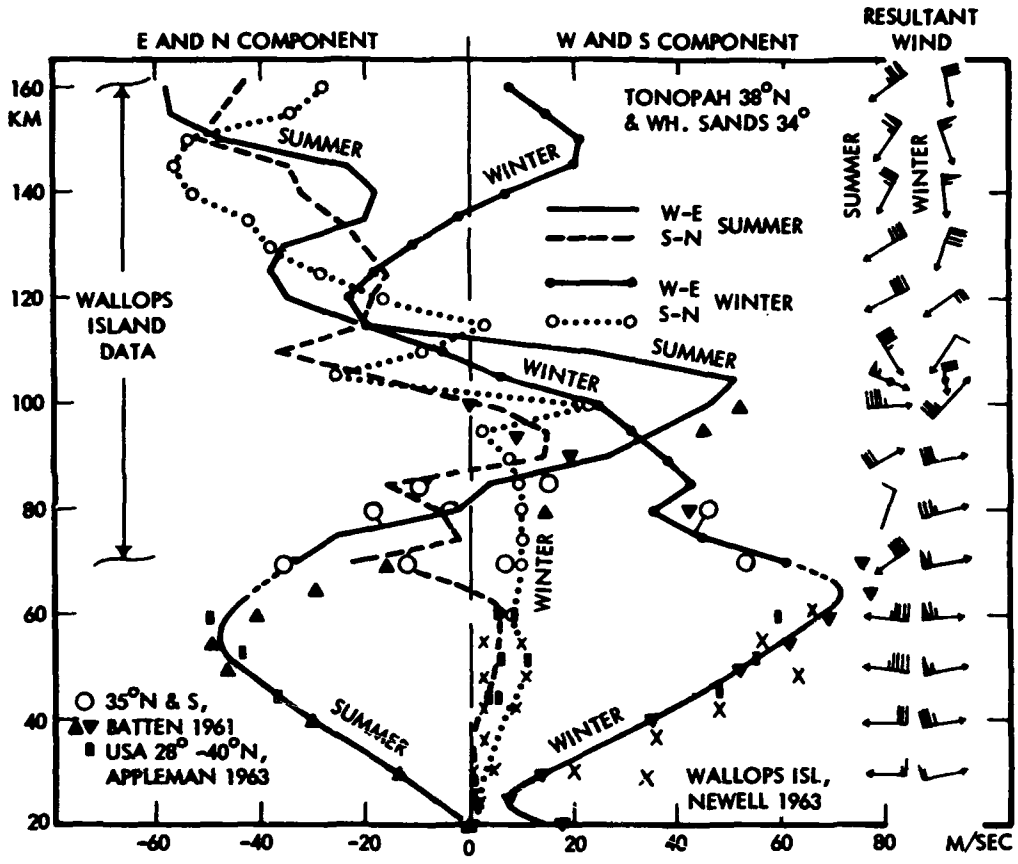

FIGURE F-3. Wind Near 38° N (After Kochanski, 1964)

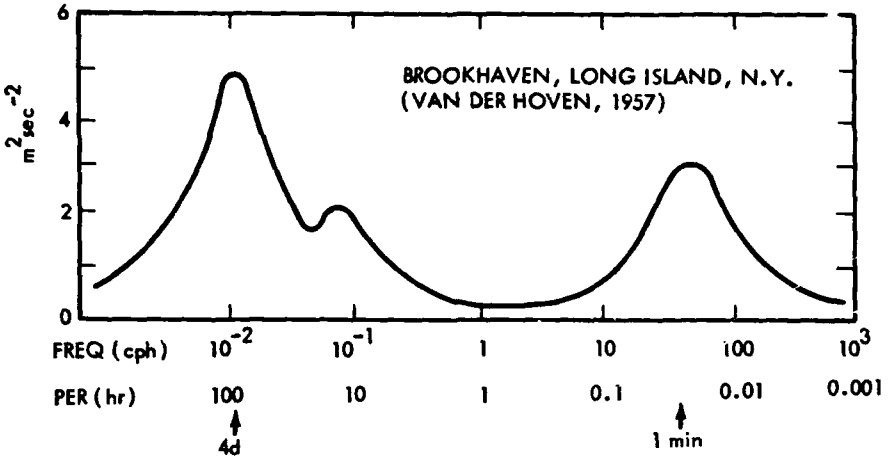

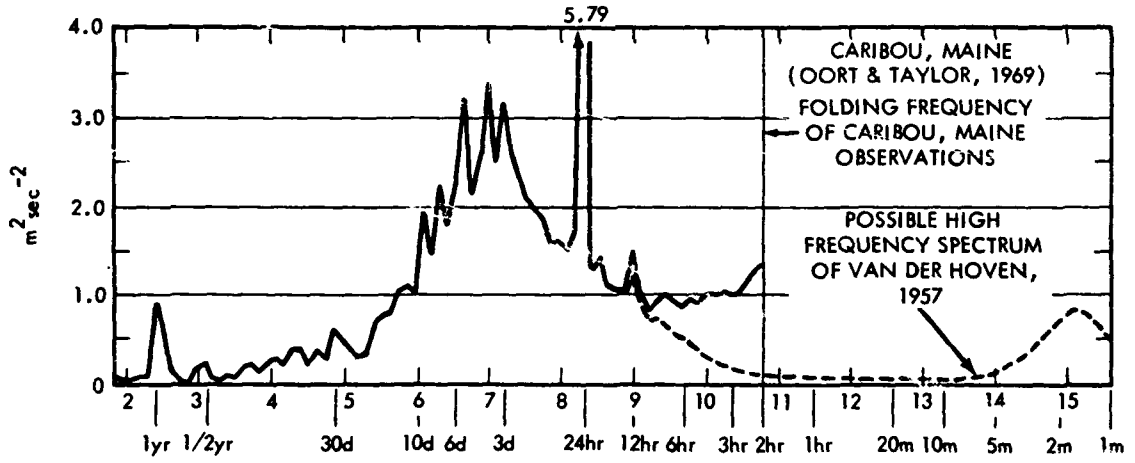

SPECTRUM WIND SPEED AT CARIBOU, MAINE (After Oort and Taylor, 1969)

FIGURE F-4. Horizontal Wind Speed Spectra

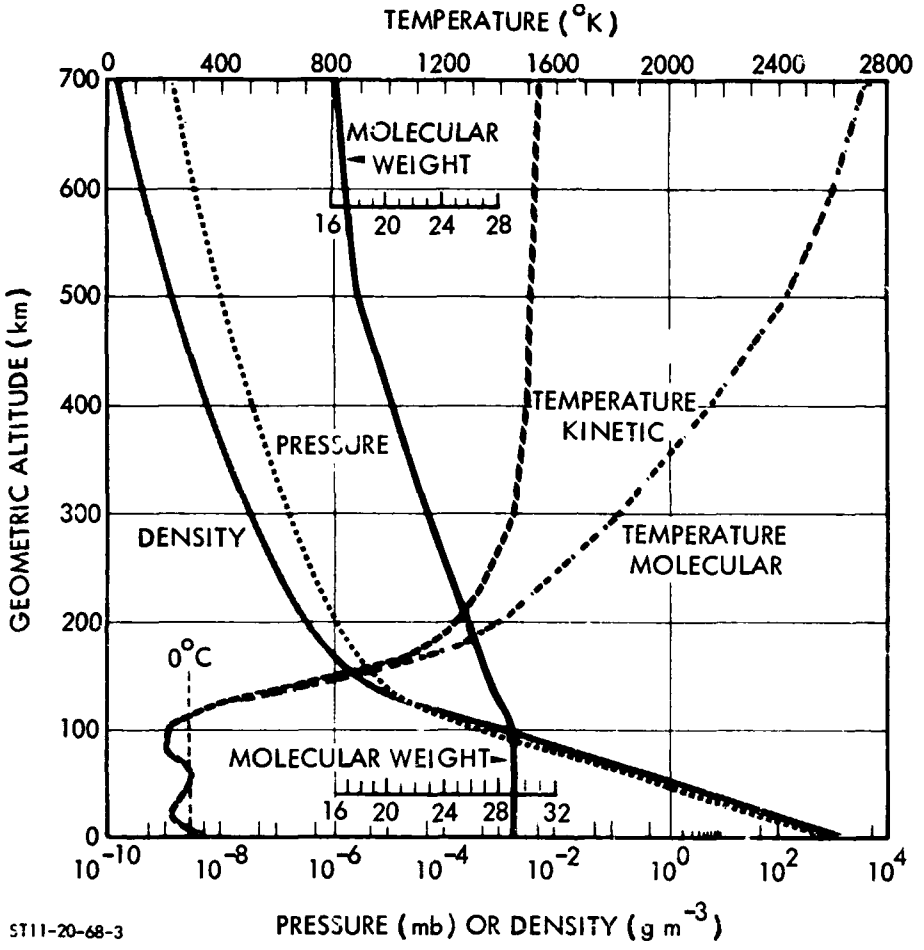

FIGURE F-5. Temperature, Pressure, Density, Molecular Weight (U.S. Standard Atmosphere, 1962) (After Valley, 1965)

ANNEX G

HEAT SOURCES AND SINKS

Domain	Heat Source/Sink
0-20	Emission from surface
	Emission by H_2O vapor (50μ)
	Emission by CO_2 (15μ)
	Absorption by H_2O vapor
	Convection/Conduction upward
20-50	Emission by CO_2 (IR)
	Emission by H_2O
	Absorption by O_3 ( )
	Conduction (down)
	Absorption by O_2, H_2O, N_2O, CH_4
50-80	Emission by CO_2 (15μ)
	Emission by O_3 (9.6μ)
	Emission by O (63μ)
	Absorption by O_3 (uv)
	Absorption by O_2 (uv)
	Particle precipitation
	Conduction (upward)
80-150	Emission by O (63μ)
	Absorption by O_2 (uv)
	Absorption by O_2, N_2 (xr)
	Particle precipitation
	Conduction (down)
	Joule heading by ionosphere dynamics
	Dissipation of gravity, tidal, Rossby waves
	Recombination of down-transported O
150-300	Absorption by N_2, O_2 (Euv)
	Particle precipitation

ANNEX H

CHEMICAL REACTIONS FOR PRODUCTION AND LOSS
OF ATMOSPHERIC CONSTITUENTS

The principal production and loss mechanisms, with greatest time and space variability, are those due to ionization and dissociation resulting from the solar electromagnetic radiation, which is wavelength and flux dependent.

The dissociation energies and ionization potentials of atmospheric species of interest, as listed by Bortner and Kummler (1968), are given in Tables H-1, H-2, and H-3. Since the more intense X-ray radiation may produce several ion-pairs per quantum, the more energetic radiation is expected to produce ion-pairs at a rate proportional to the next smaller integer value of (J/IP), wherein J is the ergs sec^{-1} deposited in each cm^3 of the radiation path, and IP is the ionization potential of the species.

Other important sources of production and loss of chemical constituents are the chemical processes, defined by Bortner and Kummler (1968), which are described in Figs. H-1 to H-31 inclusive. Only the most important reactions and their rate coefficients are shown.

The species shown in the Figs. H-1 to H-31 are in the following order:

a. Major neutral species: H_2O, CO_2, O_2 (Fig. 5-21)

b. Minor neutral species: O, $O(^1D)$, $O_2(^1\Delta)$, $O_2(^1\Sigma)$, O_3, N, NO, NO_2, N_2O, H, H_2, OH, HO_2, H_2O_2

c. Positive ions: N_2^+, N^+, O^+, O_2^+, NO^+

d. Negatively charged species: e, O_2^-, O^-, O_3^-, CO_3^-, NO_2^-, NO_3^-

e. Metallic species: of form M, MO, MO_2, M^+ of metals Na, Mg and Cu.

For each of the reactions shown, a rate coefficient is given in cgs units, that is in cm^2 sec^{-1} per particle for two body and in cm^6 sec^{-1} per $(particle)^2$ for three body reactions. Particle densities are in cm^{-3} and temperature in ^oK. M is used to represent a collision partner. All values for rate constants are given by the constants a, b, and c for a rate constant of the form

$$R = a \left(\frac{T}{300}\right)^b \exp(-c/T).$$

The rate coefficients may have error of factors 2 to 10.

Bortner and Kummler (1968) list 33 atmospheric species, with approximately 8 reactions each, or 244 reactions.

TABLE H-1. DISSOCIATION ENERGIES, IONIZATION POTENTIALS, AND ELECTRON AFFINITIES OF SPECIES OF INTEREST

	D(ev)	IP(ev)	EA(ev)
O^-	-	13.618	1.478
N	-	14.532	
O_2	5.115 (O-O)	12.063	0.43
N_2	9.759 (N-N)	15.580	
NO	6.507 (N-O)	9.267	0.3
O_3	1.051 ($O-O_2$)	12.80	1.9
NO_2	3.116 (O-NO)	9.78	4.0
N_2O	1.677 (N_2-O)	12.894	
NO_3	2.122 ($O-NO_2$)		
Ar	-	15.759	
H^-	-	13.598	0.754
H_2	4.477 (H-H)	15.425	
OH	4.395 (O-H)	13.34	1.83
H_2O	5.116 (H-OH)	12.619	
HO_2	2.04 ($H-O_2$)		
H_2O_2	2.22 (HO-OH)		
CO	11.108 (C-O)	14.013	
CO_2	5.453 (O-CO)	13.769	
CO_3			
Li		5.390	
Na		5.138	
K		4.339	
Cs		3.893	
Mg		7.644	
Ca		6.111	
Ba		5.210	
Si		8.149	
Fe		7.87	

Bortner and Kummler: "The Chemical Kinetics and the Composition of the Earth's Atmosphere," G.E. Reentry Systems Science Report GE-9500-ECS-SP-1, 24 July 1968.

TABLE H-2. WAVELENGTHS CORRESPONDING TO IONIZATION POTENTIALS, A

N_2	796
N	853
O	911
H	912
O_2	1029
NO_2	1269
NO	1339
Si	1547
Fe	1601
Mg	1649
Ca	2062
Na	2453
K	2905

TABLE H-3. WAVELENGTHS CORRESPONDING TO DISSOCIATION ENERGIES

		D(ev)	λ_D (A)	
$O_2 \rightarrow$	$O(^3P) + O(^3P)$	5.115	2425	
$O_2 \rightarrow$	$O(^3P) + O(^1D)$	7.082	1751	x
$NO \rightarrow$	$N(^4S) + O(^3P)$	6.507	1907	
$NO \rightarrow$	$N(^4S) + O(^1D)$	8.474	1464	
$NO \rightarrow$	$N(^2D) + O(^3P)$	8.891	1395	x
$O_3 \rightarrow$	$O(^3P) + O_2(^3\Sigma)$	1.051	11804	
$O_3 \rightarrow$	$O(^1D) + O_2(^3\Sigma)$	3.018	4111	
$O_3 \rightarrow$	$O(^3P) + O_2(^1\Delta)$	2.028	6117	
$O_3 \rightarrow$	$O(^1D) + O_2(^1\Delta)$	3.995	3105	x
$O_3 \rightarrow$	$O(^3P) + O_2(^1\Sigma)$	2.678	4633	
$O_3 \rightarrow$	$O(^1D) + O_2(^1\Sigma)$	4.645	2671	x
$NO_2 \rightarrow$	$O(^1D) + NO(^2\pi)$	3.116	3981	x

- Effective dissociation processes

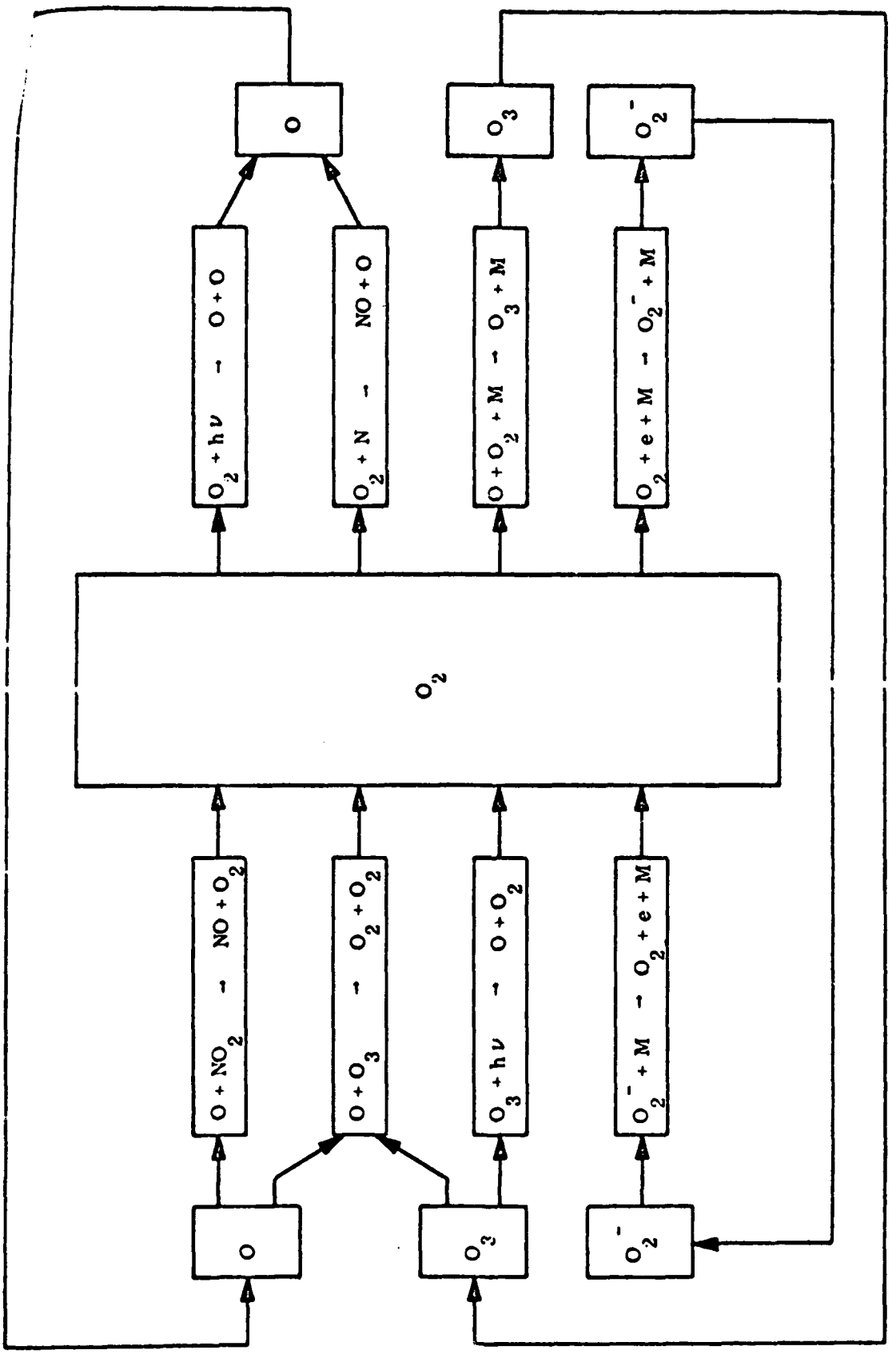

FIGURE H-1. Chemical Kinetics of Oxygen Molecules

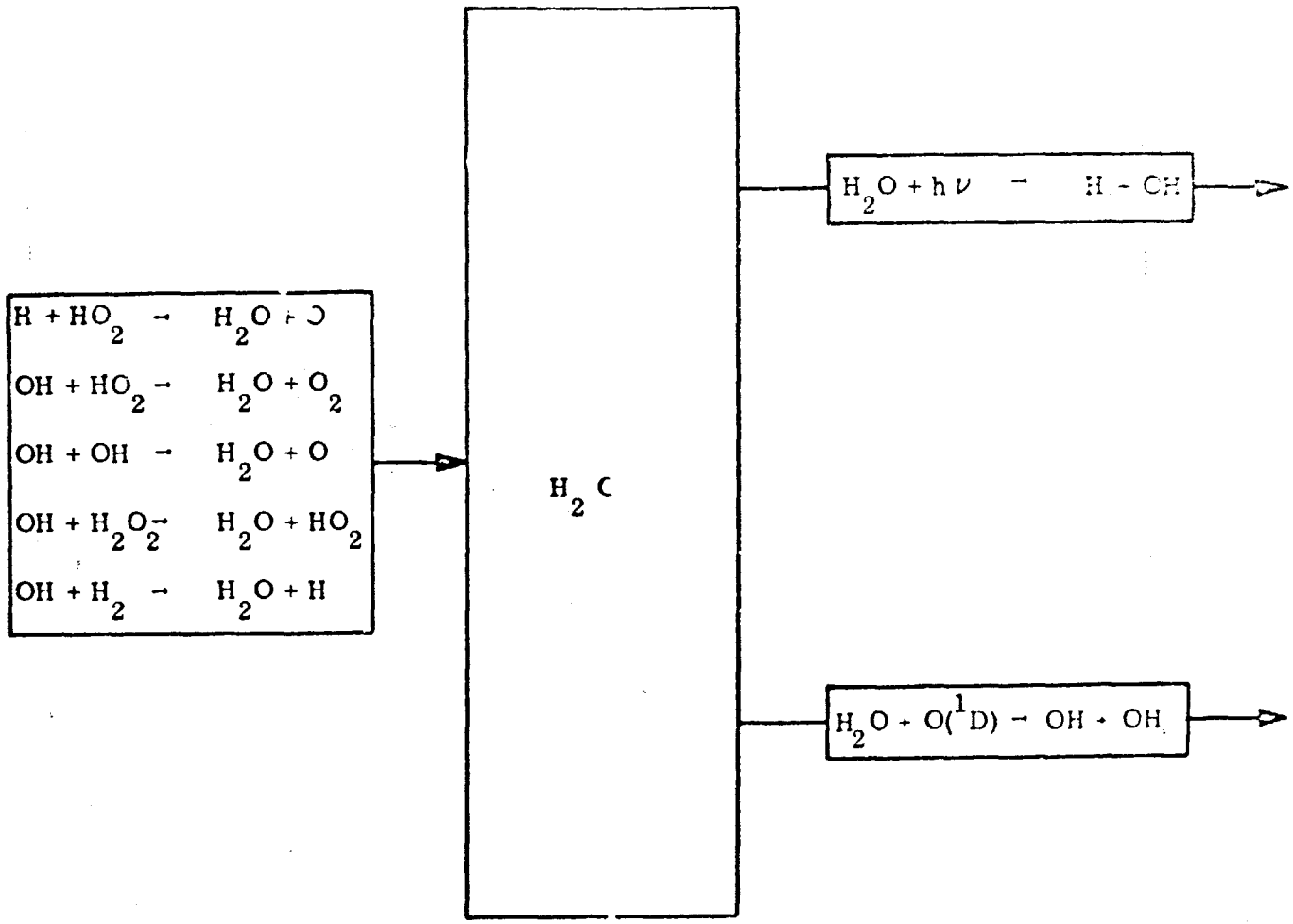

FIGURE H-2. Chemical Kinetics of Water Vapor

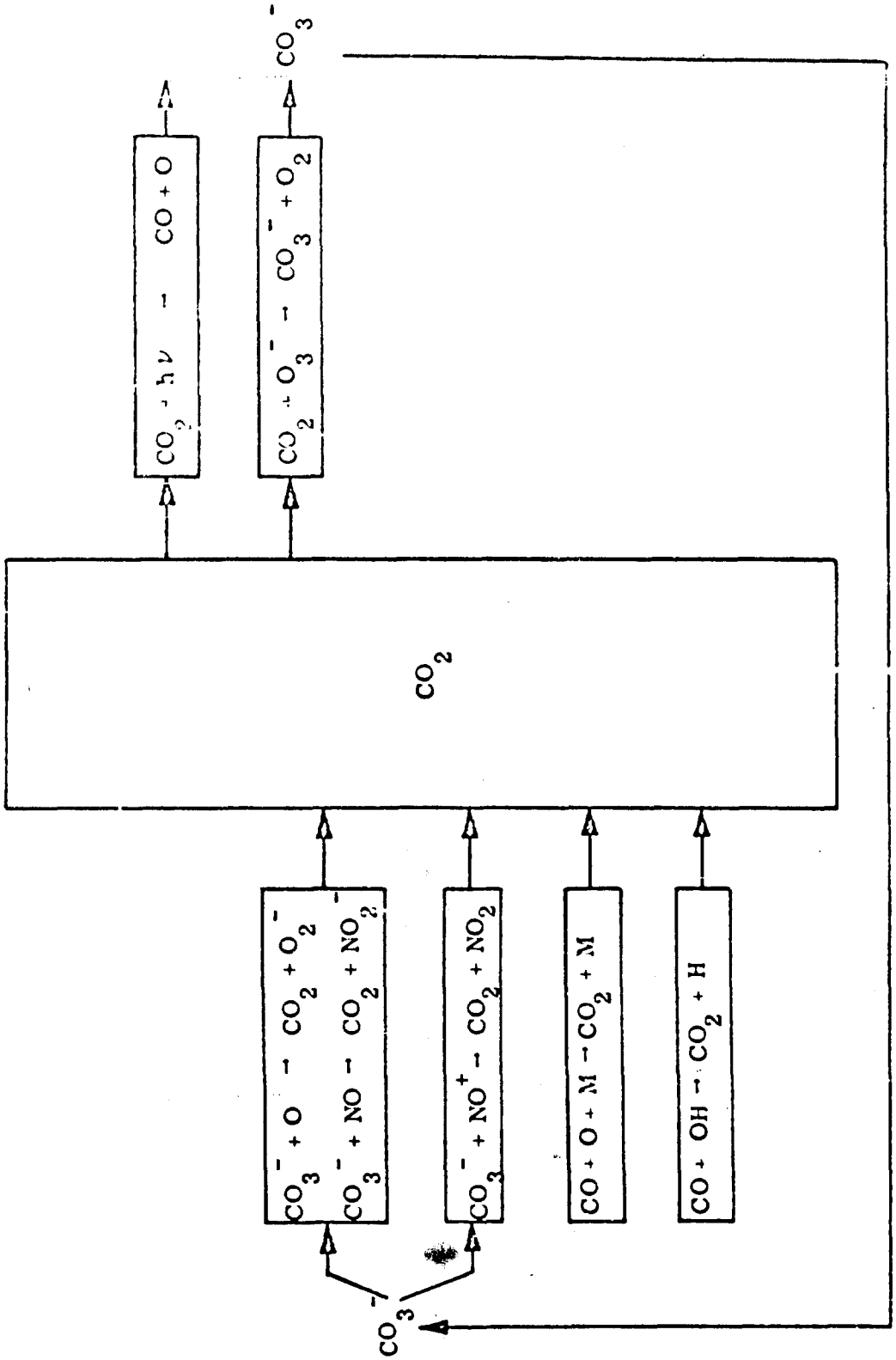

FIGURE H-3. Chemical Kinetics of Carbon Dioxide

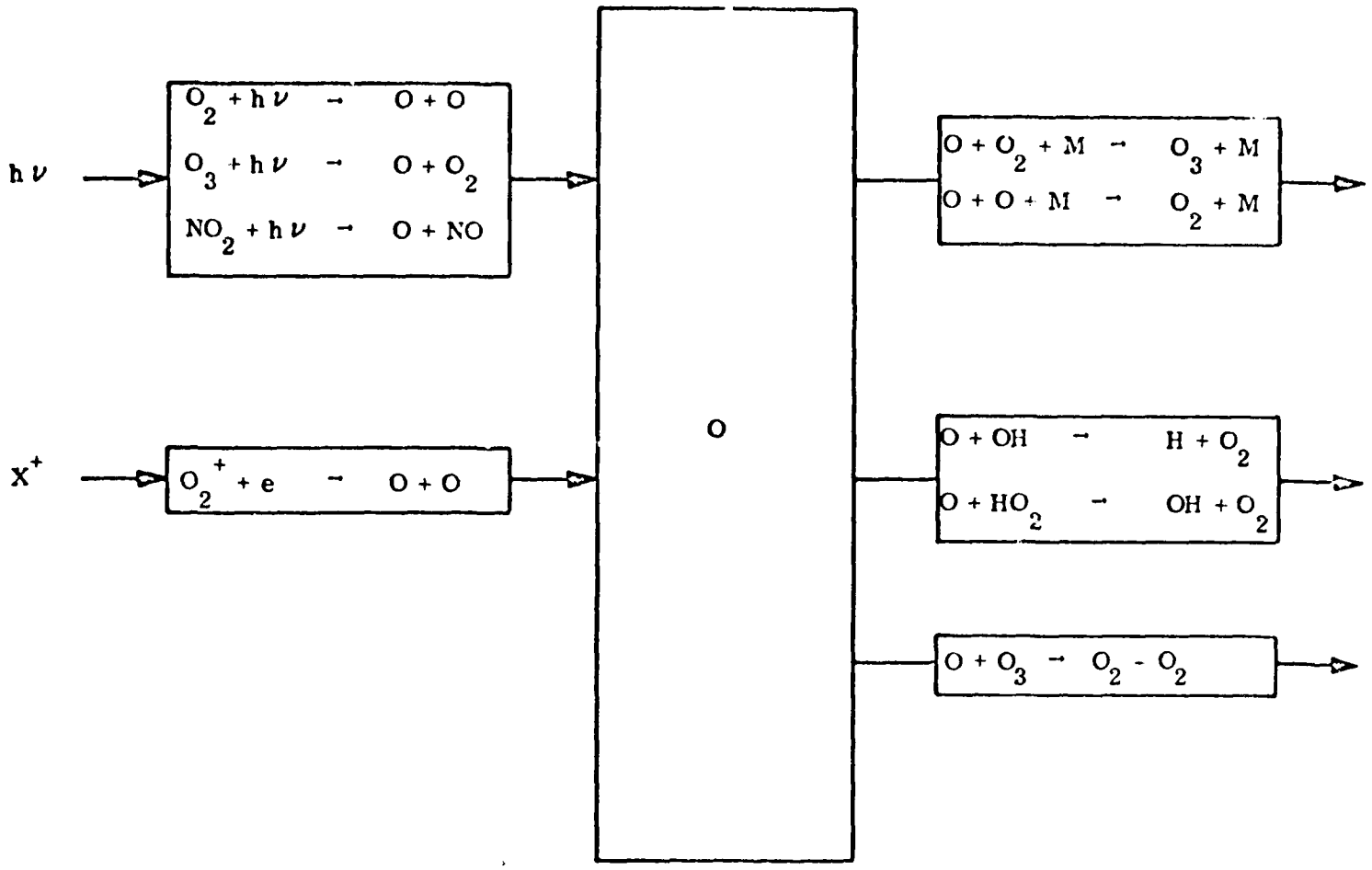

FIGURE H-4. Chemical Kinetics of Oxygen Atoms

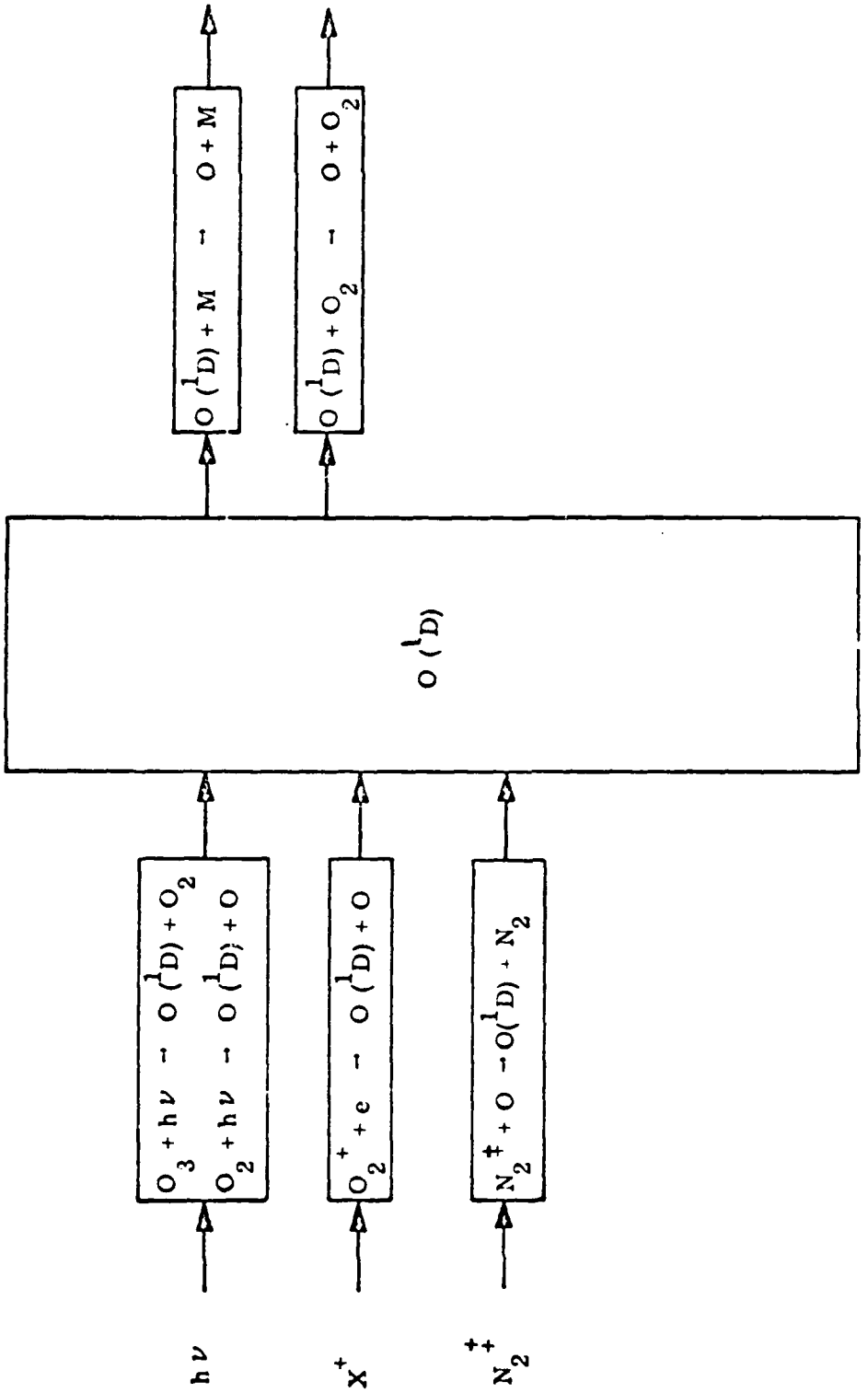

FIGURE H-5. Chemical Kinetics of Excited Oxygen Atoms

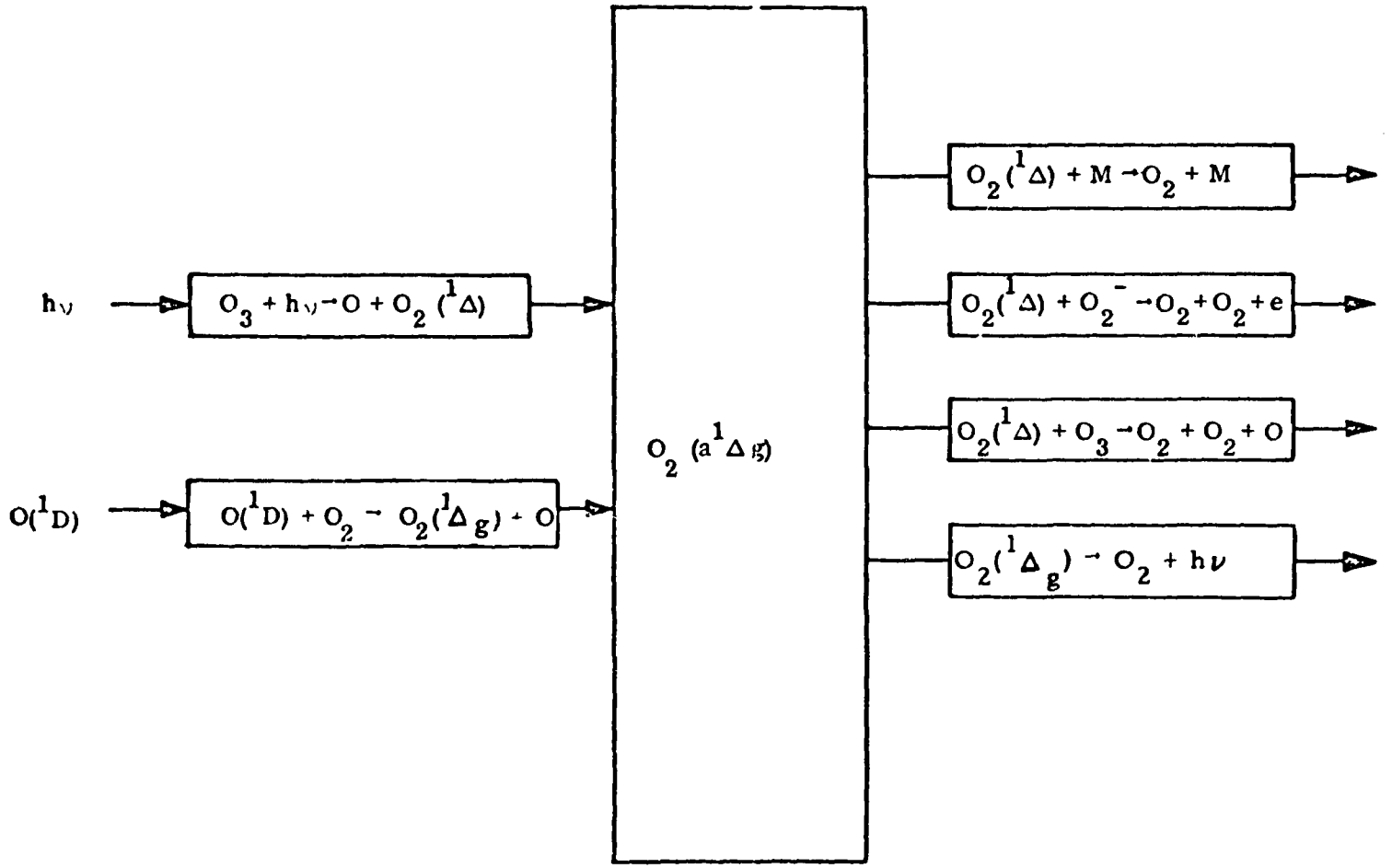

FIGURE H-6. Chemical Kinetics of O_2 ($a^1\Delta g$)

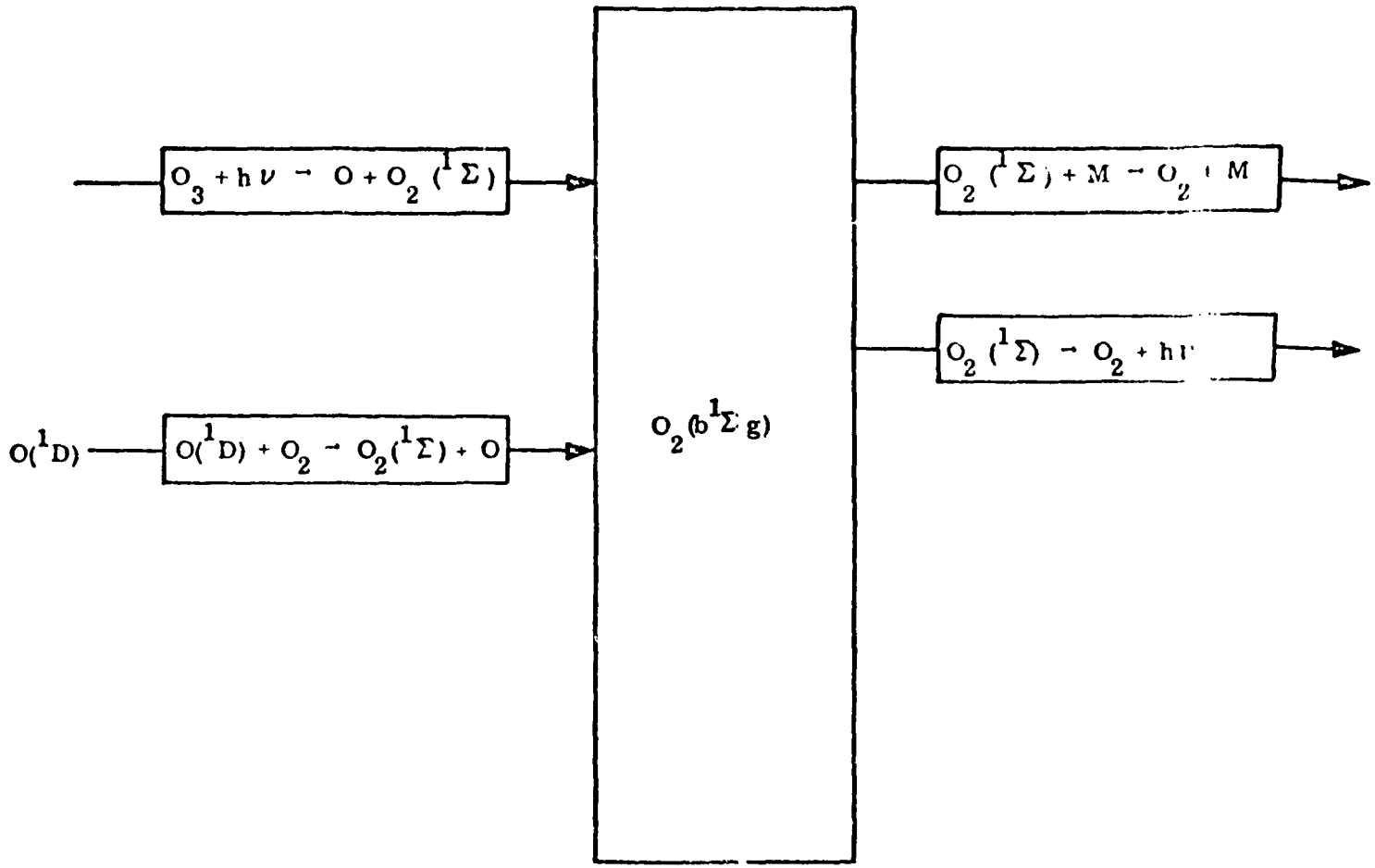

FIGURE H-7. Chemical Kinetics of $O_2(b^1\Sigma g)$

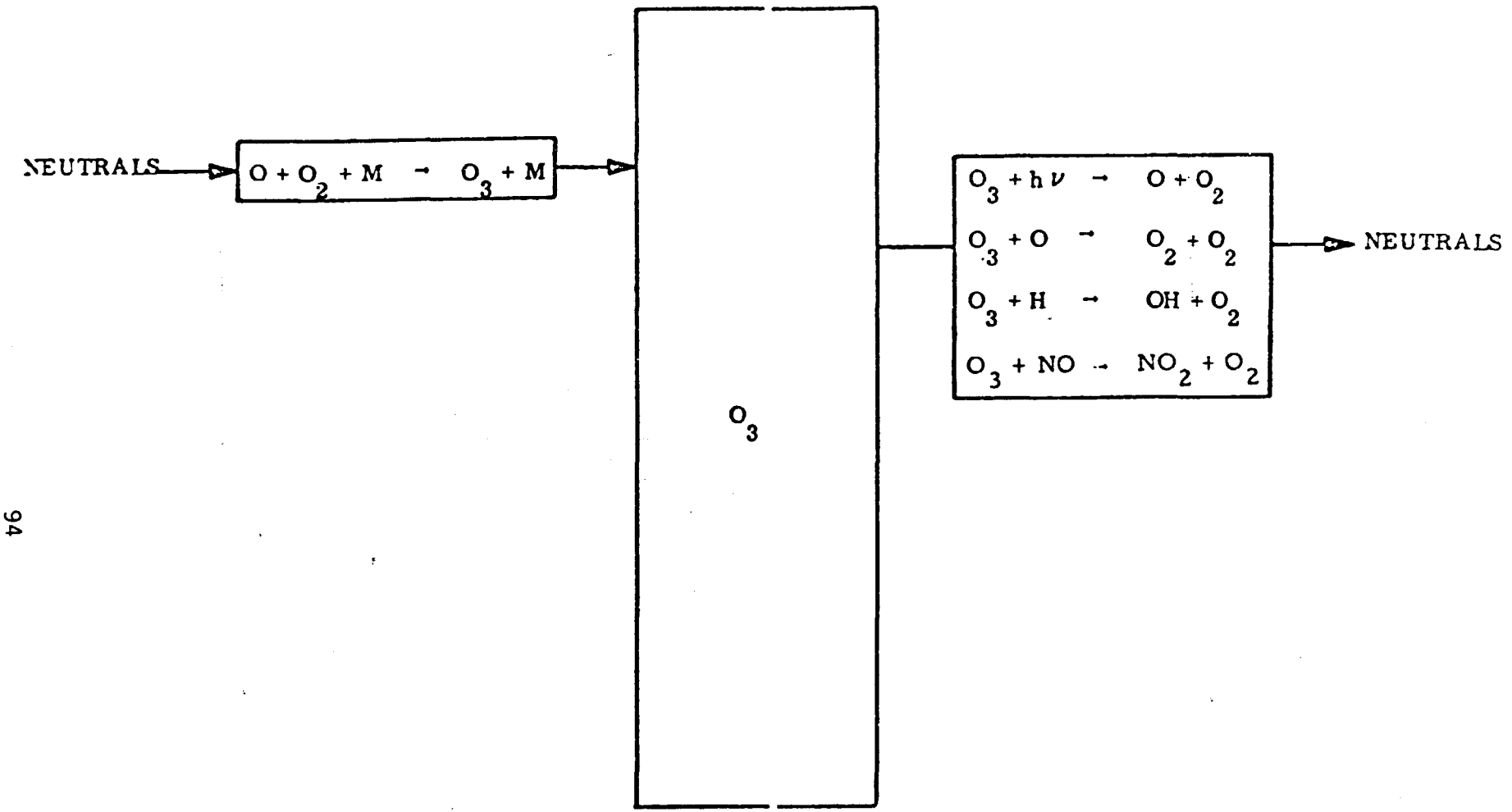

FIGURE H-8. Chemical Kinetics of Ozone

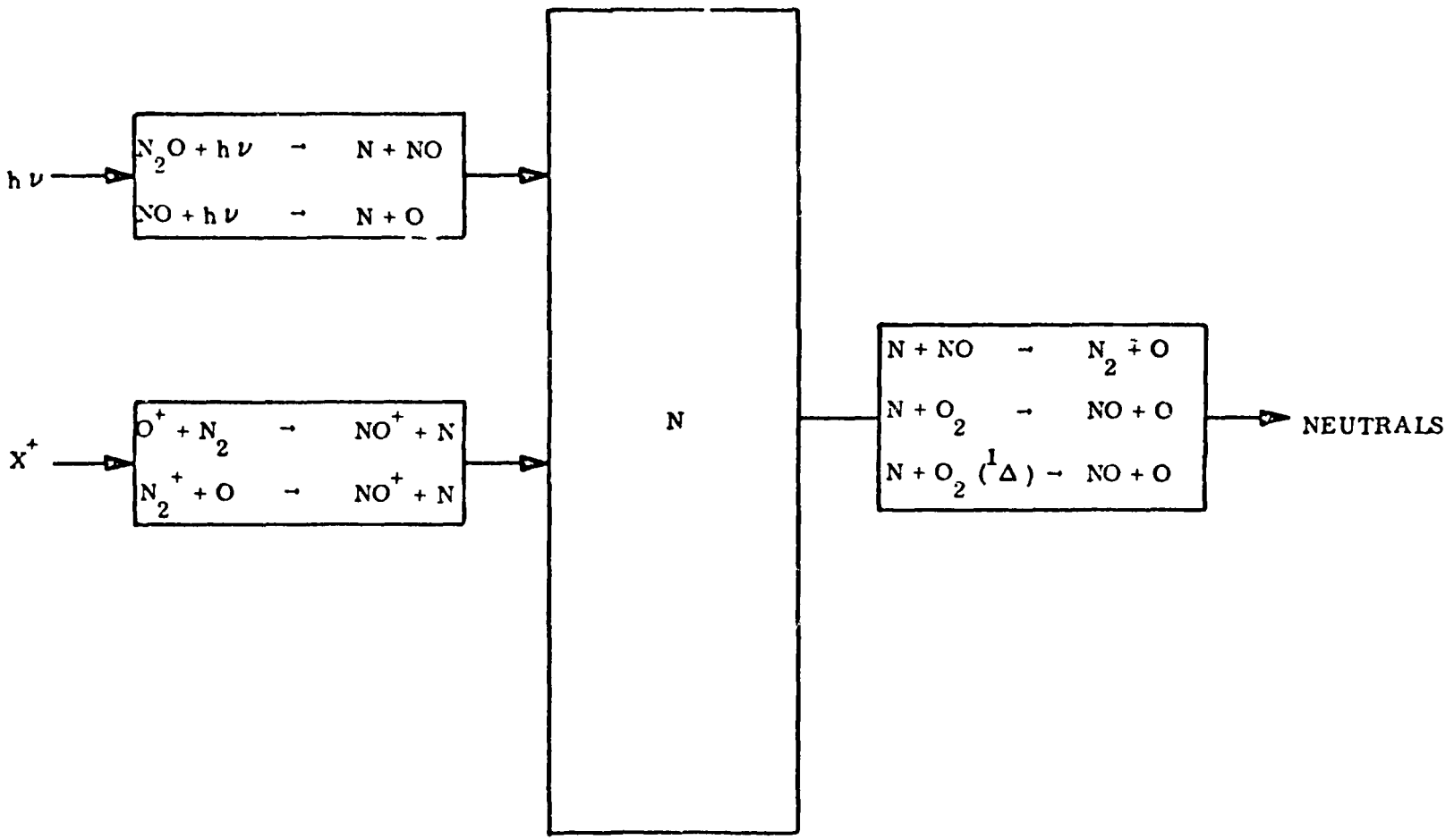

FIGURE H-9. Chemical Kinetics of Nitrogen Atoms

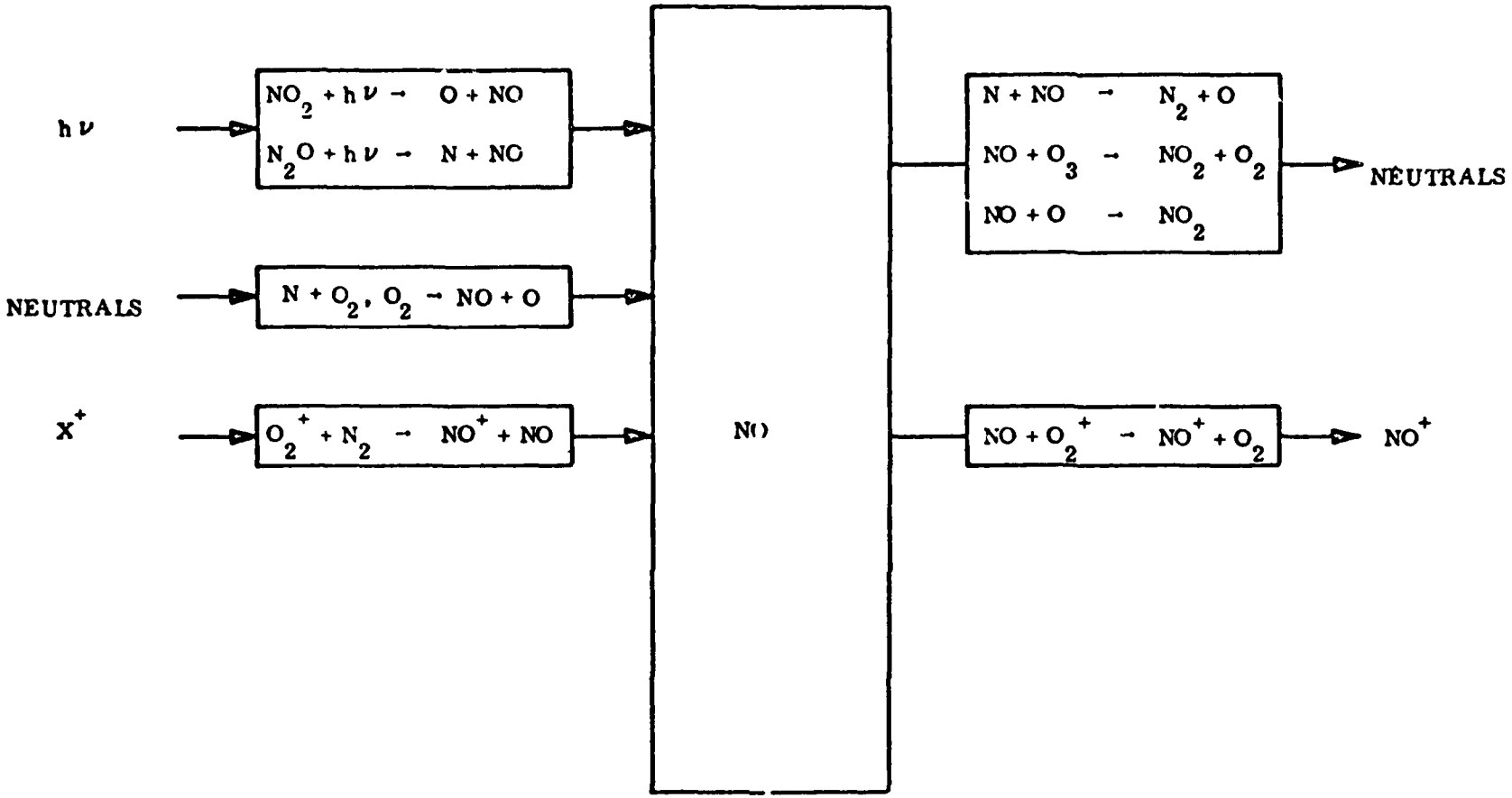

FIGURE H-10. Chemical Kinetics of Nitric Oxide

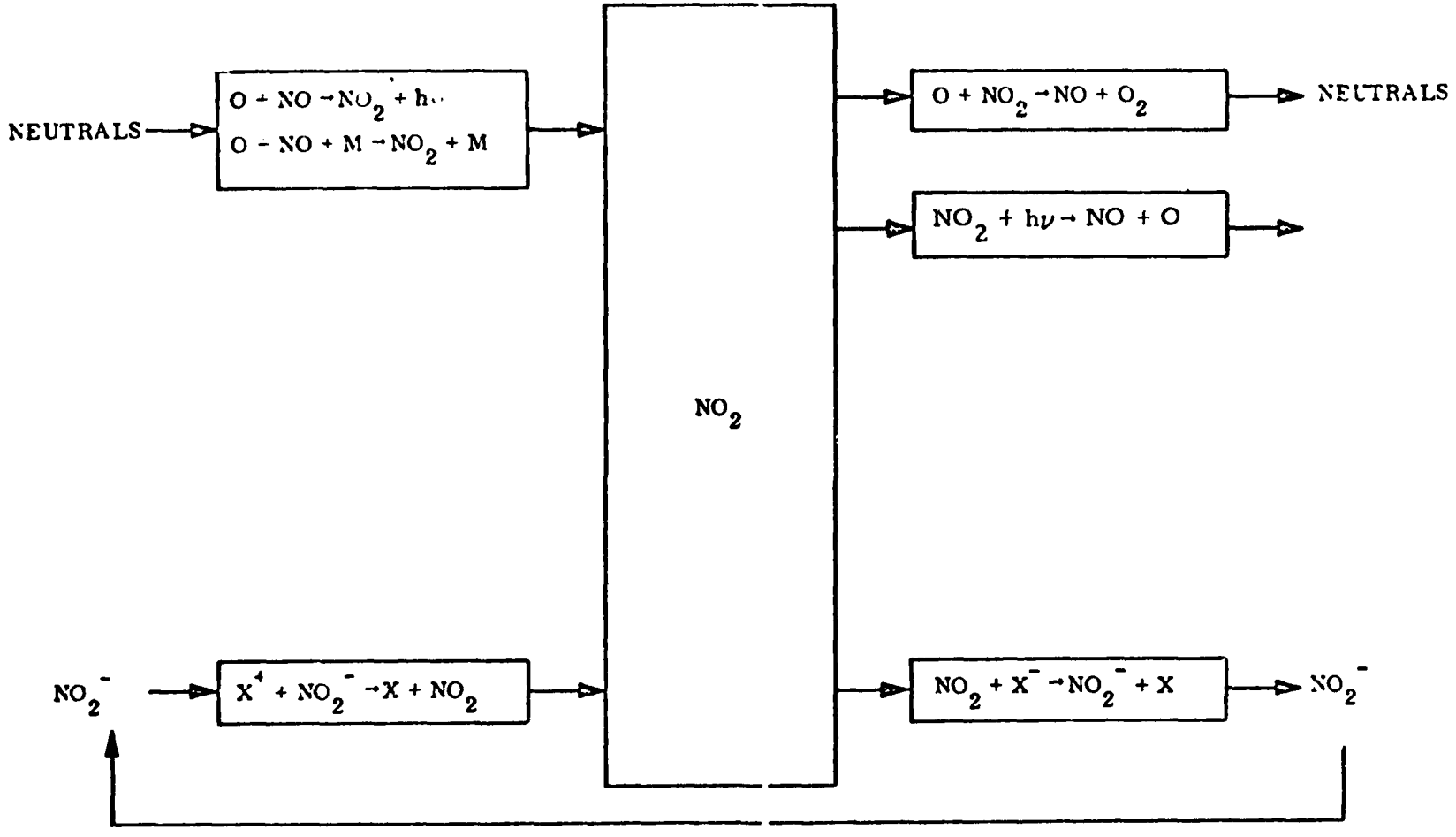

FIGURE H-11. Chemical Kinetics of Nitrogen Dioxide

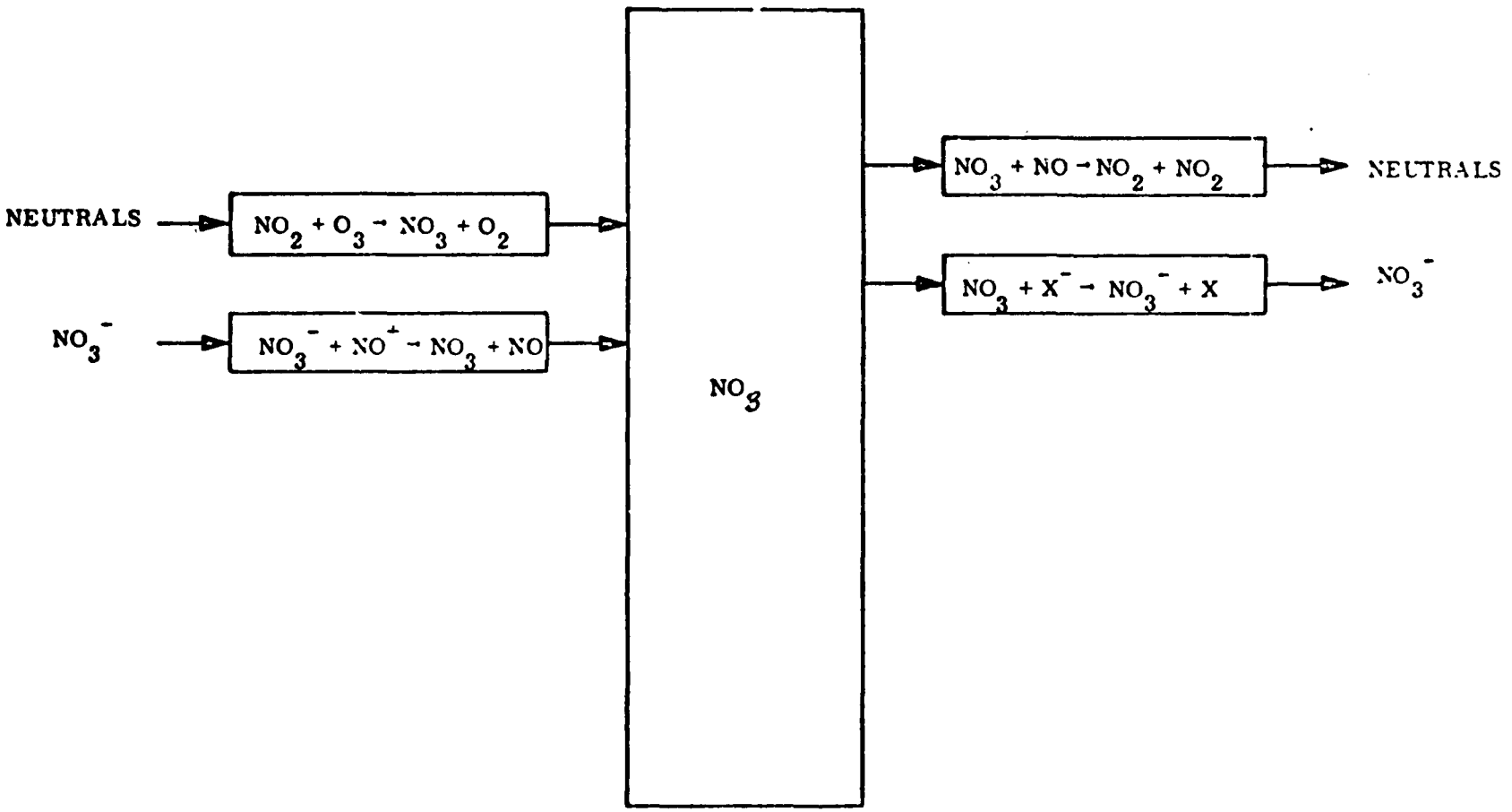

FIGURE H-12. Chemical Kinetics of Nitrogen Trioxide

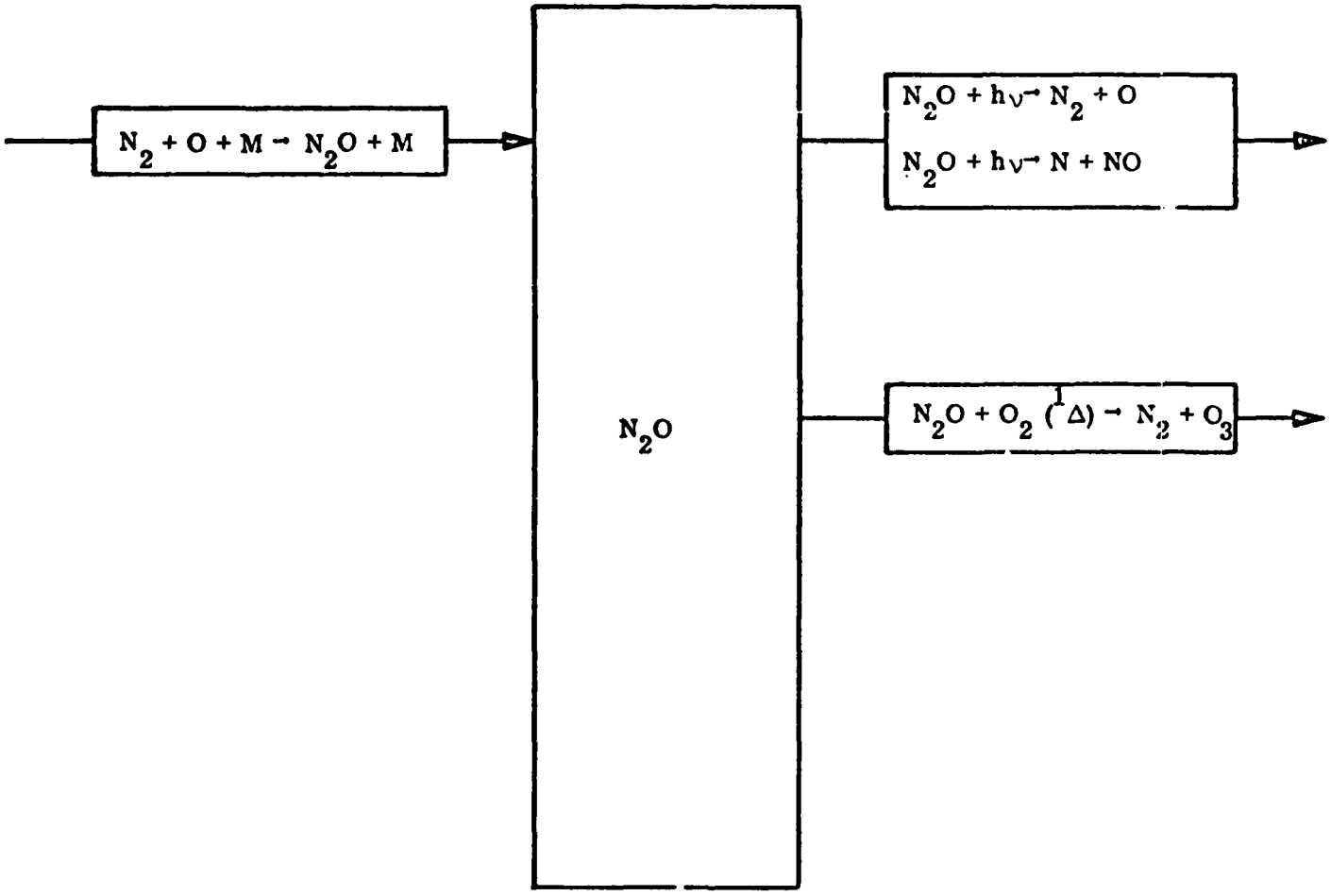

FIGURE H-13. Chemical Kinetics of Nitrous Oxide

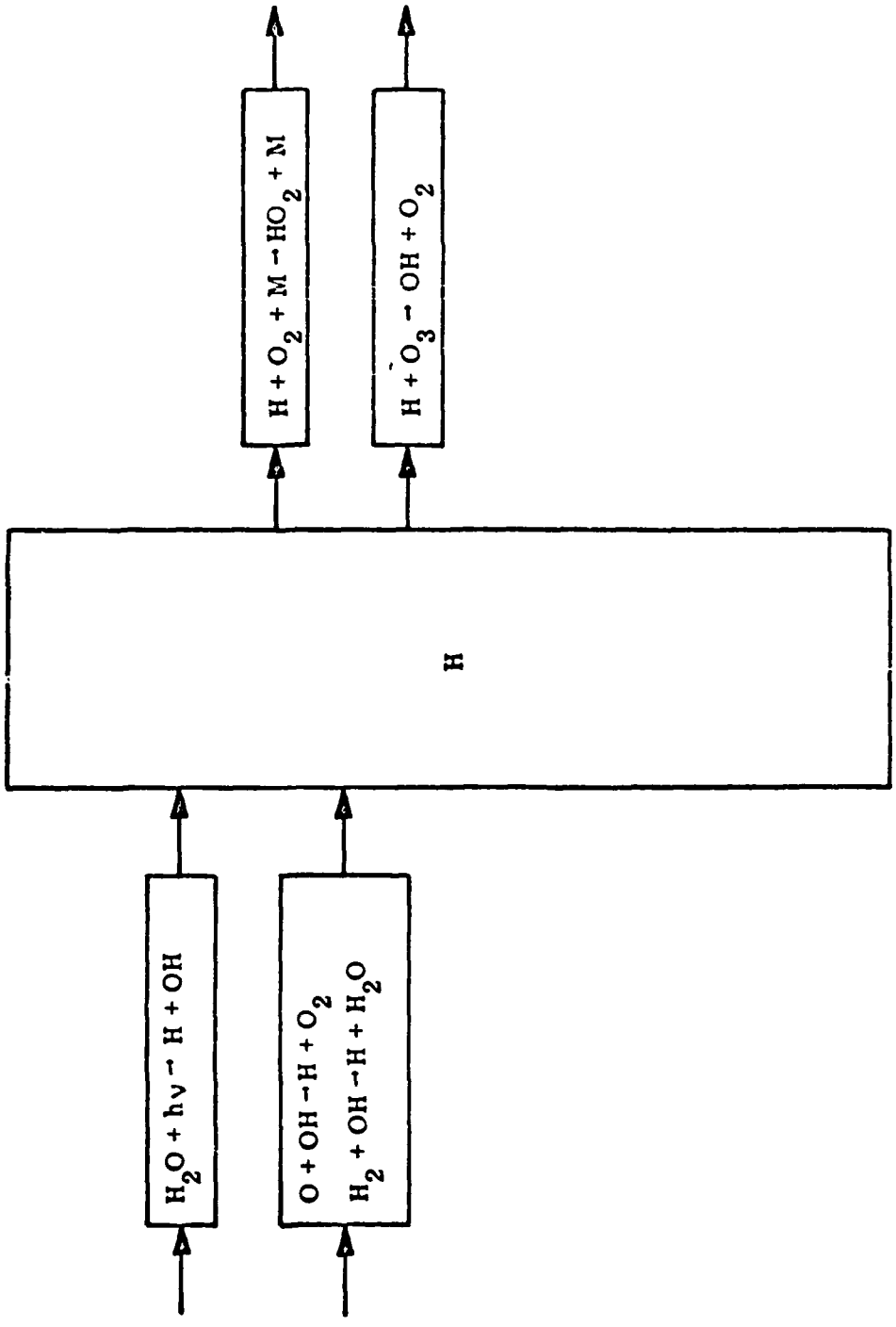

FIGURE H-14. Chemical Kinetics of Hydrogen Atoms

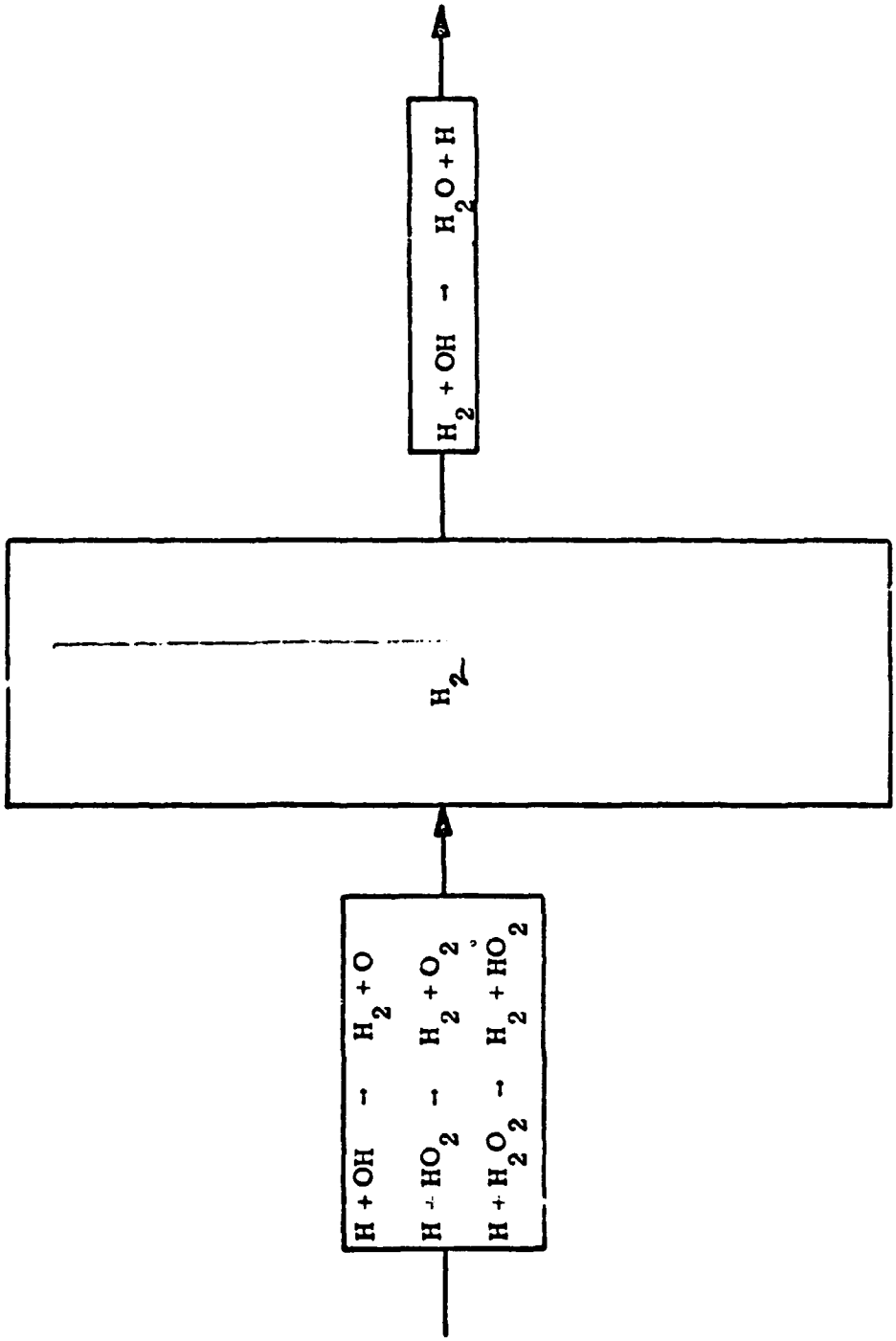

FIGURE H-15. Chemical Kinetics of Hydrogen Molecules

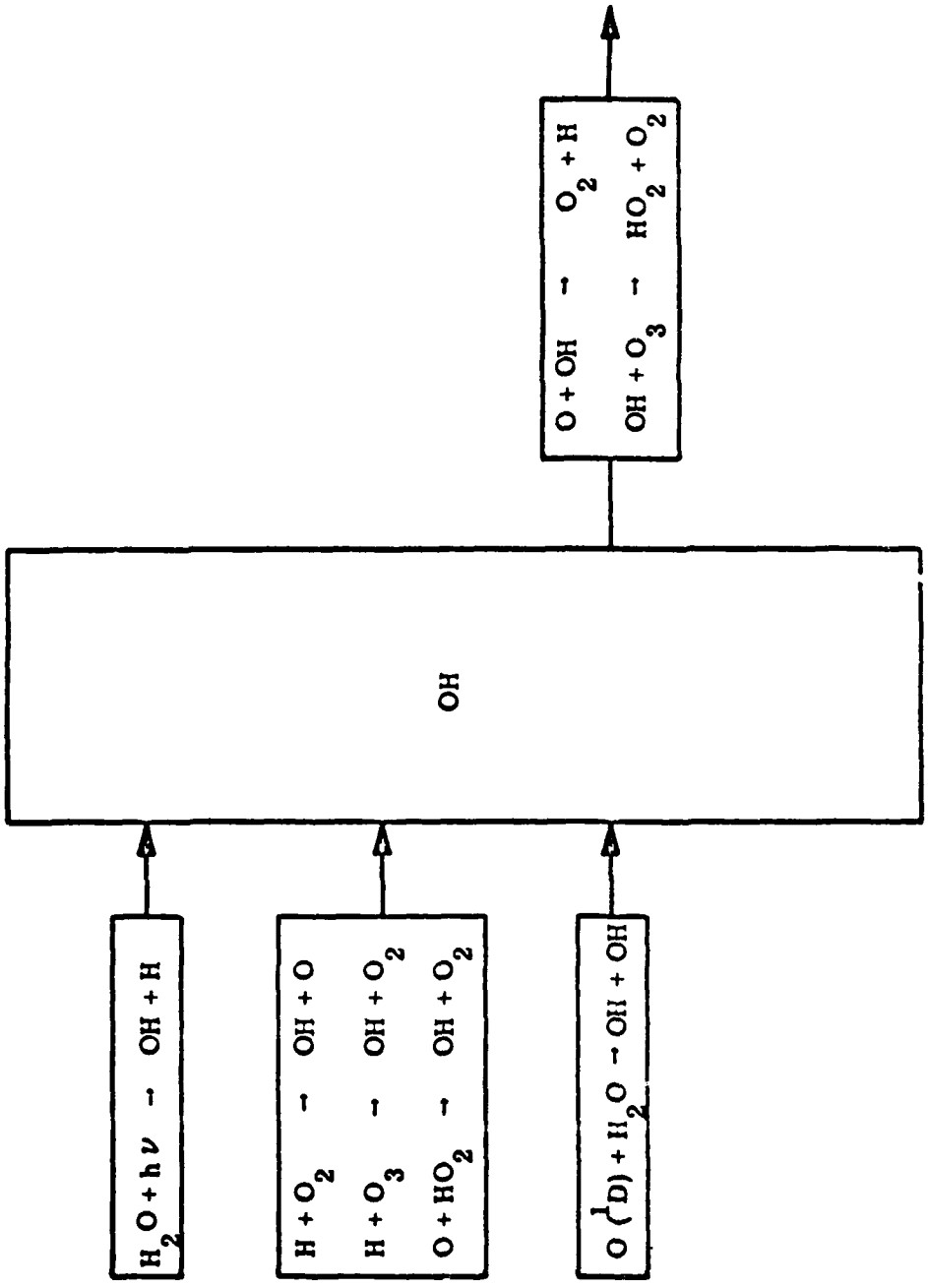

FIGURE H-16. Chemical Kinetics of Hydroxl Radicals

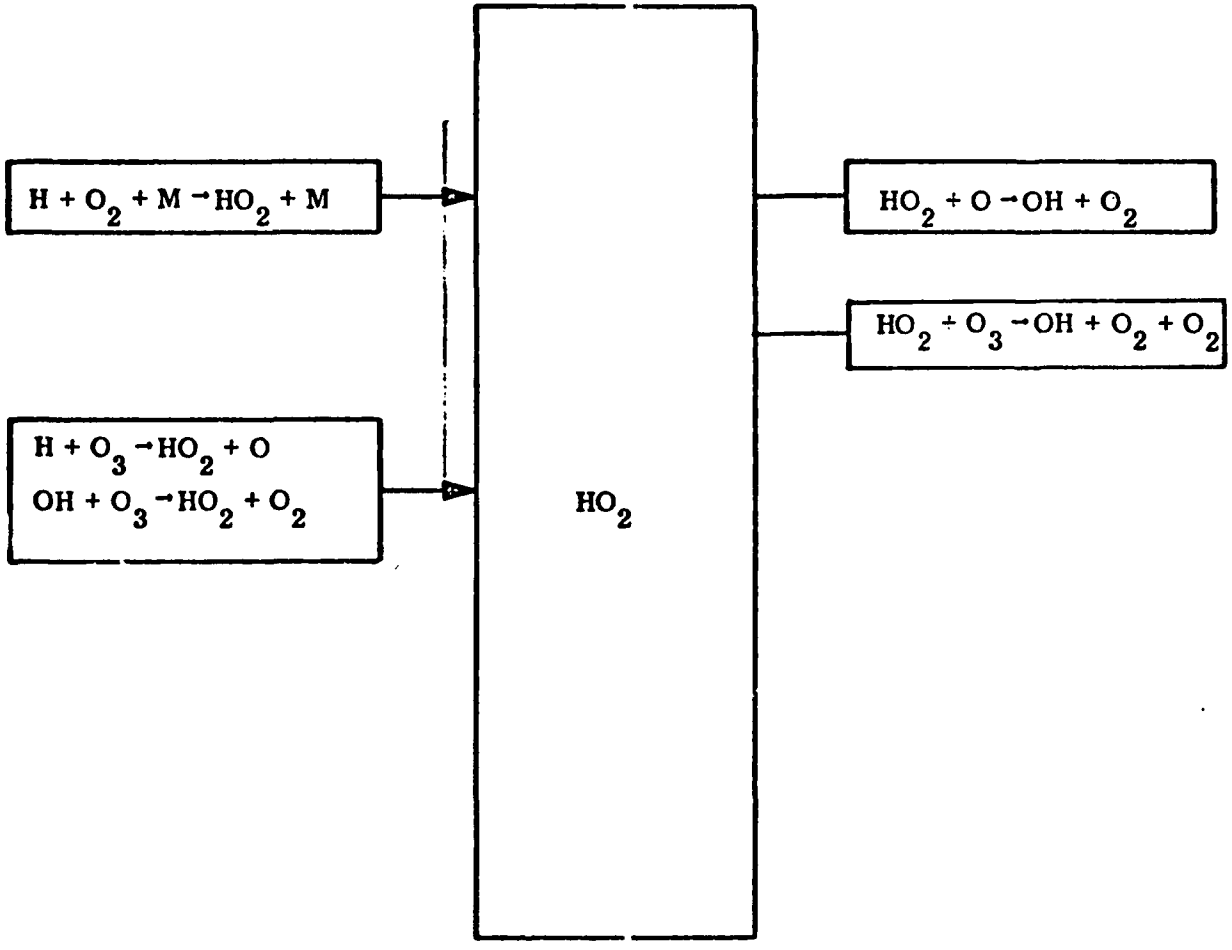

FIGURE H-17. Chemical Kinetics of HO_2 Radicals

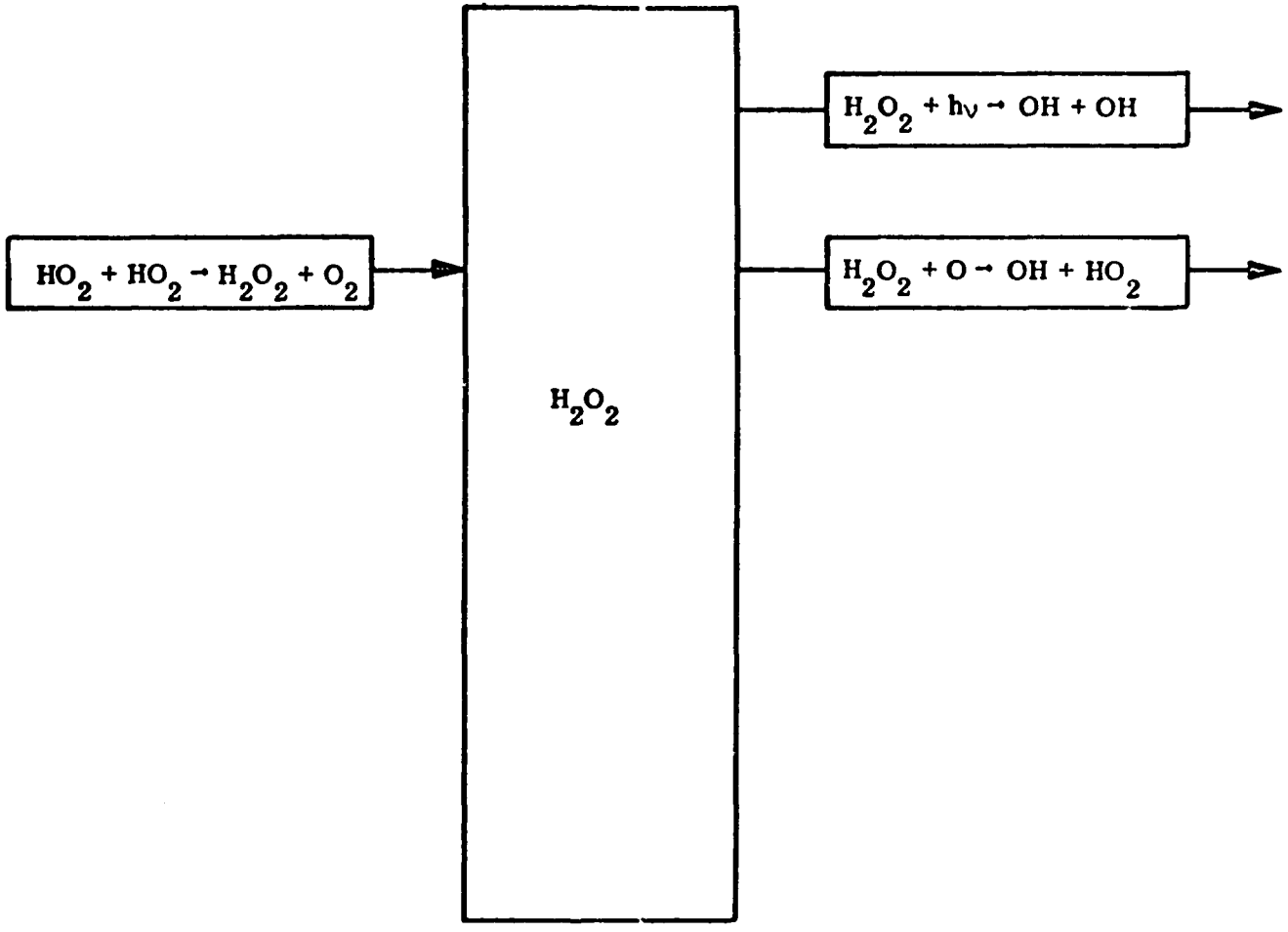

FIGURE H-18. Chemical Kinetics of Hydrogen Peroxide

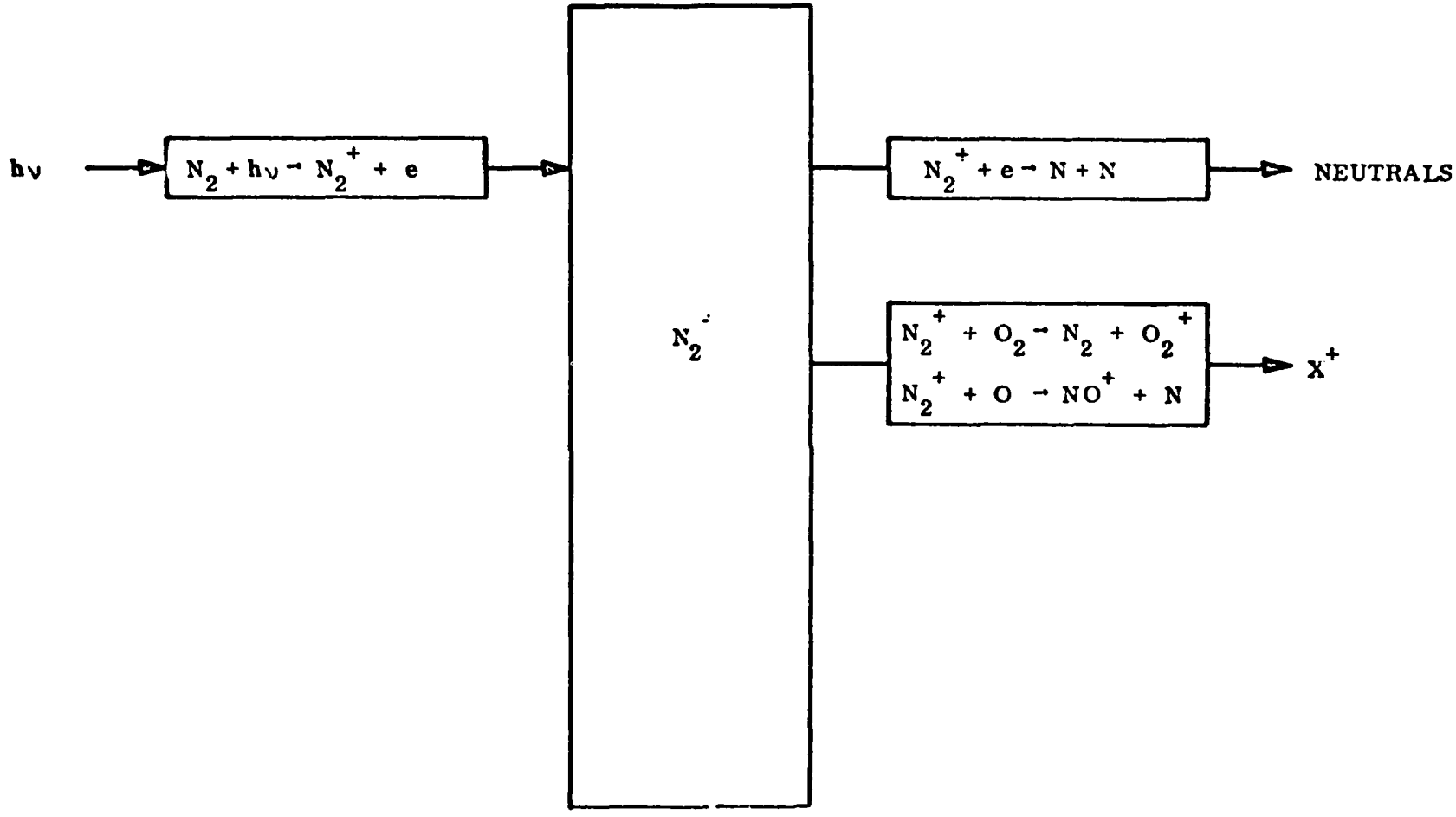

FIGURE H-19. Chemical Kinetics of Molecular Nitrogen Ions

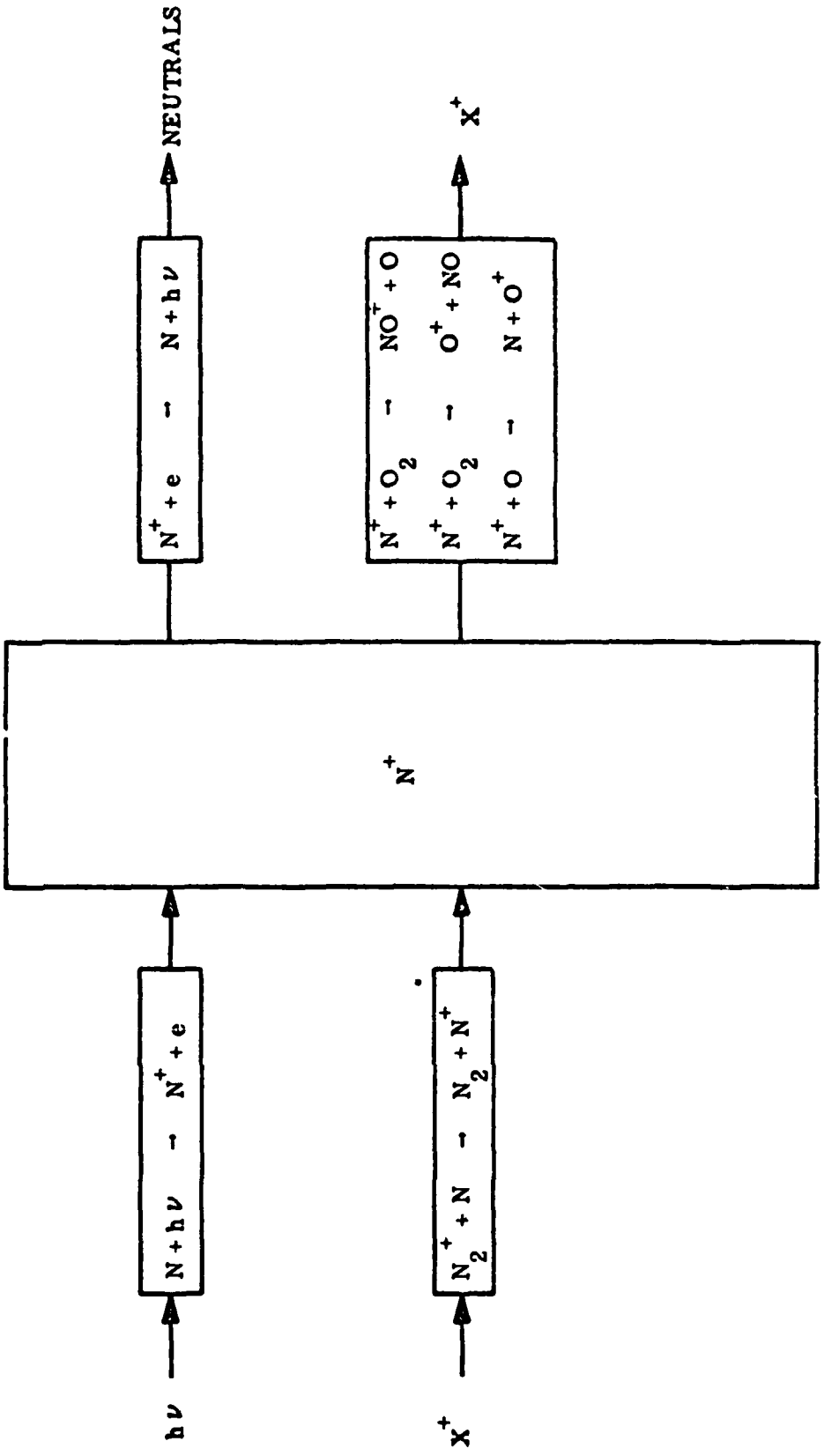

FIGURE H-20. Chemical Kinetics of Atomic Nitrogen Ions

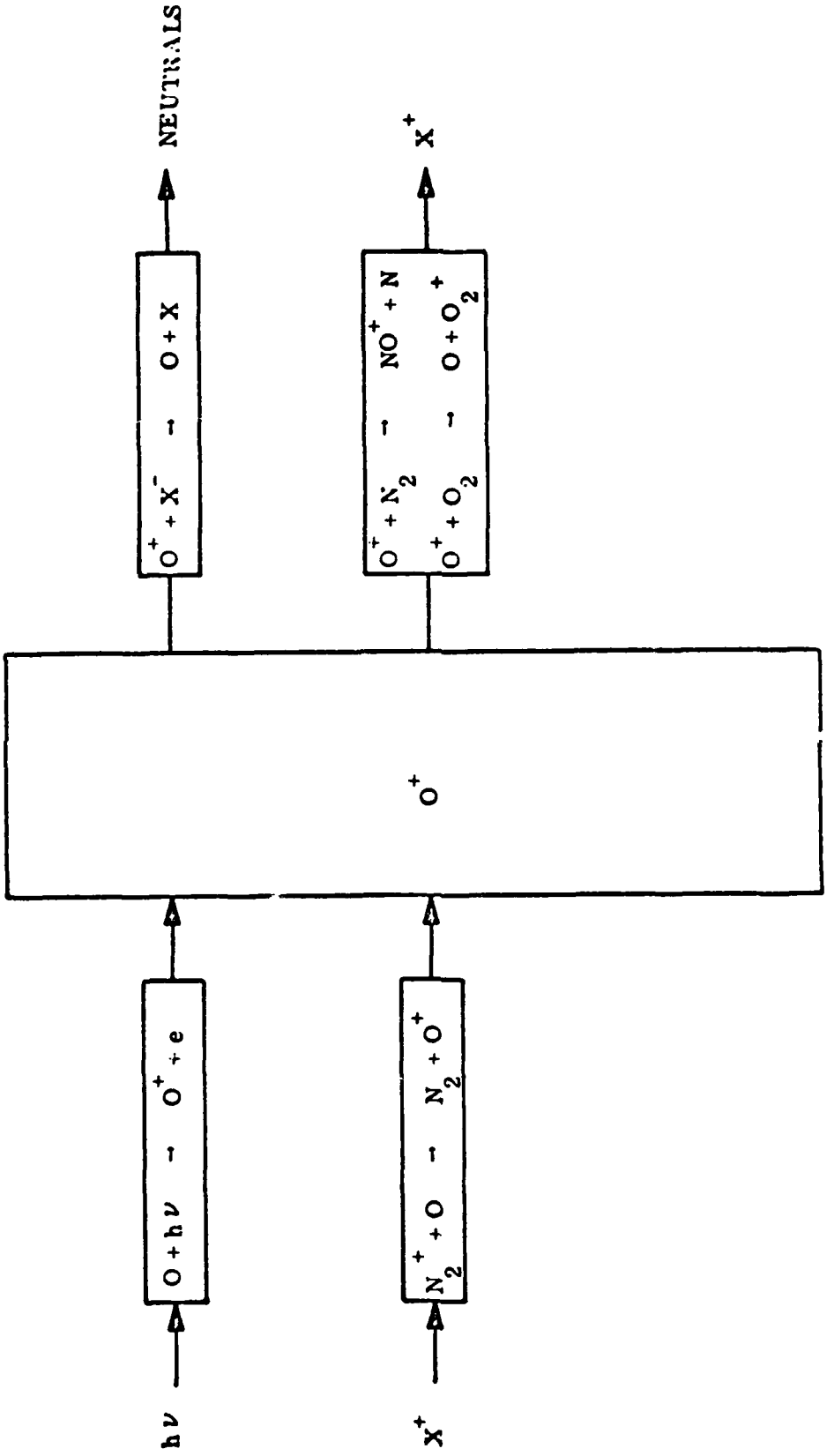

FIGURE H-21. Chemical Kinetics of Atomic Oxygen Ions

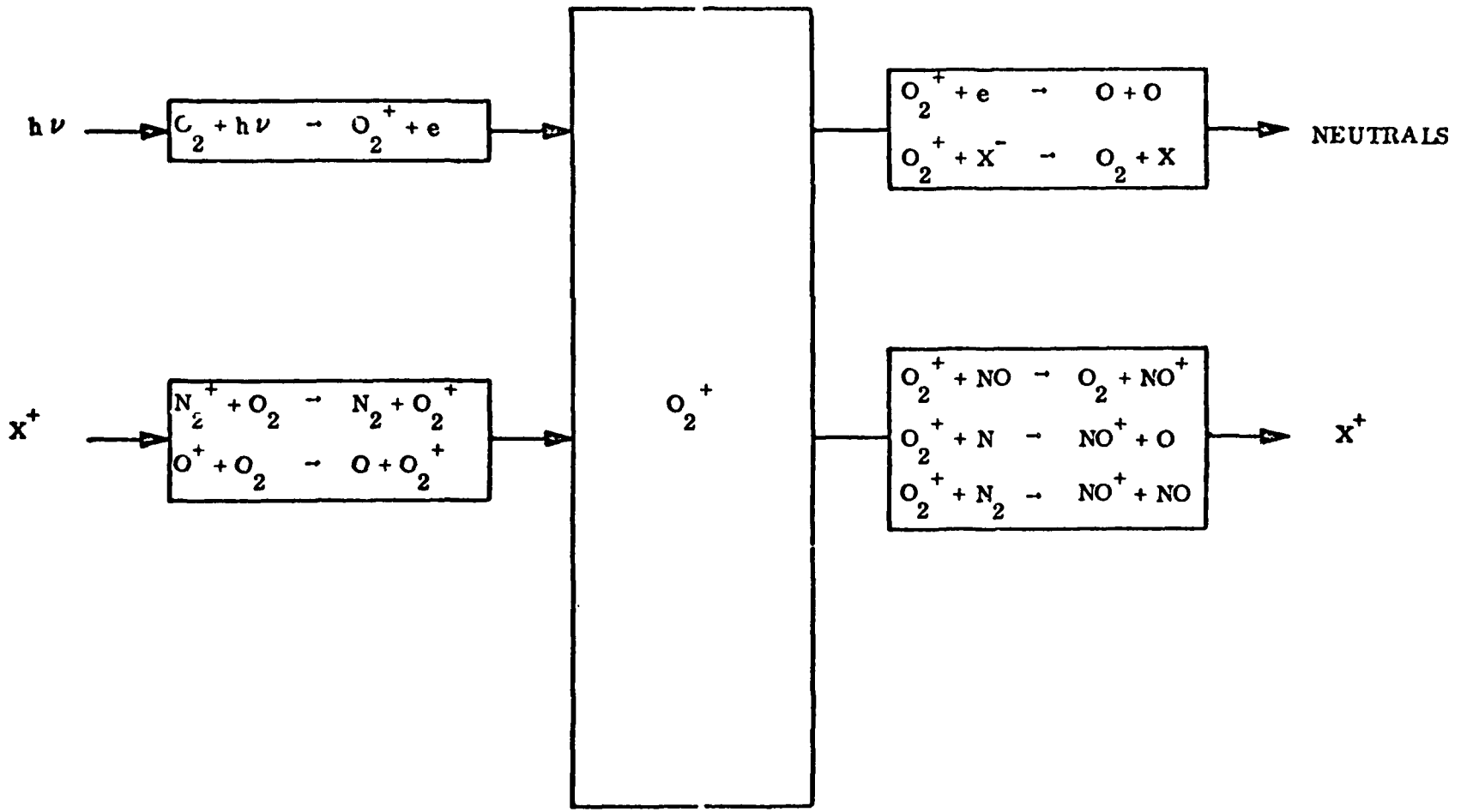

FIGURE H-22. Chemical Kinetics of Molecular Oxygen Ions

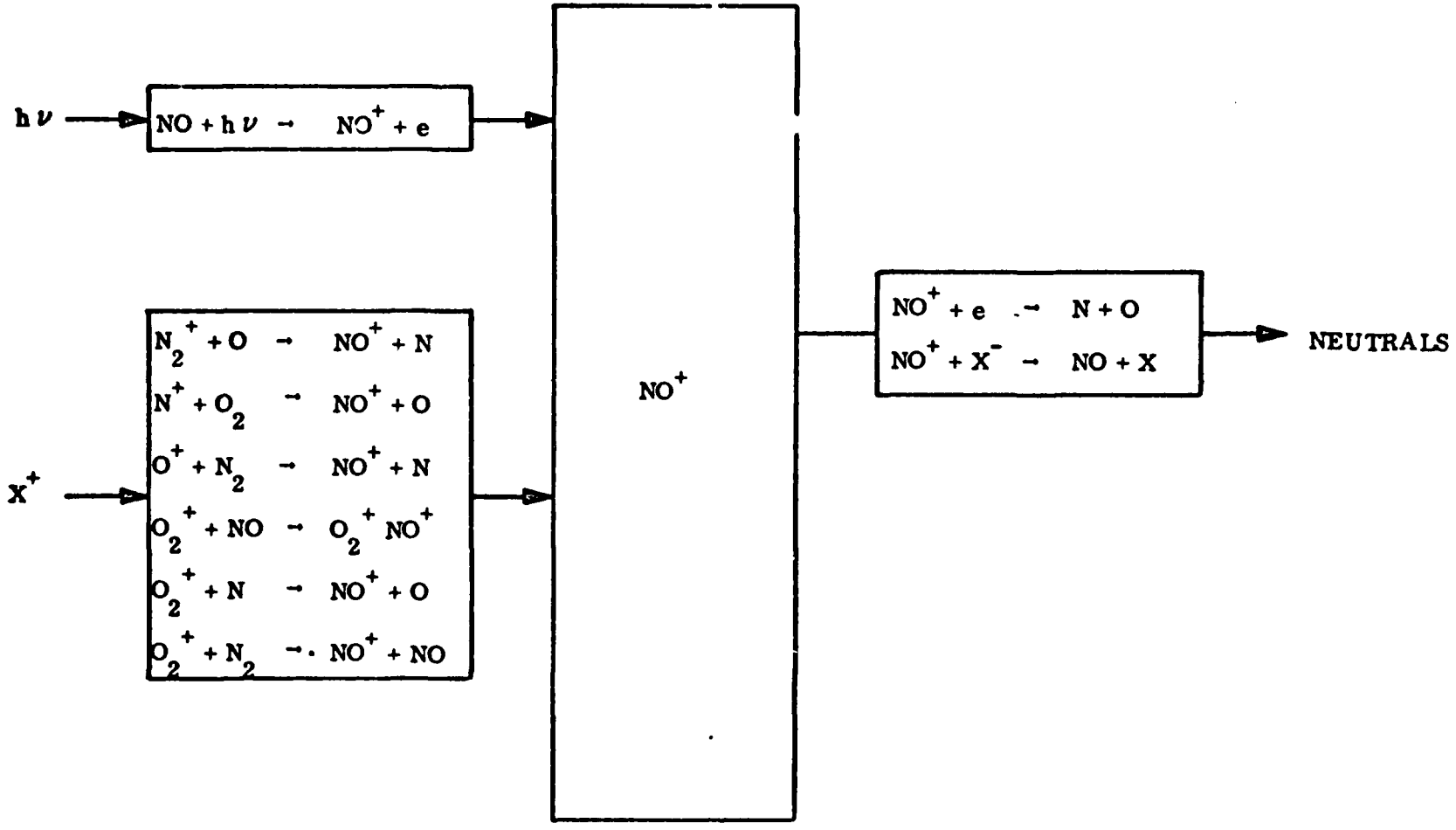

FIGURE H-23. Chemical Kinetics of Nitric Oxide Ions

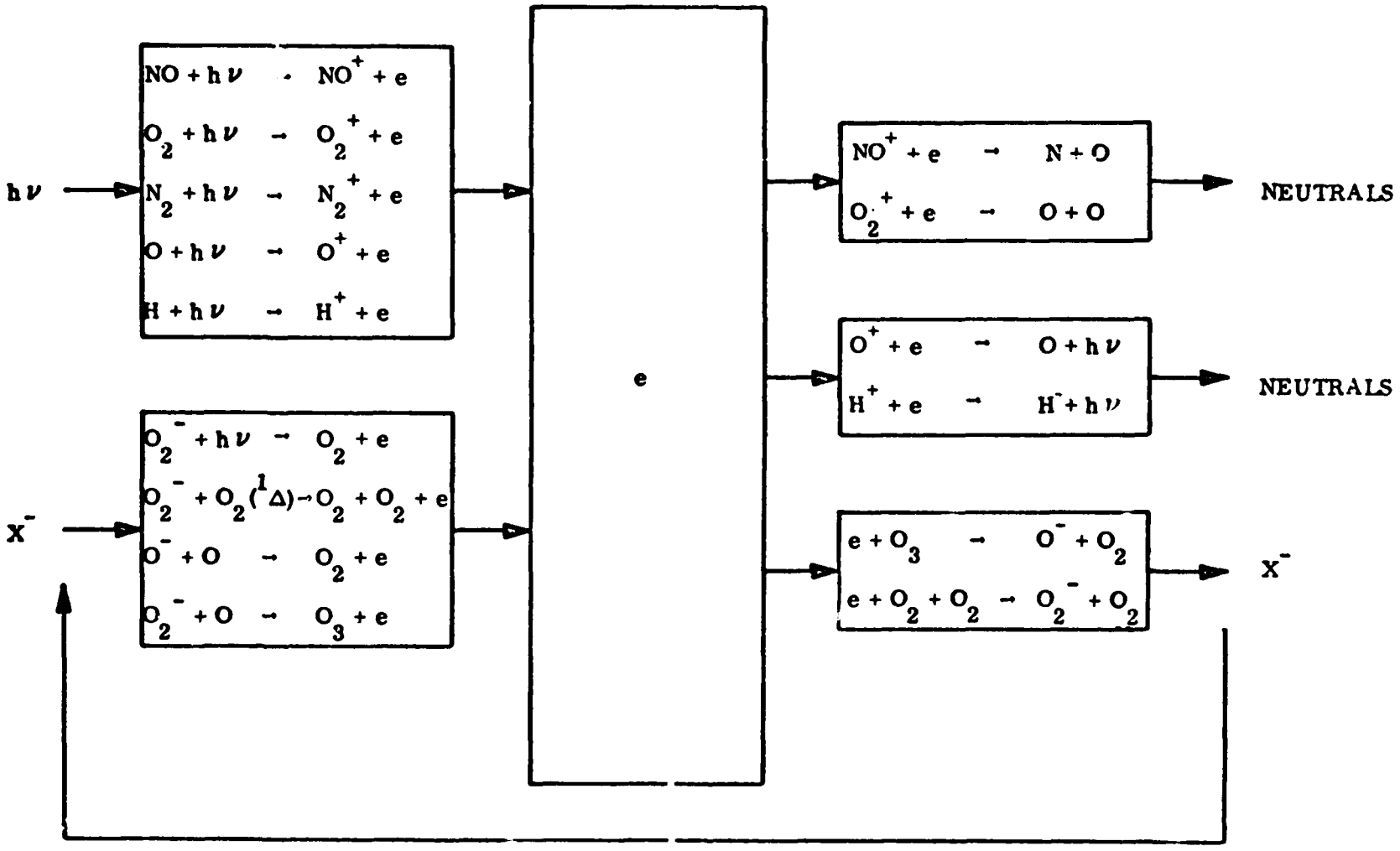

FIGURE H-24. Chemical Kinetics of Free Electrons

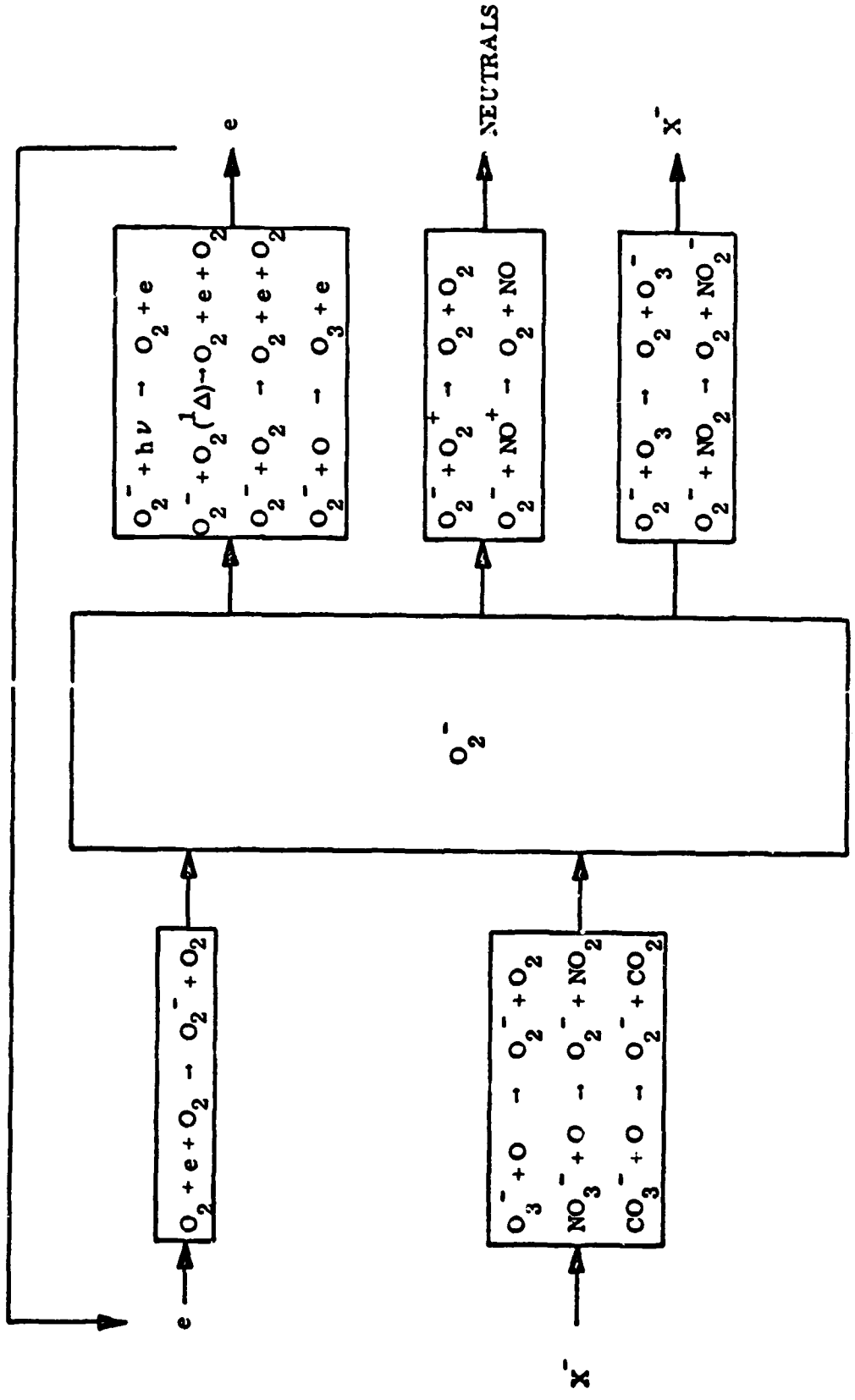

FIGURE H-25. Chemical Kinetics of Negative Molecular Oxygen Ions

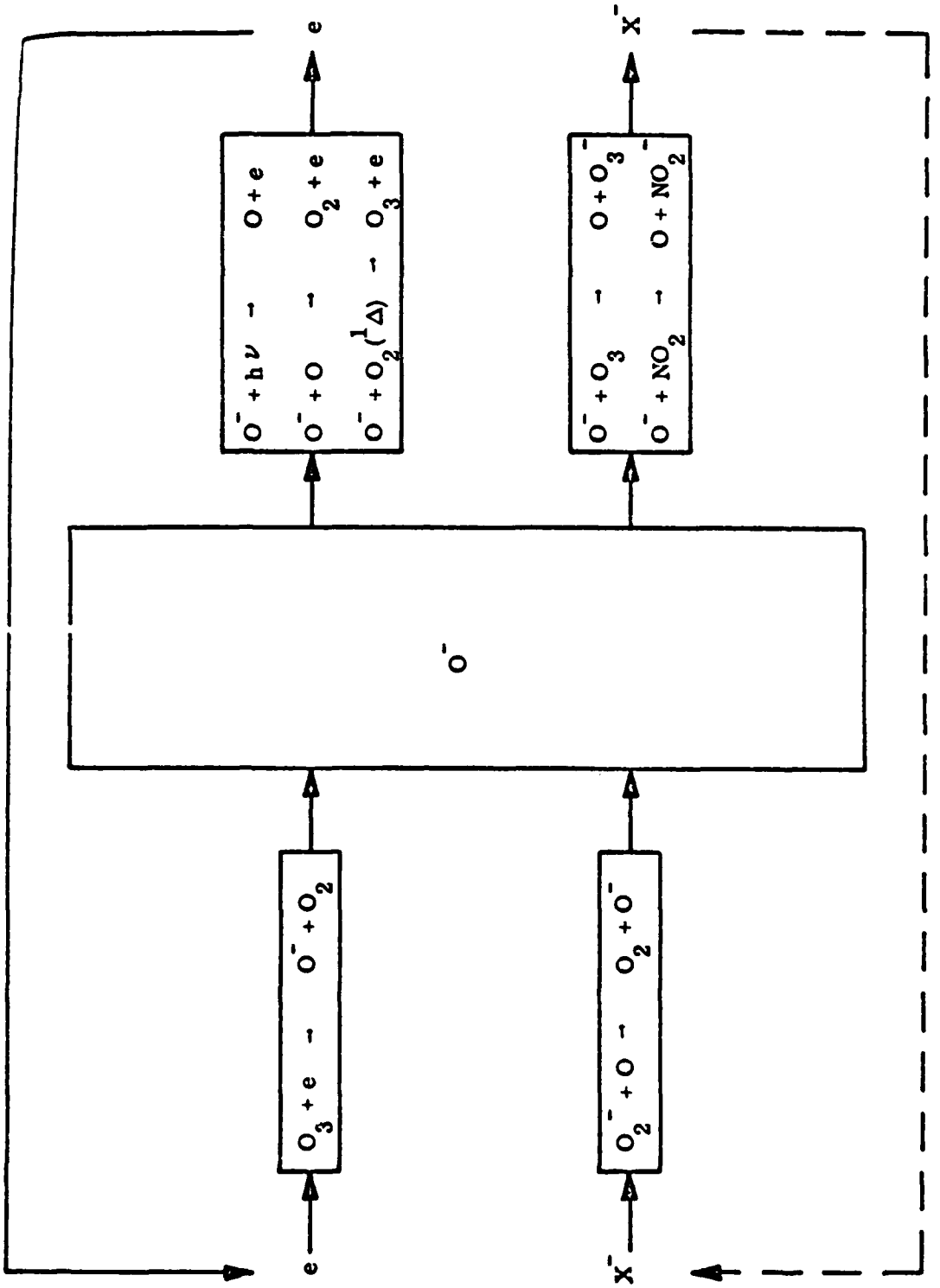

FIGURE H-26. Chemical Kinetics of Negative Atomic Oxygen Ions

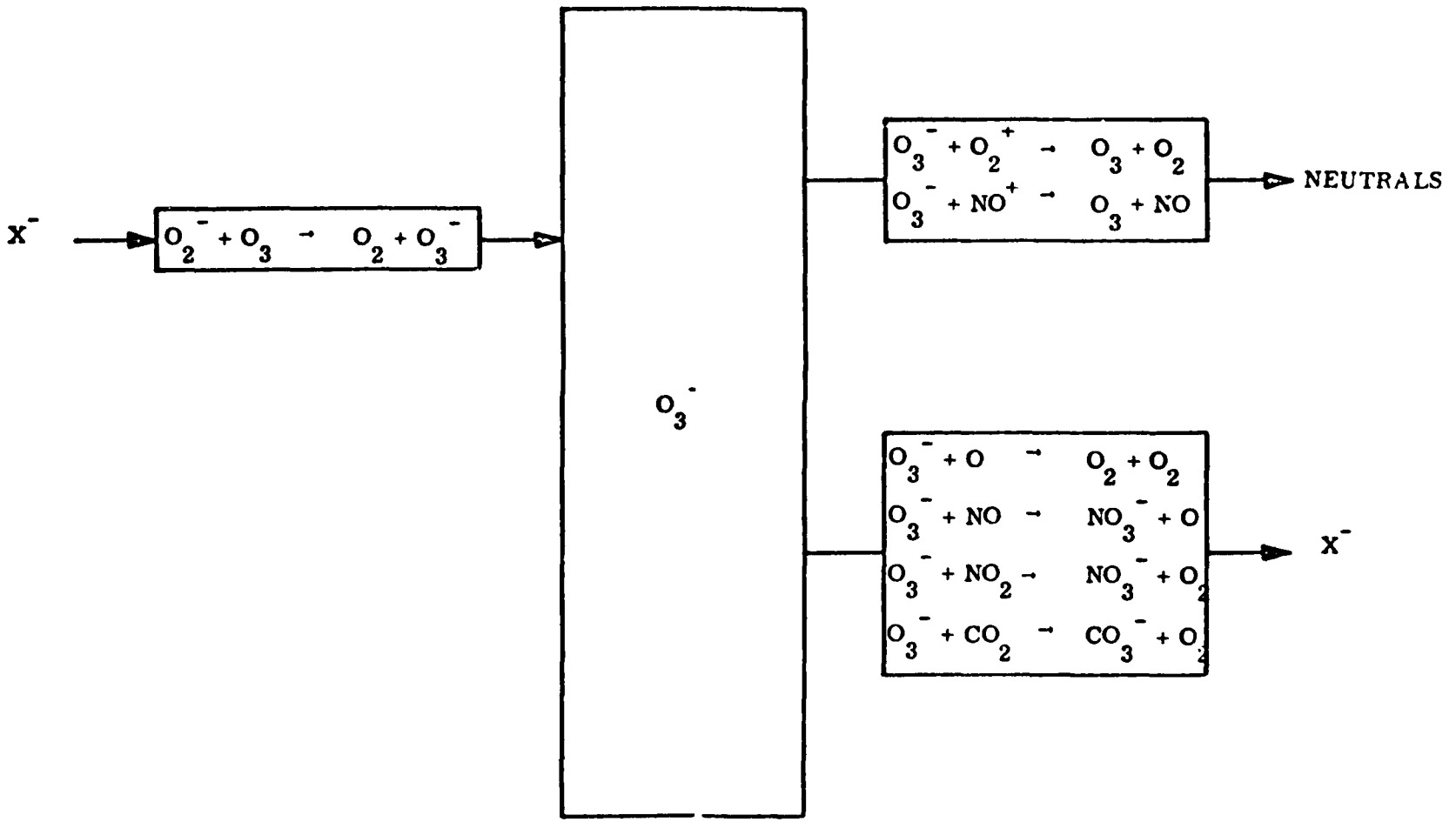

FIGURE H-27. Chemical Kinetics of Negative Ozone Ions

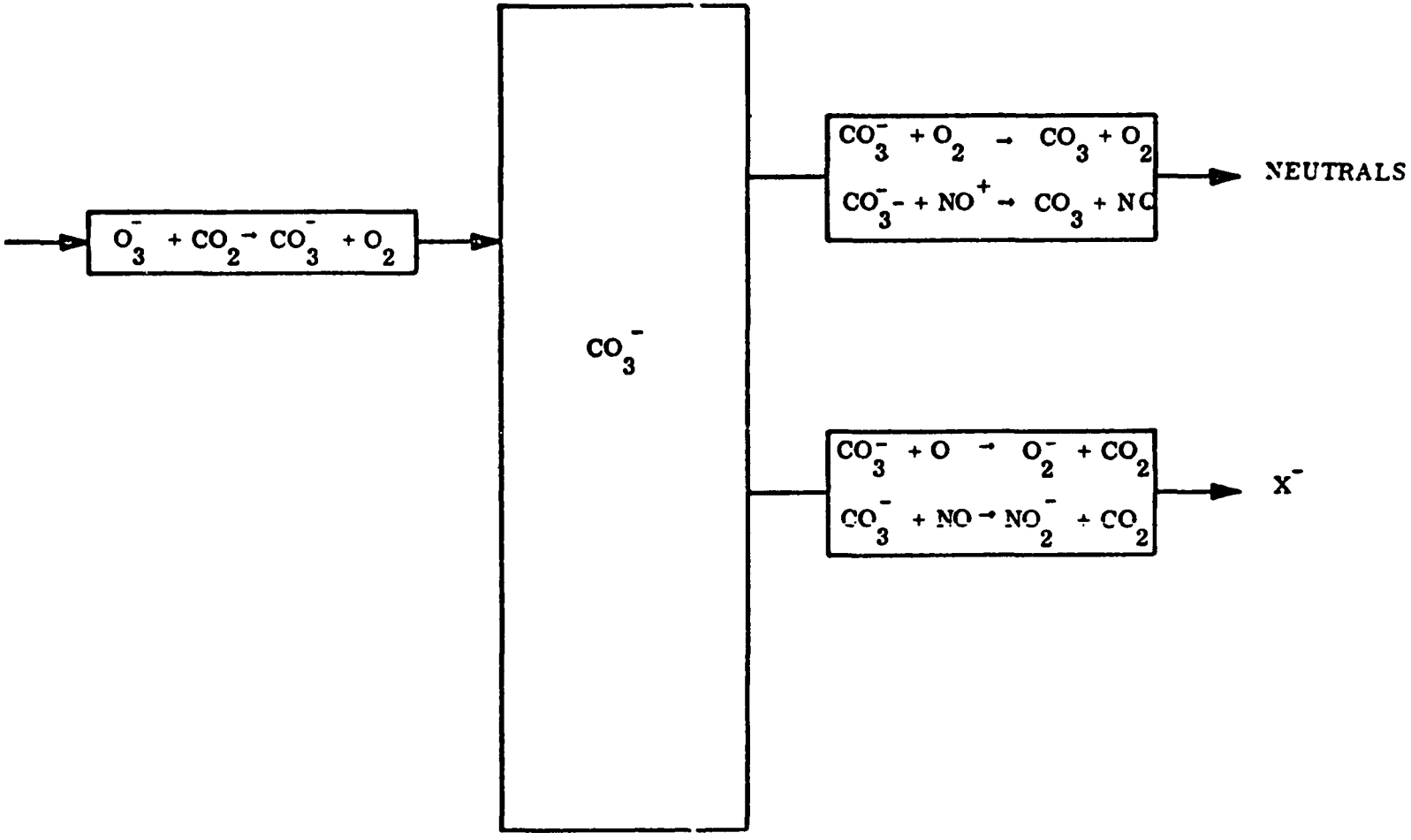

FIGURE H-28. Chemical Kinetics of Negative Carbon Trioxide Ions

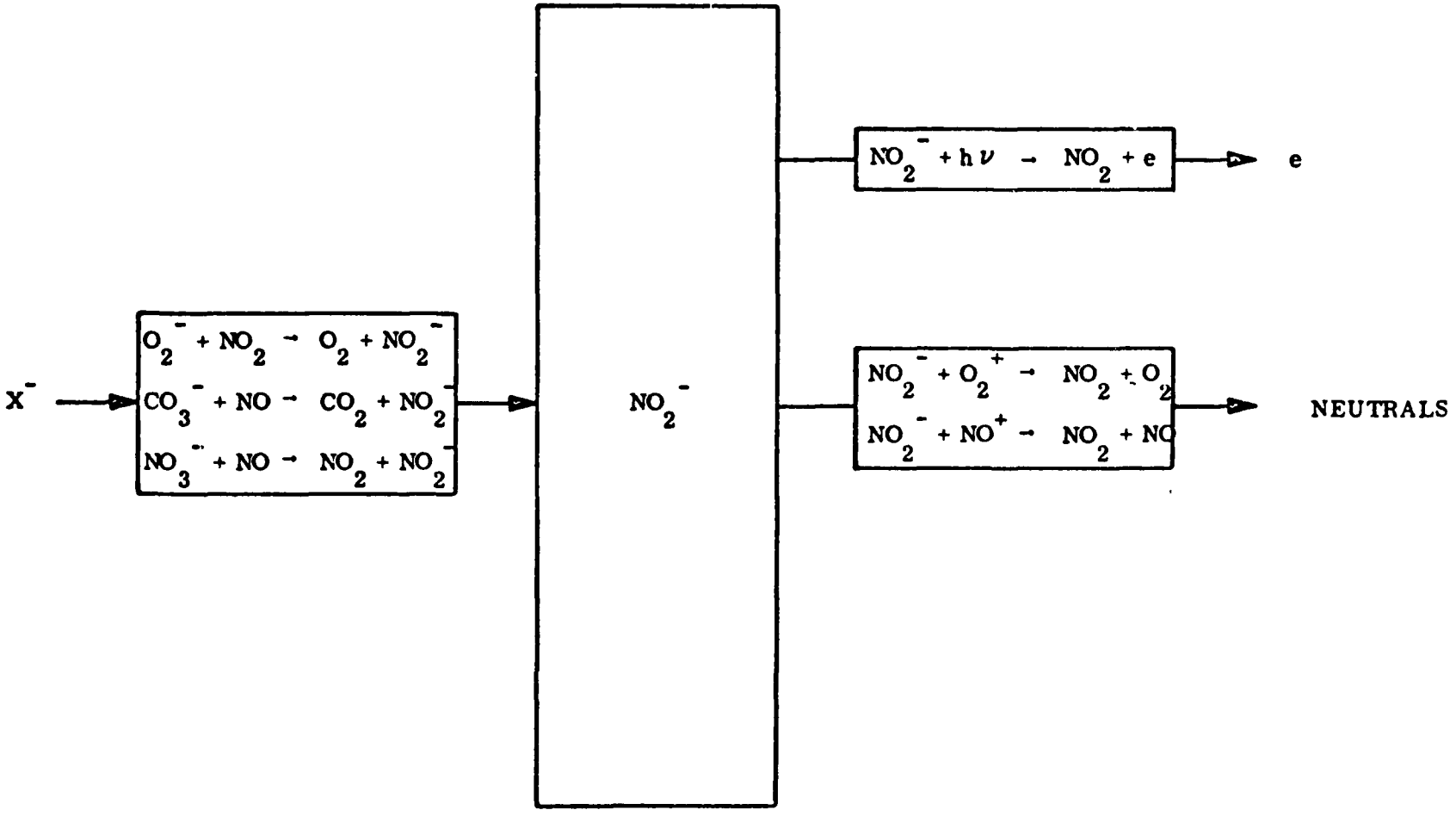

FIGURE H-29. Chemical Kinetics of Negative Nitrogen Dioxide Ions

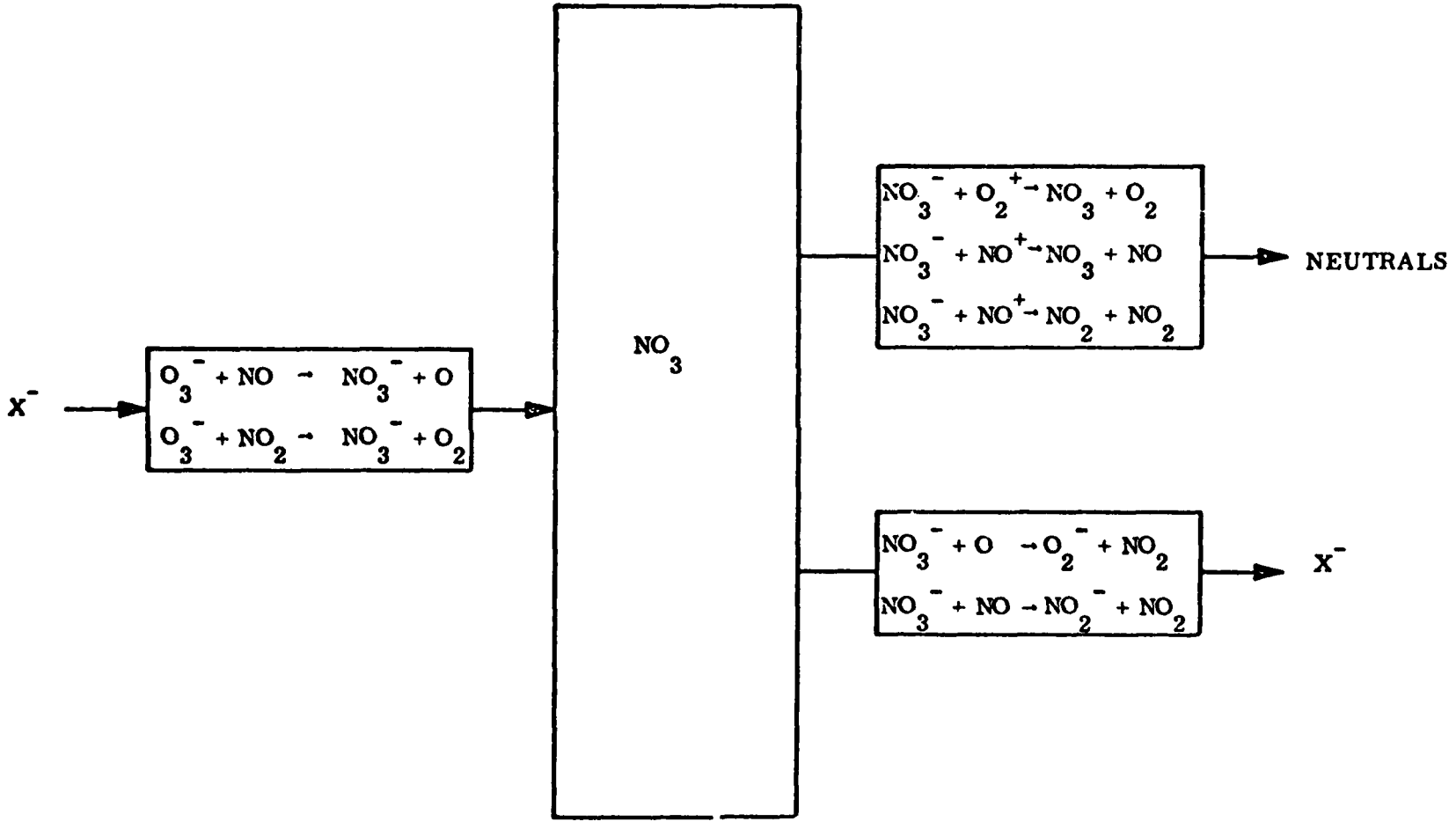

FIGURE H-30. Chemical Kinetics of Negative Nitrogen Trioxide Ions

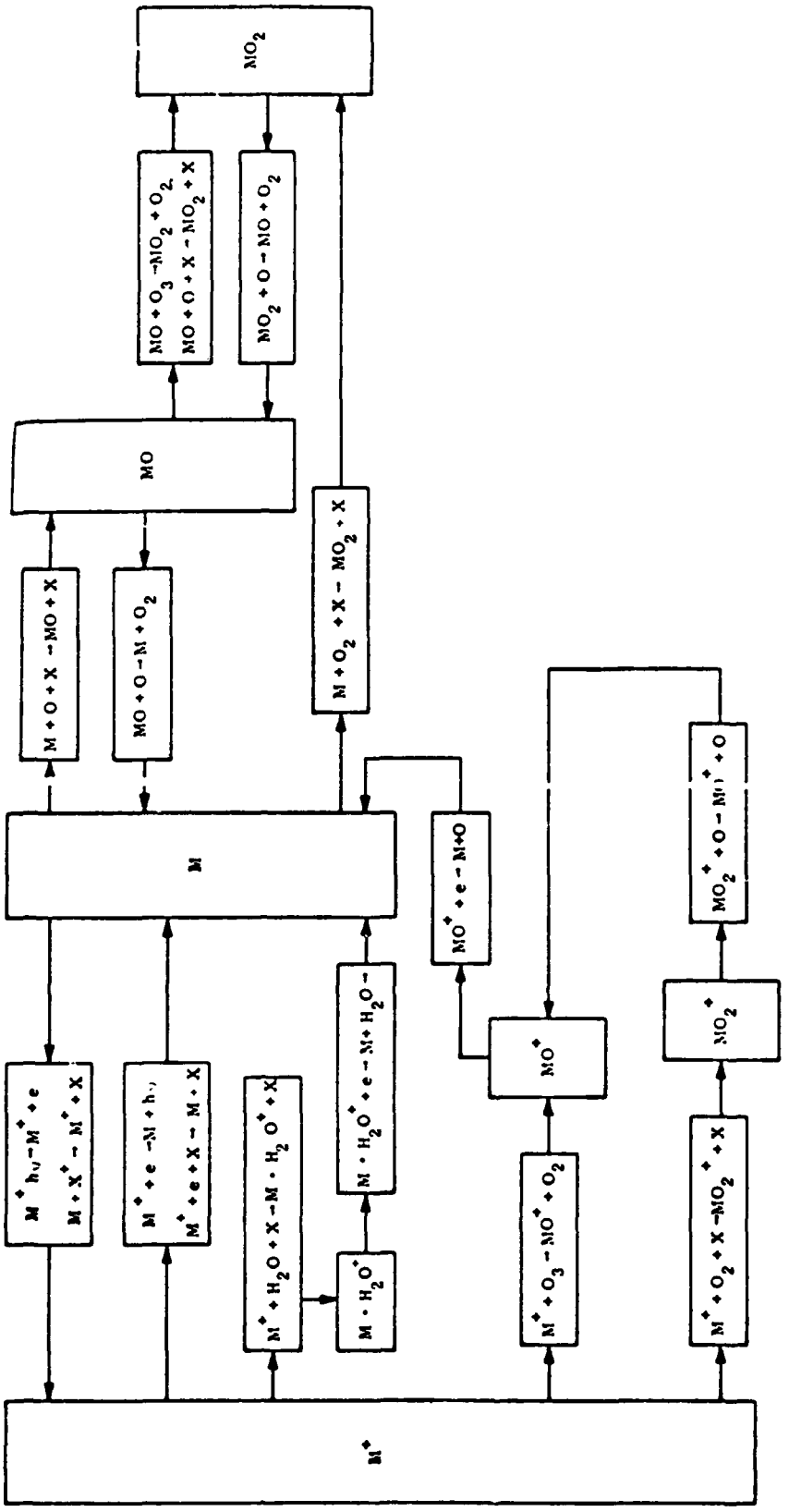

FIGURE H-31. Chemical Kinetics of Metal Atoms, Metal Oxide Molecules and Metal Ions of Na, Mg, Cu.

ANNEX I

RADIATION ENERGY AND HEAT EQUATIONS

INTRODUCTION

The Stratosphere-Mesosphere-Thermosphere as given in Appendix E is based on the grid structure and differenceing schemes of the Leith Tropospheric model, with radiation energy, heat equations, electromagnetic effects, etc., as added features. In order to get some idea of the extra computational load imposed by the added features, each was to be assessed in order. After looking at the radiation energy and heat equations, it became apparent that the remaining effects would not contribute significantly to the load and their detailed analysis was abandoned.

This Annex presents the analysis of the radiation energy and heat equations.

EQUATIONS

The radiation energy equation uses as its variable input data the values I_m, which are received from the SOLRAD HI satellite. These values are assumed to change hourly. The equation convolves this information along with other known information about the constituents of the upper atmosphere to produce coefficients for a set of simultaneous linear equations. The solution of these equations produces the number density of each constituent of the atmosphere at each designated level in the model.

The stratosphere is divided into 6 layers, the mesosphere into 8 layers, the lower thermosphere into 6 layers, and the upper thermosphere into 8 layers, for a total of 28 layers.

The data sets involved in the radiation energy equation and their origin or disposition are given in the following list:

$\sigma_{i,j}$(or $\sigma_{m,\ell}$) - Given array (time independent)

F(X) - Given table (30 to 100 values)

I_m - SOLRAD-HI input values

IP_ℓ - Given constants

$J_{\ell,m}$ - Intermediate results

$\Sigma J_{\ell,m}$ - Intermediate results (save for heat equation)

S_ℓ - Input to simultaneous equations (see Eq. I-1 below)

n_ℓ - Results of simultaneous equations

N_j - Recursion formula

G - Matrix of values selected from S_ℓ and R_ℓ using Annex H

R_ℓ - Given constants that go into G-matrix.

The equations to be solved and the definition of the indices are given below in Table I-1. The indices are as follows:

TABLE I-1. EQUATION INDICES

Domain	Computation Cycle		Limits
	t	t-1	
Components		j	≤ 42
Wave bands		i	≤ 20
Altitude levels	k	k - 1	31

Equations, based on Equations 32 and 33 of this Appendix are the following:

$$S_\ell = \frac{1}{IP_\ell} \sum_{m=m_o}^{M} \underbrace{\sigma_{m,\ell}\left\{I_m \exp\left[-F(X) \sum_j \sigma_{i,j} N_j (k-1)\right]\right\}}_{J_{\ell,m}}, \quad \text{(I-1)}$$

$$n_{\ell} = \left[\begin{array}{l}\text{Solution of } \ell \times \ell \\ \text{simultaneous} \\ \text{equations}\end{array}\right] , \qquad \text{(I-2)}$$

$$N_j(k) = N_j(k - 1) + n_j(k - 1) , \qquad \text{(I-3)}$$

where $n_{\ell}(k)$ are the results of the solution of the $\ell \times \ell$ simultaneous equation set. (See Equation 37 of this Appendix.)

$$Q^{t+1} = Q^t + \Delta t \left[\sum_{\ell} n_{\ell} \sum_{m} J_{\ell,m}\right] . \qquad \text{(I-4)}$$

TIMING ANALYSIS

The indices involved are given more precisely in Table I-2:

TABLE I-2. INDICES BY DOMAIN

	Number of Components (j and ℓ)	Wave Bands Range of m (m_o to M)	Number of Wave Bands (i and m)
Stratosphere	18	11 to 20	10
Mesosphere	30	11 to 20	10
Lower Thermosphere	42	1 to 16	16
Upper Thermosphere	30	8 to 11	4

Equation I-1 may be broken down into 6 logical computation sequences:

$$a = \sum_{j} \sigma_{i,j} N_j(k - 1)$$

$$b = F(X) \cdot a$$

$$c = \text{Exponential of } b$$

$$d = I_m \cdot c$$

$$e = \sum_{m_o} \sigma_{m,\ell} \cdot d$$

$$f = \frac{1}{IP_\ell} \cdot e$$

The total computation for the equation can be determined by substituting the proper integer indices for ℓ, m, and j and the number of microsec for each of the 6 computational sequences in the following formula:

$$\text{Total Computation} = \ell[m(j \cdot a + b + c + d + c) + f].$$

However, it is more appropriate to determine the time required per point, since all previous estimates and timings are made on the basis of a point. This posed a small problem, which was solved by calculating a weighted average for ℓ, m, and j, determined by the number of layers in each of the domains. Thus the weighted average for ℓ and j was 30, and for m it was 9.

The CDC-7600 was used as the basis for the execution time per section, because of a good timing estimate given for the Leith troposphere model which is running on the 7600 at the Lawrence Radiation Laboratory in Livermore, California.

Without overhead, the 6 sections were timed as follows:

Section	Number of CDC-7600 Cycles
a	19
b	77
c	95
d	15
e	23
f	32

Using these values and the weighted averages for ℓ, m, and j, we have:

$$\text{Time per point} = 27.5 \text{ ns per cycle} \times 30[9(30.19 + 210) + 32]$$

$$= 5.8 \text{ ms per point.}$$

Equation I-2 can be divided into 2 logical sections: (a) location of the coefficients from given and calculated values and their formation into a matrix suitable for solution, and (b) solution of the simultaneous equations.

The first of these sections consists of the manipulation of indexes to select the proper coefficients. A set of predetermined pointers can be developed for each domain to minimize the complexity of this process. Without showing the detail, this section required approximately 0.15 ms per point.

The solution of the simultaneous equations was based on a popular subroutine used at LRL on the CDC-6600. For actual matrices of equivalent density but for a 10 x 10, the time required on the 6600 was approximately 1.0 millisec. Since the solution time using this routine goes up approximately linearly as a function of the number of nonzero values in the matrix, we can extrapolate that it will require about 9 millisec for the 30 x 30 matrix, which is the weighted average size for the S-M-T Model. Using a factor of 5:1 for the CDC-7600 over the CDC-6600 results in an estimate of 1.8 millisec for solution on the CDC-7600.

Equation I-3 is simple and requires an average of 31 iterations for an estimated 25 microsec of CDC-7600 computer time.

Equation I-4, the heat equation, is simple by virtue of the fact that partial results of earlier radiation calculations can be used to achieve this result. The equation is estimated to require approximately 20 microsec of CDC-7600 time.

The total time for Equations I-1 through I-4 is found to be about 7.75 millisec per point without considering overhead and

bookkeeping instructions. Since maximum times have been used in all of the previous analyses, it is felt that the overhead will be more than offset by the difference that would occur from overlap of arithmetic instructions.

The Troposphere hydrodynamic model after Leith, which is being run on the CDC-7600 at the Lawrence Radiation Laboratory, Livermore, has been estimated to take about 180 microsec per point. Thus, from a comparative standpoint, the radiation energy and heat equations would take approximately 43 times as much time as is required for the hydrodynamical computations.

Since it was determined at this point that the desired result had been realized, no further analyses were made on the remaining features of the S-M-T Model. They were, however, estimated to be small in comparison to the radiation energy calculation.

BIBLIOGRAPHY

Aikin, A. C., and S. J. Bauer, Introduction to Space Science, Hess and Mead, Gordon and Breach Publishers, 2nd Edition, pp. 160-162, 1968.

Anderson, K. A., et al., "Energetic Electron Fluxes in and Beyond the Earth's Outer Magnetosphere," J. Geophysical Research, Vol. 70, No. 5, pp. 1039-1050, March 1, 1965.

Arakawa, A., "Computational Design for Long Term Numerical Integration of the Equations of Fluid Motion," J. of Computational Physics, Vol. 1, 1966.

Bagrinovski, K. A., and S. K. Godunov, , "Different Schemes for Multi-dimensional Problems," Doklady Akademiia Nauk, USSR, Vol. 115, p. 431, 1957.

Batchelor, G. K., "The Application of the Similarity Theory of Turbulence to Atmospheric Diffusion," Quart. Journal of Royal Meteorological Society, Vol. 76, p. 133, 1950.

Bates, D. R., "The Thermosphere," Proc. of Royal Society of London, Vol. A236, pp. 206-211, 1956.

Bedinger, J. F., and E. Constantinides, "Investigation of Temporal Variations of Winds," Final Report Contract No. NAS 5-11572, GCA-TR-69-3N, August 1969.

Bjorgum, O., "Turbulence from a Naval Point of View and Examination of the Physical Basis of Hydrodynamics," Universitetet Arbok Matematisk-Natur-Vietenskapelig, Serie, Bergen, Norway, No. 3, 1944.

Bortner, M., and R. Kummler, "The Chemical Kinetics and the Composition of the Earth's Atmosphere," General Electric Re-Entry Systems, Scientific Report #1, GE-9500-ECS-SR-1, July 24, 1968.

Byron-Scott, Ronald, "A Stratospheric General Circulation Experiment Incorporating Diabatic Heating and Ozone Photochemistry," McGill University, Montreal, Canada, DDC No. AD 655 058, April 1967.

Crank, J., and P. Nicholson, "A Practical Method for Numerical Integration of Solutions of Partial Differential Equation of Heat Conduction Type," Proc. Cambridge Philos. Society, Vol. 43, p. 50, 1947.

DuFort, E. C., and S. R. Frankel, "Stability Conditions in the Numerical Treatment of Parabolic Differential Equations," Mathematical Tables and Other Aids to Computation, Vol. 7, p. 135, 1953.

D'Yakonov, E. G., "On Several Difference Schemes for the Solution of Boundary Problems," Zhurnal Vychislitelnoi Matematiki i Matematicheskoi Fiziki, Moscow, Vol. 2, p. 57, 1962.

Friedman, M. P., "A Three-Dimensional Model of the Upper Atmosphere," SAO Special Report 250, Smithsonian Institution, Astrophysical Observatory, Cambridge, Mass., September 19, 1967.

Godske, C. L., et al., "Dynamic Meteorology and Weather Forecasting," American Meteorological Society, Boston, Mass., and Carnegie Institute of Washington, Washington, D.C., 1957.

Gosling, J. T., et al., "Vela 2 Measurements of the Magnetopause and Bow Shock Positions," J. Geophysical Research, Vol. 72, No. 1, pp. 101-112, January 1, 1967.

Izakov, M. N., and S. K. Morozov, "The Heating Function of Thermosphere by Solar Radiation in Schumann-Runge Continuum," Institute for Space Research, Academy of Sciences of the USSR, Report to be presented at the XIII Session of COSPAR, Leningrad, May 1970.

Izakov, M. N., "On the Theoretical Models of Structure and Dynamics of the Earth's Thermosphere," Institute for Space Research, Academy of Sciences of the USSR Dδ-6, Moscow, 1970.

Jackson, J. D., Classical Electrodynamics, John Wiley and Sons, New York, 1962.

Jeffreys, H., The Earth: Its Origin, History, and Physical Constitution, Cambridge University Press, 1962.

Kasahara, Akira, "The Influence of Orography of the Global Circulation Patterns of the Atmosphere," NCAR Manuscript 424, National Center for Atmospheric Research, Boulder, Colo., June 1967.

Kasahara, A., and W. Washington, "NCAR Global General Circulation Model of the Atmosphere," Monthly Weather Review, Vol. 95, No. 7, pp. 389-402, July 1967.

Kochanski, Adam, "Atmospheric Motions from Sodium Cloud Drifts," J. Geophysical Research, Vol. 69, No. 17, pp. 3651-3662, September 1, 1964.

Laasonen, P., "Wser eine Methodi Zür Lösung der Wärme leitungs gleishung," Acta Math., Vol. 81, p. 309, 1949.

Leith, C. E., "Numerical Simulation of the Earth's Atmosphere," Methods in Computational Physics, Vol. 4, Academic Press, New York, pp. 1-28, 1965.

Leith, C. E., "Numerical Simulation of Turbulent Flow," Properties of Matter Under Unusual Conditions, Interscience Publishers (John Wiley), New York, 1969.

Leith, C. E., "Atmospheric Predictability and Two-Dimensional Turbulence," NCAR MS 70-87. To appear March 1971 J. Atmosp. Sci.

Marchuk, G. I., and N. N. Yanenks, "Applications of the Method of Splitting (Fractional Steps) to the Solution of Mathematical Physics," IFIP Congress, New York, 1965.

Mintz, Y., "Very Long Term Global Integration of the Primitive Equations of Atmospheric Motion," World Meteorological Organization, Technical Note WMO 162 TP 69, 1965.

Murgatroyd, R. J., "The Physics and Dynamics of the Stratosphere and Mesosphere." Submitted to Rep. Prog. Physics, 1970.

Nagata, T., et al., "Observations of Mesospheric Ozone Density in Japan," IQSY-COSPAR Symposium, London, July 1967.

Newell, R. E., "The General Circulation of the Atmosphere Above 60 km," Meteorological Monographs, Vol. 8, No. 31, April 1968.

Olson, W. P., "Variations in the Earth's Surface Magnetic Field from the Magnetopause Current System," Planet Space Science, Vol. 18, pp. 1471-1484, Pergamon Press, 1970.

Oort, A. H., and A. Taylor, "On the Kinetic Energy Spectrum Near the Ground," Monthly Weather Review, Vol. 97, No. 9, September 1969.

Phillips, N.A., "An Example of Non-linear Computational Unstability," The Atmosphere and the Sea in Motion, B. Bolin, editor, Rockefeller Institute Press, New York, 1959.

Richardson, L.F., "Atmospheric Diffusion Shown on a Distance-Neighbor Graph," Proceedings of Royal Society, London, Series A, Vol. A110, p. 709, 1926.

Richardson, L. F., Weather Prediction by Numerical Process, Cambridge University Press, MB6, 1922.

Richtmyer, R. D., and K. W. Morton, Difference Methods for Initial Value Problems, Interscience Publishers, John Wiley & Sons, New York, 1967.

Saul'ev, V. K., "On a Method of Numerical Integration of the Equation and Diffusion," Doklady Academiia Nauk, USSR, Vol. 115, p. 1077, 1957.

Shimazaki, Tatsuo, "Dynamic Effects on Atomic and Molecular Oxygen Density Distributions in the Upper Atmosphere: A Numercial Solution to Equations of Motion and Continuity," J. of Atmospheric & Terrestrial Physics, Vol. 29, pp. 723-747, Pergamon Press Ltd., 1967.

Shimazaki, Tatsuo and A. R. Laird, "A Model Calculation of the Diurnal Variation in Minor Neutral Constituents in the Mesosphere and Lower Thermosphere Including Transport Effects," J. Geophysical Research, Space Physics, Vol. 75, No. 16, pp. 3221-3235, June 1, 1970.

Smagorinsky, J., "General Circulation Experiments with the Primitive Equations: I. The Basic Experiment," Monthly Weather Review, Vol. 91, No. 3, pp. 91-151, March 1963.

Smagorinsky, Joseph, et al., "Numerical Results from a Nine-Level General Circulation Model of the Atmosphere," Monthly Weather Review, Vol. 93, No. 12, pp. 727-768, December 1965.

U. S. Standard Atmosphere Supplements, ESSA, NASA, USAF, 1966.

Valley, Shea L., "Handbook of Geophysics and Space Environments," Ionospheric Wind Velocity (about 110 km) Distribution at Puerto Rico and Rostov, Russia, 1965, p. 12-35.

Van der Hoven, Isaac, "Power Spectrum of Horizontal Wind Speed in the Frequency Range from 0.0007 to 900 cycles/hour," Journal of Meteorology, Vol. 14, pp. 160-164, April 1957.

Weidner, D. K., et al., "Models of Earth's Atmosphere (120 to 1000 KM)" NASA/SP-8021, May 1969.